2016

Distributed Optimization And Control Of Islanded Microgrids

Md Rishad Hossain
University of South Carolina

DISTRIBUTED OPTIMIZATION AND CONTROL OF ISLANDED MICROGRIDS

by

Md Rishad Hossain

Bachelor of Science
Bangladesh University of Engineering and Technology, 2005

Master of Business Administration
University of Dhaka, 2014

Submitted in Partial Fulfillment of the Requirements

For the Degree of Doctor of Philosophy in

Electrical Engineering

College of Engineering and Computing

University of South Carolina

2016

Accepted by:

Herbert L. Ginn III, Major Professor

Charles W. Brice, Committee Member

Andrea Benigni, Committee Member

Jamil A. Khan, Committee Member

Cheryl L. Addy, Vice Provost and Dean of the Graduate School

DEDICATION

To my elder brother, Md Anwar Hossain, for whom it was possible

To my parents who dreamt big, very big

To my beloved wife, Fatima Farzana, for her patience and support during this work

To my lovely son, Mahathir Rishad Hossain, for the happiness he brought to us

ACKNOWLEDGEMENTS

My sincere appreciation to my advisor, Dr. Herbert L. Ginn for his guidance and support during the course of my PhD studies in University of South Carolina. His valuable advice, encouragements along with belief and patience led me to come up with this work. I would always remember his support in both academic and personal matters.

I like to thank my advisory committee members, Dr. Charles Brice, Dr. Andrea Benigni and Dr. Jamil A. Khan, for their time, helpful comments and advice.

I would like to acknowledge the sponsor that made my Ph.D. work possible. My work was supported by the U.S. Office of Naval Research.

I am also grateful to my friends Gholamreza Dehnavi, Hossen Asiful Mustafa and Nowrin Hasan Chamok for their help and support.

None of this work would have been possible without love and support from my elder brother, Md Anwar Hossain. My deepest gratitude to my father, Md Nazir Hossain and to my mom, Anwara Khanm for their dedication, support and patience during my life.

I would like to thank my beloved wife, Fatima Farzana, for her patience, continuous encouragement and to my lovely son, Mahathir Rishad Hossain who used to spend his afternoons by the window waiting anxiously for his dad.

ABSTRACT

A microgrid may have numerous multi-functional power electronic converters connecting sources, loads, and storage to the system. Systems where converters are the interface between many of the main sources of energy and load centers have the ability to direct the flow of energy if the control of the converters is coordinated. The influence of energy flow in a microgrid by coordinated action of converters is referred to here as 'energy routing'. Energy routing allows for reduction of systems losses by optimizing source operating points and reducing transmission and distribution path losses. Energy ramp rates at various points in the system can also be manipulated by coordinated control of energy flow through the converters.

Converters can be coordinated centrally or in a distributed fashion. A distributed coordination system approach can enable system level converter control while avoiding single points of failure that are inherent in a centralized hierarchical control system, and that is robust and expandable. Research performed in the area of distributed control indicates that a control based on a multi-agent system (MAS) has the potential to satisfy the distributed converter control requirements. Here an optimization technique is developed that can be distributed for parallel computation by MAS type control systems.

An optimization algorithm will be presented that dynamically determines global optimal values of discretized command variables to the converters in a distributed fashion in order to ensure most economic fuel usage of the sources and minimization of

distribution loss simultaneously. Converter command variables are discretized in order to formulate the optimization problem as a Mixed Integer Quadratic Programming (MIQP) problem. The MIQP framework allows decomposition of the optimization algorithm as well as pruning of the search span by a factor of hundreds. Thus, it provides very fast convergence to the optimal solution and ensures that the communication requirements are feasible for real-time system level coordination.

In order to validate the distributed optimization and control method developed in this research, a simplified shipboard DC power distribution system and CERTS (Consortium for Electric Reliability Technology Solutions) microgrid are used for case studies. These are isolated microgrids with converters between all sources of energy and the main buses as well as between all load centers and the main buses. Energy routing through the branches is directly maintained by controlling the command variables input to the converters. Sources as well as storage are indirectly manipulated to their optimal set points by these discretized command variables. Simulation based validation is performed for both test systems.

TABLE OF CONTENTS

DEDICATION iii

ACKNOWLEDGEMENTS iv

ABSTRACT v

LIST OF TABLES ix

LIST OF FIGURES x

CHAPTER I INTRODUCTION TO MICROGRIDS 1

1.1 LITERATURE REVIEW 2

1.2 RESEARCH OBJECTIVE 6

1.3 ORGANIZATION OF THE DISSERTATION 8

CHAPTER II COMPONENTS OF MICROGRIDS 9

2.1 SOURCES 9

2.2 LOADS 10

2.3 CONVERTER / INVERTER 10

2.4 ENERGY STORAGE SYSTEM 12

CHAPTER III DESCRIPTION OF THE EXAMPLE MICROGRIDS 23

3.1 SHIPBOARD POWER SYSTEM 23

3.2 CERTS MICROGRID 26

CHAPTER IV SYSTEM LOSS OF A POWER SYSTEM AND ITS COMPONENTS 30

4.1 UNIT COMMITMENT 30

4.2 ECONOMIC DISPATCH 31

4.3 DISTRIBUTION LOSS 36

4.4 STORAGE SYSTEM LOSS 41

4.5 OVERALL SYSTEM LOSS 42

CHAPTER V OPTIMIZATION ALGORITHM 43

5.1 SCALING AND CHANGE OF VARIABLES 44

5.2 SEARCH AND PRUNE 46

5.3 AGGRESSIVENESS VS SUB-OPTIMALITY 48

CHAPTER VI SOFTWARE AGENT AND COMMUNICATION 50

6.1 COMMUNICATION OF THE DISCUSSED ALGORITHM 51

6.2 MULTI-AGENT BASED COMMUNICATION 54

CHAPTER VII RESULTS 59

7.1 MINIMIZATION OF DISTRIBUTION LOSS 61

7.2 ECONOMIC DISPATCH AND MINIMIZATION OF DISTRIBUTION LOSS SIMULTANEOUSLY 66

7.3 ECONOMIC DISPATCH AND MINIMIZATION OF DISTRIBUTION LOSS SIMULTANEOUSLY CONSIDERING MINIMUM GENERATION SETTING ... 74

7.4 SYSTEM LOSS MINIMIZATION OF CERTS MICROGRID 80

CHAPTER VIII CONCLUSION 85

REFERENCES 87

APPENDIX A - LOSS IN SHIPBOARD MICROGRID 94

APPENDIX B - LOSS IN CERTS MICROGRID 96

APPENDIX C - SCALING AND CHANGE OF VARIABLES 98

LIST OF TABLES

Table 4.1. Specific Fuel Consumption of Main Generator 32

Table 4.2. Efficiency of the Main Generator 34

Table 4.3. Efficiency and Loss of the Main Generator 34

LIST OF FIGURES

Figure 1.1. General architecture of a Microgrid 2

Figure 2.1. Controlled Voltage/Current Source 11

Figure 2.2. ESS used as Peak Shaver 12

Figure 2.3. Simple Battery Model 15

Figure 2.4. Modified Thevenin Equivalent Battery Model [23] 15

Figure 2.5. ESS behavior around its SOC limit 22

Figure 3.1. Architecture of example Ship Microgrid 24

Figure 3.2. Pulsed Load Characteristics 25

Figure 3.3. CERTS microgrid architecture 27

Figure 3.4. CERTS microgrid test case during islanded operation 29

Figure 4.1. Unit Commitment problem 31

Figure 4.2. Economic Dispatch problem 32

Figure 4.3. Output Power vs Specific Fuel Consumption in p.u. [45] 33

Figure 4.4. Fuel loss characteristics of the Main Generator 35

Figure 4.5. Ohmic loss basics 36

Figure 4.6. Simplified Ship Microgrid 37

Figure 4.7. Electrical representation of the simplified ship microgrid 39

Figure 4.8. Electrical representation of CERTS microgrid test case 40

Figure 5.1. Loss due to z_1 46

Figure 5.2. Loss due to pruned z_1 47

Figure 5.3. Search tree 48

Figure 5.4. Optimal Region 48

Figure 6.1. Communication design of the control system [35] 52

Figure 6.2. Flow diagram of the distributed control 53

Figure 6.3. Asynchronous message passing paradigm based on content-based publish-subscribe design 54

Figure 6.4. Comparison between complexity of bidding and publish-subscribe agent technologies 55

Figure 6.5. Integrated agent-based system including MATLAB model in lower section and JADE platform in upper section, joined using MACSim toolbox 57

Figure 6.6. Work flow diagram of designing integrated agent-based controller 58

Figure 7.1. Shipboard Power system for the test scenario 60

Figure 7.2. CERTS microgrid for the test scenario 61

Figure 7.3. Load profiles in the shipboard system for the test scenario 62

Figure 7.4. Converter operating points for minimization of Distribution Loss 63

Figure 7.5. Load sharing in Zone1 64

Figure 7.6. Load sharing in Zone2 65

Figure 7.7. Generators' contribution for minimization of Distribution Loss 65

Figure 7.8. Zonal Voltages 66

Figure 7.9. Converter operating points dictated by the system control 67

Figure 7.10. Power contribution of ESS due to different loading conditions in the shipboard system 69

Figure 7.11. Change of SOC due to discharge of the ESS 69

Figure 7.12. Generators' contributions in the shipboard system 70

Figure 7.13. Comparison of loss due to dynamic optimization vs rating based sharing .. 71

Figure 7.14. Bus cross-tie current 72

Figure 7.15. Load sharing in Zone1 73

Figure 7.16. Load sharing in Zone2 73

Figure 7.17. Load profiles in the shipboard system for the test scenario 75

Figure 7.18. Converter operating points dictated by the system control 76

Figure 7.19. Power contribution of ESS due to different loading conditions in the shipboard system 76

Figure 7.20. Change of SOC due to discharge of the ESS 77

Figure 7.21. Generators' contributions in the shipboard system 78

Figure 7.22. Bus cross-tie current 78

Figure 7.23. Load sharing in Zone1 79

Figure 7.24. Load sharing in Zone2 79

Figure 7.25. Loads in the CERTS Microgrid 80

Figure 7.26. Optimal Ratios 81

Figure 7.27. Generators' Set Points 81

Figure 7.28. Generator1's Contribution 82

Figure 7.29. Generator2's Contribution 82

Figure 7.30. Generator3's Contribution 82

Figure 7.31. Total Load of the System 83

Figure 7.32. Total Generation of the System 83

CHAPTER I

INTRODUCTION TO MICROGRIDS

A Microgrid (MG) is a special category of distributed generation and load system that is distinguished by its size and the ability to operate independently as a self-contained power system. Energy sources in a microgrid are commonly interfaced through power electronic converters. A microgrid may take the form of shopping center, industrial park, college campus, an electric ship and so on. A microgrid may be or may not be connected to a large scale utility grid [1].

Microgrids can be classified into several types based on the position they have and the type of power they provide. Common types of microgrids are Grid Connected Microgrid, Islanded Microgrid, AC Microgrid, DC Microgrid and Hybrid Microgrid. Power electronics and their coordination by a system level control system play a very important role to control power flow in a microgrid.

Microgrids that are connected to a large scale power grid are called grid connected microgrid. Figure 1.1 depicts a grid connected microgrid. Its connection to the grid doesn't mean that it's always exchanging power with the grid. Power flow can be controlled (inflow, outflow, no flow) by using an energy management system (EMS). Microgrids that operate freely without any connection with large scale power grids are called islanded microgrids. Shipboard power systems are a good example of this type. Islanded microgrids must be fully self-subsistent. Microgrids that deal with AC power

only are called AC Microgrid. If a grid connected microgrid provides AC power only, it would be called as grid connected AC microgrid. DC Microgrids provide DC power only. If an islanded microgrid deals with DC power only, it would be called as islanded DC microgrid. Microgrids that deal with both DC and AC power are called Hybrid Microgrids [2].

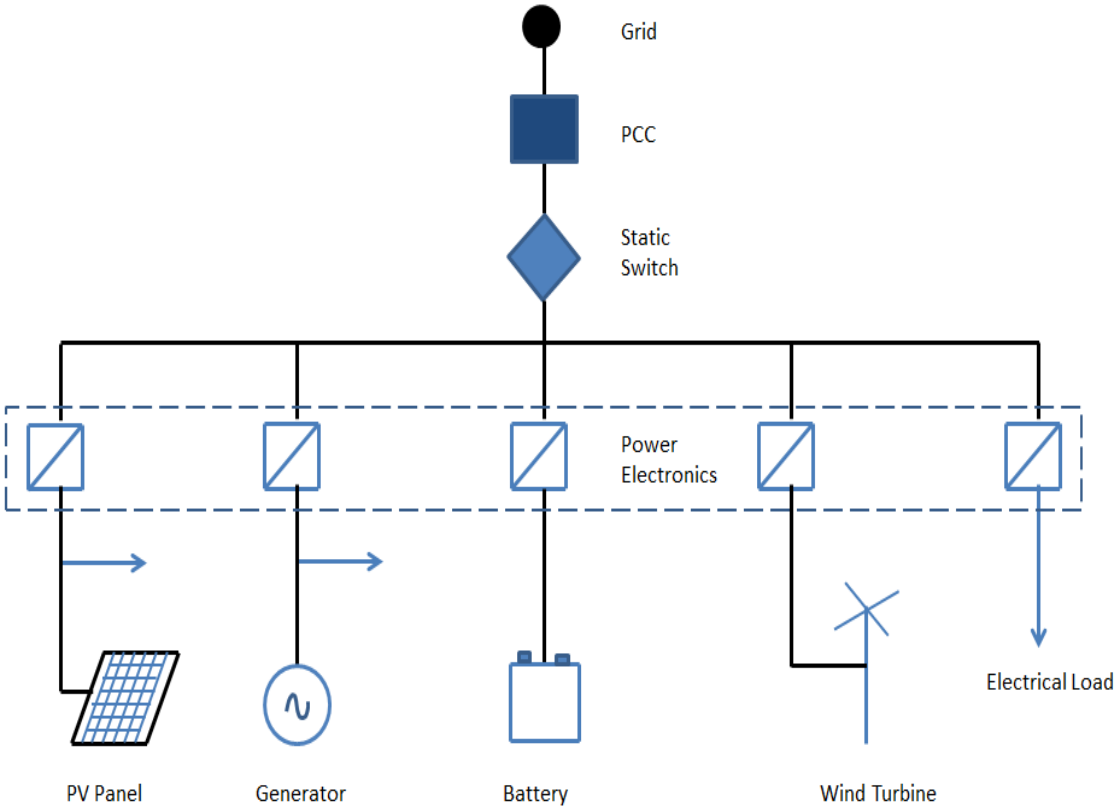

Figure 1.1. General architecture of a Microgrid

1.1 LITERATURE REVIEW

Researchers have suggested many methods for control of microgrids. Suggestions vary depending on the objectives considered. Some place emphasis on global optimal solution, some on time of convergence, and others on stability, reliability, scalability or a

mix [3-18]. In order to ensure greater command on the system, some sort of communication is a must. Hence droop based or decentralized communication free articles are not considered here.

Authors in [3] presented a scheme for an energy management system in the form of distributed control agents. The control agents' task is to ensure supply of the various load demands while taking into consideration system constraints and load priorities. A graph theoretic self-stabilizing maximum flow algorithm for the implementation of the agents' strategies has been developed to find a global solution using local information and minimum amount of communication. The algorithm has been adapted there to find a solution to the power flow problem of the electric shipboard system. Communication among agents makes use of the blackboard architecture. A fundamental problem in graph theory is the maximum flow problem for which parallel algorithms run in polylogarithmic time on a polynomial number of processors. Solutions to the reconfiguration problem have been found in 0.5 to 1.5 seconds which makes it not good enough for real-time reconfiguration.

A dynamic load management method to support for the next generation integrated shipboard power system has been validated in [4]. The problem is formulated as a dynamic optimization problem to maximize the energized loads in the system without violating any constraint. The objective of dynamic load management is to serve as many loads as possible considering priorities subject to the constraints of system. The simulation results indicated that the dynamic load management could maximize the energized loads without violating any system constraints in real-time. Though it's a real

time load management system, it doesn't intend to optimize the system loss. The objective function of this management doesn't deal with a cost function.

Authors in [5] have suggested particle swarm optimization combined with improved pre-prepared power demand (IPPD) table to optimize fuel consumption of a multi-machines microgrid. The work consisted in its entirety in a techno-economic study whose objective was to minimize fuel consumption and thereby generated pollution of a small central cogeneration multi-machine. This work was carried out by Secant method combined with Improved Pre-prepared Power Demand (IPPD) table which obtains the unit status information and then the optimal solution is achieved by Secant method at each power demand for 24 hours. It doesn't provide dynamic solution to load management and also is not applicable to distributed control.

Feasibility of employing modified Particle Swarm Optimization (PSO) approaches for efficient solving of Economic Dispatch Problems (EDP) considering generator constraints has been demonstrated in [6]. To enrich the searching behavior and to avoid being trapped into local optimum, a chaotic sequence based on logistic map is incorporated as a randomizer instead of traditional uniform random function approaches. This paper includes network loss or distribution loss in its objective function. But distribution loss is lumped together and expressed as function of generating units which doesn't truly represent simultaneous EDP and transmission loss optimization.

A decentralized economic dispatch approach for microgrids has been analyzed in [7] such that each DG unit makes local decisions on power generation based on a multi-agent coordination with guaranteed convergence. Heterogeneous wireless network architecture is established. Each node uses an ad hoc communication device for basic information

exchange, while some dual-mode nodes are equipped with optional cellular communication devices which can be activated to improve the convergence speed of multi-agent coordination. Two multi-agent coordination schemes are proposed to utilize the cellular communication links based on the single-stage and hierarchical operation modes, respectively. However, the basic objective function of this article is considered as a Linear Programming problem and so it can't fit non-linear distribution loss into its structure.

A dynamic economic dispatch method has been proposed in [8]. Considering microgrid as a discrete time system, the dynamic economic dispatch is to find the optimal control strategy for the system in finite time period. Based on this idea, the dynamic economic dispatch model for microgrids has been established and then the corresponding dynamic programming algorithm is designed. An energy storage system has also been used in the proposed model. This method is computation costly and may not work for real-time coordination.

Economic dispatch using reduced gradient method is implemented in [9] for the optimization of energy in an islanded microgrid. Renewable energy sources like Wind Turbine and Solar system along with Battery storage has been modeled in the discussed article. Cost functions of the sources include operation, maintenance and investment costs. Optimization is obtained by minimizing the cost function of the system while meeting the load demand. However, ramp rates of the fuel based sources and distribution loss have not been considered in this article and it can't support distributed control configuration.

Time of convergence in most of the discussed articles varies around 0.5 to 2 seconds. The work to date coordinates microgrids at a top level and does not seek to coordinate the power electronic converters in real-time for controlling the flow of energy and hereby dictate the sources rather they command directly on the sources to achieve objectives. However, direct communication based coordination at the converter level may provide a greater degree of energy flow control aimed at system optimization.

1.2 RESEARCH OBJECTIVE

A microgrid may have numerous multi-functional power electronic converters connecting sources, loads, and storage to the bus. Systems where converters are the interface between many of the main sources of energy and load centers have the possibility to direct the flow of energy if the control of the converters is coordinated. The influence of energy flow in a microgrid by coordinated action of converters is referred to here as 'energy routing'. Energy routing allows for reduction of systems losses by optimizing source operating points and reducing transmission and distribution path losses.

Converters can be coordinated centrally or in a distributed fashion however, centralized control is vulnerable to a single point of failure. A distributed coordination system approach can enable system level converter control while avoiding single points of failure that are inherent in a centralized hierarchical control system, and that is robust and expandable. Distributed control provides an avenue to expand the system with an evenly distributed computation workload, hence it becomes useful for larger system optimization. A Multi-Software platform that can work autonomously in a particular

environment having intelligence to choose optimum strategies (commonly known as Multi-agent System, MAS in short) can be implemented to achieve distributed control of the converters in a microgrid [19-21].

The main objective of this research is to establish a framework for distributable optimization algorithms used in system level control of microgrids that would ensure system optimization dynamically. Multiple agents, having little or weak communication among themselves, will take part in the process to determine optimum power sharing for the converters. Optimal energy routing would ensure minimum ohmic losses and maximize efficiency of the sources while maintaining their operating limits. Any change in loads would be followed by new operating points of the system dynamically.

In order to validate the distributed control method developed in this research, a shipboard power distribution system and CERTS (Consortium of Electric Reliability Technology Solutions) microgrid structure will be used for case studies. The shipboard system is an isolated microgrid with converters between all sources of energy and the main buses as well as between all load centers and the main buses. CERTS microgrid is radial in structure with three feeders having energy manager, microsource controller and protection scheme. Both of the test systems are described in detail in Chapter III.

The goal is to establish a multi-agent based distributed control system that determines the optimal operating points of the converters that would minimize system loss. These two test systems have attributes that form a superset of attributes found in other microgrids. Therefore, a distributable optimization framework that can optimize operation for these microgrids in real-time should be broadly applicable for most other microgrid systems.

1.3 ORGANIZATION OF THE DISSERTATION

Components of Microgrids are discussed in Chapter II. Battery model and its state of charge estimation methods have also been reviewed in this Chapter. Chapter III is about description of the notional shipboard distribution system and the CERTS Microgrid. Components of system loss of a power system such as Unit Commitment, Economic Dispatch, Distribution Loss etc. would be discussed in Chapter IV. Optimization algorithm and its formulation would be explored in Chapter V. Chapter VI is about software agent, multi-agent system and communication among them. Results of the optimization algorithm on the discussed microgrids would be presented and discussed in Chapter VII. Chapter VIII outlines key conclusions and contributions of this work along with ideas for continuation of the research.

CHAPTER II

COMPONENTS OF MICROGRIDS

Microgrids are self-subsistent systems, therefore they should have many of the components that a large scale power grids have. Some of the most common components of a microgrid are briefly described in this chapter.

2.1 SOURCES

Microgrid's sources are responsible to provide its own load demand. If the microgrid isn't grid connected and the demand is higher than capacity, some loads would be unfed. Microgrids' sources are mainly of two broad types, Fuel based Generators and Alternative Energy Sources.

Fuel based generators like gas turbine or diesel generators are most common sources in the microgrids where some priority loads must be fed on demand. Fuel based generators constitute a reliable and steady solution for load demand. Generators used in the microgrids may or may not be of same rating.

Alternative energy sources play very important role in microgrids. Photo Voltaic (PV) panel and Wind Turbine are currently the most common types of renewable energy sources in microgrids. As they are dependent on nature, for example PV panels for sunlight and Wind Turbines for air flow, their output isn't as steady as the Fuel Generators. Special control measures need to be used to harness energy from nature.

2.2 LOADS

Microgrid may have loads of different types and priority. Grid connected microgrids have the provision to exchange power between microgrid and large scale grid. If the grid's demand is higher than its generating capacity, it can request the microgrid to provide some power. In that case, the grid itself appears as a lumped load to the microgrid. Microgrids have their own electrical, electro-mechanical, and electro-chemical loads. If the load demand is higher than the microgrid sources' generation capacity, then a grid connected microgrid would ask the grid to provide power to feed excess load. Islanded microgrids have to shed low priority loads to meet the microgrids capacity constraint if installed total load is ever greater than generation capacity.

2.3 CONVERTER / INVERTER

Power Electronic Converters are used to connect sources, storage systems and loads to a microgrid. They can be used for AC to DC, DC to AC conversion or AC to AC, DC to DC scaling. The application level control dictates the operation of the power electronics system in order to meet the goal determined by the system level control. From the viewpoint of the application level controller, they appear as one of the three possible equivalent devices: Controlled Voltage Source, Controlled Current Source, or Controlled Impedance. Converters are used as controlled voltage source when particular components of a voltage need to be added or controlled into the voltage drop across a line. Active filter, Static Synchronous Series Compensator, Interline Power Flow Controller etc. are some of the applications of converters used as controlled voltage source.

Converters are used as controlled current source when particular components of the

current need to be drawn from or injected into a system. STATCOM, mini-HVDC, Energy Storage System Interface are some of the applications of converters used as controlled current source. Differences between the 'Controlled Voltage Source' and 'Controlled Current Source' converters lie mainly in the data acquisition and application level control that deals with the reference signal generation [19].

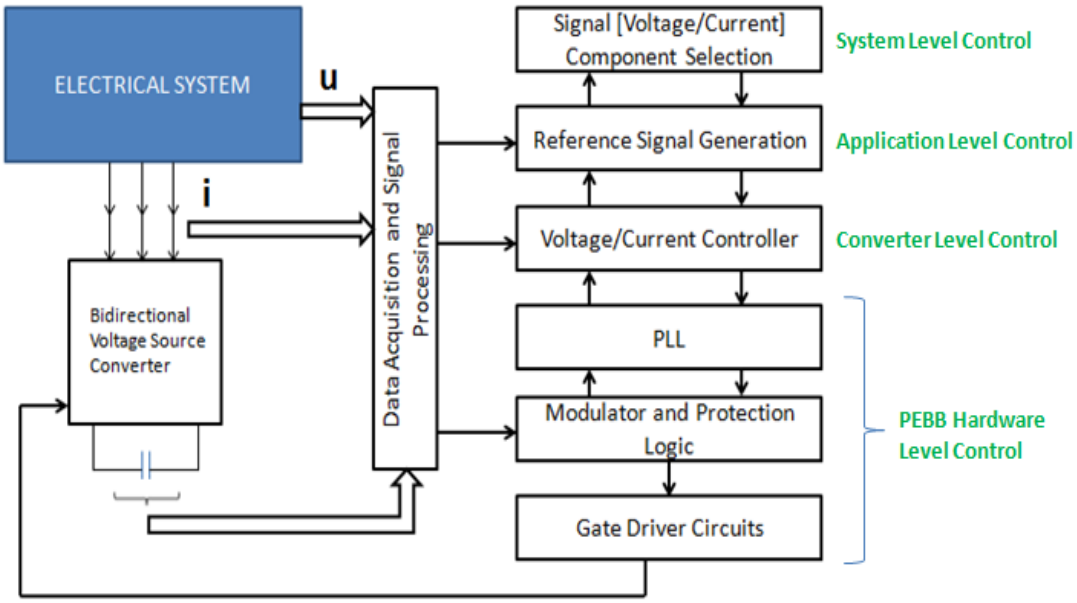

Figure 2.1. Controlled Voltage/Current Source

Figure 2.1 depicts the typical control hierarchy for grid connected converters. The Application Level Control generates either the voltage reference or the current reference signal for the converter according to the mission determined by the system level control. The converter level and hardware level controls cause the power electronics hardware to behave accordingly. Controlled Impedances are quite similar to their voltage sourced converter based counterparts with the exception of their operating range. The operating

limits for this class of device vary dynamically with the state of the power system. Static Var Compensator (SVC) is a good example of this type.

2.4 ENERGY STORAGE SYSTEM

Energy storage systems (ESS) are used to serve different purposes in different types of microgrids. Often they are used as peak shavers which means the ESS supplies energy when load demand at its peak and recharged while demand is low and there is adequate supply available. A typical peak shaver profile is shown in Figure 2.2 [22].

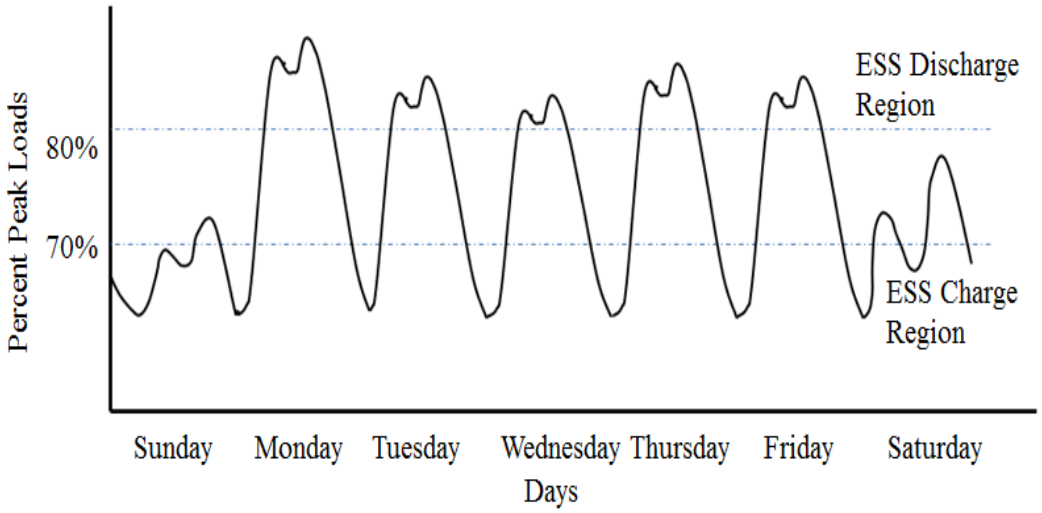

Figure 2.2. ESS used as Peak Shaver

Sometimes ESS is used dynamically as other sources to ensure minimum system loss. Two types of energy storage are mostly used in microgrids, Mechanical Energy Storage and Electro Chemical Energy Storage. There is a number of mechanical energy storage systems among which flywheel fits the best for the microgrid. Flywheels store kinetic energy which is then converted to electrical energy. Current flywheels can store up to

about 125 Wh kg^{-1} of energy [22]. Electro chemical batteries are the most popular storage system. They can be used for a wide range of applications, from assisting the very large-scale electrical grid down to tiny portable devices. The amount of charge a battery contains at a specific time (with respect to full charge) is called 'State of Charge'. State of charge (SOC) plays a very important role to prevent over-charging, over-discharging and to ensure battery life. SOC estimator plays key role behind using a battery dynamically in a microgrid. In a Battery, SOC tells the amount of Charge that the systemcan still provide. In simple mathematical form, it can be expressed as,

$$SOC = \frac{Q_{available}}{Q_{ref}} \times 100 \tag{2.1}$$

SOC measurement is important not only to know about residual capacity, it ensures system efficiency. Incorrect determination of SOC may cause Overcharging or over discharging which may lead permanent damage to the Battery or accelerate ageing [23]. As electrochemical energy storage is an integral part of the discussed shipboard power system, battery model and its SOC estimation methods are briefly discussed next.

2.4.1 BATTERY MODEL

Batteries revolutionized the way electricity can be stored. From portable cell phones to high-tech space equipment, batteries find innumerable applications. A battery stores chemical energy and converts it into electrical energy as and when required through an external circuit. Batteries used for the microgrid level operation consists of many electrochemical cells. Although the terms battery and cell are often used used interchangeably, cells are the building blocks of which batteries are constructed. Batteries

consist of one or more cell connected electrically. Series combination adds terminal potential whereas parallel combination boost up energy capacity. The basic components of a cell are electrodes (positive and negative), separator and electrolyte. During cell operation, ions are created and consumed at the electrode-electrolyte interfaces by oxidation/reduction reactions. The electrolyte can either be a solid or liquid chemical. It has high conductivity for ions. Electrolyte completes the internal circuit between the electrodes. Parameters associated with battery modeling like Internal Resistance, Polarization Capacitance, Rate of Charge and Discharge are briefly discussed below. .

Internal resistance can also be categorized into three sub-types like Charging/Discharging resistance, Overcharging/Over-discharging resistance and self-discharge resistance. Charging/Discharging resistances are associated with the resistance of the electrolyte, plate and fluid resistance. Value of these resistances varies over battery age, frequency of use and temperature. Self-discharge resistance is caused by the electrolysis of water at high voltage levels and slow leakage across the battery at low voltage. This resistance is more temperature sensitive and inversely proportional to temperature. Overcharge or over-discharge resistances are associated with electrolyte diffusion during over charging and over discharging.

Polarization capacitance is associated with the chemical diffusion within the battery. It depends on SOC and temperature [24].

Rate of charge and discharge should not be too high to ensure service life of the battery. Also frequency of charging and discharging cycles affect the battery life significantly. Most commonly used battery model is shown in Figure 2.3. It consists of an ideal battery along with an internal resistance R_{int}. While this model seems to be very

simple, it does not take into consideration the varying nature of the internal resistance due to temperature and electrolytic concentration. Also it does not distinguish between charging and discharging resistances.

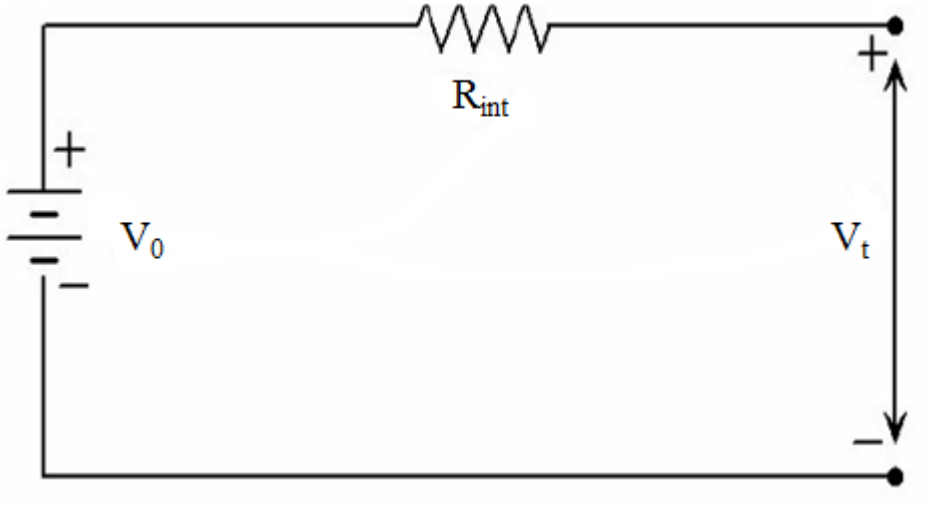

Figure 2.3. Simple Battery Model

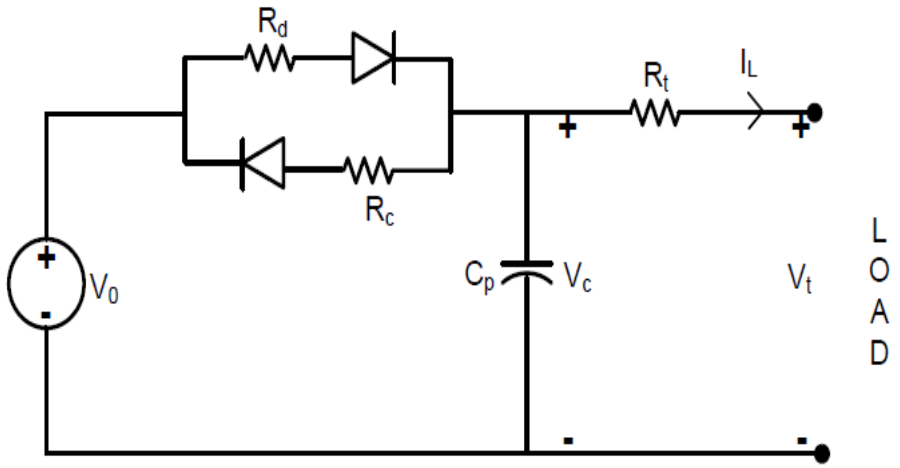

Figure 2.4. Modified Thevenin Equivalent Battery Model [23]

Battery Model that would be used to estimate SOC is shown in Figure 2.4. This is called Modified Thevenin Equivalent Battery Model. Two ideal diodes have been used in

the model just to show direction of use of the internal resistance. R_C is the internal resistance while charging and R_d while discharging. Charging and discharging impedance of the battery are not always equal. That is why they have been separated by using two ideal diodes to avoid interference in the estimation process. Here V_0 is the Open Circuit Voltage, R_t is the Terminal resistance and C_P is the Polarization Capacitance.

2.4.2 SOC ESTIMATION METHODS

A battery is a chemical energy storage source, and this chemical energy cannot be directly accessed. This issue makes the estimation of the SOC of a battery difficult. Accurate estimation of the SOC remains very complex and is difficult to implement, because battery models are limited and there are parametric uncertainties. Many examples of poor accuracy and reliability of the estimation of the SOC are found in practice.

The various methods of estimation are classified according to methodology. The classification of these SOC estimation methods differs in different literatures [25-37]. However, they can be broadly categorized into four types as Direct Measurement, Book-keeping Estimation, Adaptive Systems and Hybrid Methods.

Direct measurement uses physical battery properties, such as the voltage and impedance of the battery. Open circuit voltage method, Terminal voltage method, Impedance method, Impedance spectroscopy method fall in this category.

Book-keeping estimation uses charging-discharging current as the input and integrates it over time to calculate the SOC. Coulomb counting method, Modified Coulomb counting method are two examples of this type.

Adaptive systems are self-designing and can automatically adjust the SOC for different discharging conditions. Various new adaptive systems for SOC estimation have been developed. Back Propagation (BP) neural network, Radial basis Function (RBF) neural network, Support vector machine, Fuzzy neural network, Kalman filter represent adaptive systems. Adaptive systems can be automatically adjusted in changing systems.

Hybrid models benefit from the advantages of each SOC estimation method and allow globally optimal estimation performance. Hybrid methods generally produce better estimation of SOC compared to individual methods. Coulomb counting and EMF combination, Coulomb counting and Kalman filter combination, Per-unit system and EKF combination are some examples of Hybrid methods [27].

Back Propagation (BP) neural network is the most popular type in artificial neural networks. The BP neural network is applied in SOC estimation due to their good ability of nonlinear mapping, self-organization, and self-learning. As the problem defined, the relationship between the input and target is nonlinear and very complicated in SOC estimation. The artificial neural network based SOC indicator predicts the current SOC using the recent history of voltage, current, and the ambient temperature of a battery. The architecture of BP neural network contains an input layer, an output layer and a hidden layer. Input layer has 3 neurons for terminal voltage, current, and temperature [28].

Radial basis Function (RBF) neural network is a useful estimation methodology for systems with incomplete information. It can be used to analyze the relationships between one major (reference) sequence and the other comparative ones in a given set [29].

The Support Vector Machine (SVM) has been applied for classification in various domains of pattern recognition. The SVM has also been applied for regression problem.

The SVM used as a nonlinear estimation system is more robust than a least-squares estimation system because it is insensitive to small changes. Hansen and Wang [30] investigated the application of a SVM to estimate the SOC of lithium-ion battery. Results show that SVM produces very good SOC estimates.

Fuzzy neural network (FNN) has been used in many applications, especially in identification of unknown systems. In nonlinear system identification, FNN can effectively fit the nonlinear system by calculating the optimized coefficients of the learning mechanism. Lee et. al. [31] investigated a soft computing technique for estimating battery SOC of individual batteries in a battery string. The soft computing approach uses a fusion of an FNN with B-spline membership functions and a reduced-form genetic algorithm.

Yatsui and Bai [32] presented a Kalman filter based SOC estimation method for lithium-ion batteries. Experimental results validate the effectiveness of Kalman filter. An extended Kalman filter (EKF) is presented in [33] to estimate the concentrations of the main chemical species which are averaged on the thickness of the active material in order to obtain the SOC of the battery, by using the terminal current and voltage measurements. A novel SOC estimation method is proposed in [34] based on unscented Kalman filter (UKF) theory. The results show that UKF method is superior to extended Kalman filter method in SOC estimation for battery.

Electrochemical Impedance Spectroscopy (EIS) is a kind of electrochemical measurement method, during EIS experiments a small amplitude ac sinusoidal potential excitation signal usually a voltage between 5 to 50 mV, over a range of frequencies of 0.001 Hz to 100,000 Hz is applied to the system being studied. Since the perturbation ac

signal is very small, on the one hand, significantly disturbing of the properties being measured can be avoided, on the other hand, the resultant polarization of the system is in a linear potential region, which makes process of measuring results becomes simple and easy.

Electrochemical impedance spectroscopy is used in [35] for the purpose of predicting the state of charge of Lithium-ion rechargeable battery. The experiment data of impedance spectroscopy is comprised of an inductive arc in the high-frequency region and two capacitive arcs in the low-frequency region, and by which the reasonable equivalent circuit of battery was established. The component parameters obtained at several state of charge values of the battery had been analyzed by a non-linear least-squares fitting procedure and some electrochemical knowledge. Through researching the changing regulation of parameters with the different States of charge, the frequency of maximum of the semicircle (f_{max}), the phase angle φ, the equivalent series capacitance (C_s) had been substantiated to be the suitable parameters for analyzing and predicting the state of charge values of the lithium-ion battery.

Researchers have suggested many methods to determine SOC of the battery. Unfortunately none of these is perfect under all conditions. For example, a longer rest period is required after charge or discharge before specific gravity can be accurately measured due to electrolyte diffusion. So measuring ‘Specific Gravity’ to determine SOC is not a feasible solution for a dynamic system. Again some methods give better result but require manual intervention which makes it useless for dynamic operation. Some have significant advantage in one condition and disadvantages in other conditions. So it’s better to combine different process in such a way that the hybrid system will enjoy

advantages and avoid disadvantages of individual methods. A hybrid of Look up Table, Open Circuit Voltage and Coulomb Count method would be used here in this research to get a better, feasible and dynamic result.

Look up Table will consist of three graphs having R_d vs. Temperature, R_C vs. Temperature & C_P vs. Temperature data. During no load condition, these values will be picked to calculate Open Circuit Voltage.

Open Circuit Voltage, V_0 , has a linear relationship with Battery SOC. So accurate determination of SOC depends on correct measurement of Open Circuit Voltage. This method will be used during no load condition i.e. while the battery is neither being charged nor discharged (rest condition). At no load condition, voltage drop due to the Terminal Resistance, R_t, equals zero which means, $V_t = V_C$. V_c can then be converged exponentially towards V_0 by using values of R_d/R_c and C_p in the Look Up Table. Then we will use the linear relationship between V_0 and SOC as below:

$$V_0(t) = aS(t) + b \tag{2.2}$$

Here S(t) is SOC at specific time 't' and 'a', 'b' are constants.

Values of 'a' and 'b' can be calculated using extreme conditions of the battery. When S(t) equals zero, from Equation (2.2) we get,

$$b = V_0(t) \tag{2.3}$$

During full charge, S(t) equals 100% or 1. It gives us the value of 'a' as,

$$a = V_0(t) - b \tag{2.4}$$

During no load condition, the SOC measurement process has the following steps:

1) Measure terminal voltage, V_t
2) Measure Temperature

3) Calculate Open Circuit Voltage $V_0(t)$ using R_d/R_C and C_P at the measured Temperature.

4) Calculate SOC(t).

Coulomb Count Method will be used to measure SOC under Loaded Condition, i.e. while $|I_L(t)|>0$. Main disadvantage of this method individually is, initial condition must be correct and any error accumulates over time. To get rid of this disadvantage, latest S(t), calculated by Open Circuit Method will be used as initial value. So there is no chance of error accumulation. However as load current of a Microgrid Storage will be much higher than current through the polarization capacitance, we will neglect capacitance current during loaded condition. If we consider discharge,

$$S(t+1) = S(t) - \frac{Q_d(t)}{Q_{ref}} = S(t) - \frac{\int_{t_1}^{t_2} I_L(\tau)d\tau}{Q_{ref}} \tag{2.5}$$

While we consider charging,

$$S(t+1) = S(t) + \frac{Q_c(t)}{Q_{ref}} = S(t) + \frac{\int_{t_1}^{t_2} I_L(\tau)d\tau}{Q_{ref}} \tag{2.6}$$

Every time when Battery will neither charge nor discharge, SOC will be measured by Open Circuit Voltage & Look up Table methods and this value will be working as the initial value of Coulomb Count Method during Loaded Condition to avoid error accumulation. Ageing effect can be incorporated by changing $Q_{ref}(t)$ with respect to step size or charging/discharging number. Frequency of use could also be covered under

ageing effect. In Figure 2.5, ESS doesn't respond to the system controller demand while it hits its SOC limit. Rather it sends a notification to the controller that it's unable to obey its demand and the power flow is redesigned accordingly.

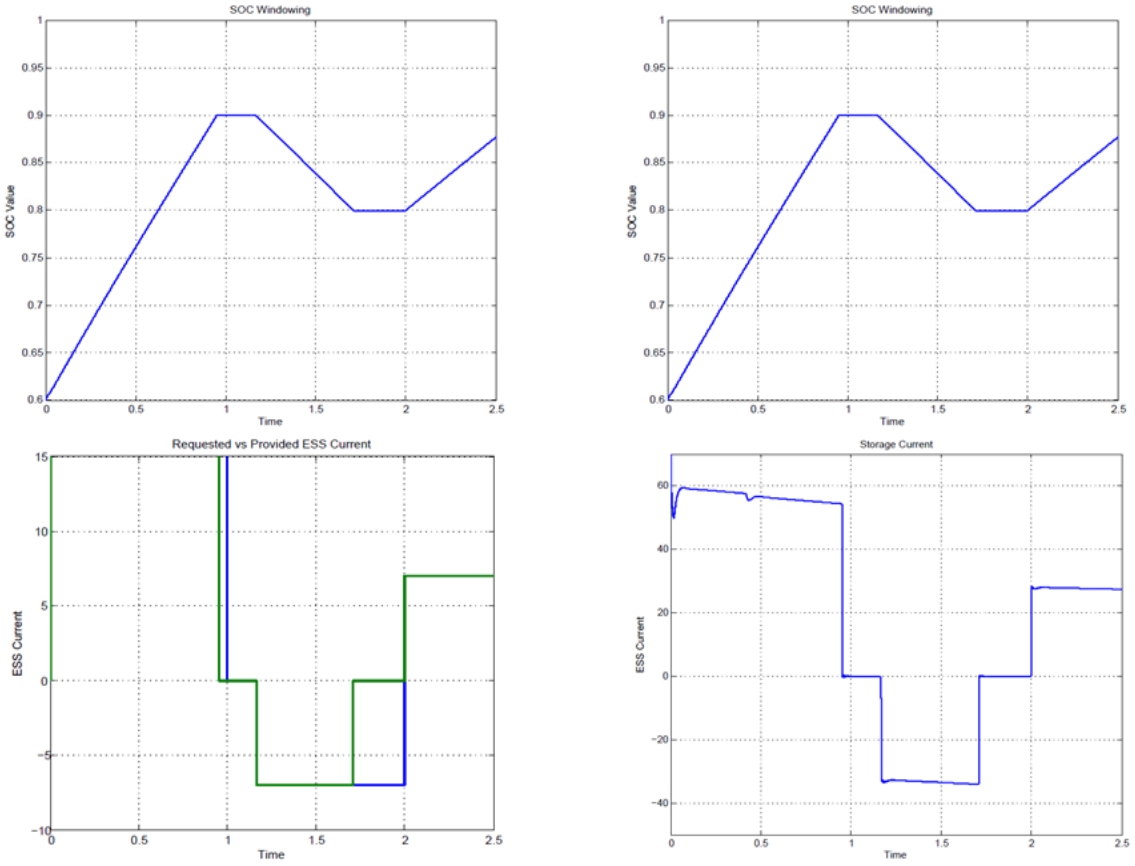

Figure 2.5. ESS behavior around its SOC limit

CHAPTER III

DESCRIPTION OF THE EXAMPLE MICROGRIDS

A notional DC shipboard power system and CERTS (Consortium for Electric Reliability Technology Solutions) microgrid would be used as case studies in this research. The shipboard system is an islanded microgrid but the CERTS microgrid can be grid-connected. As this research is about the islanded microgrids only, CERTS microgrid is only considered during the grid-disconnected condition [38-40].

3.1 SHIPBOARD POWER SYSTEM

The system that would be first used for discussion and validation of this research is a DC shipboard islanded microgrid. The example system, shown in Figure 3.1 is a subset of a notional DC shipboard distribution system. All major sources and load centers are interfaced to the system by appropriate converter systems also referred to as power conversion modules (PCMs). It has both fuel based generators (of different rating) and an electrochemical energy storage system (ESS). The ESS can serve the shipboard microgrid both as source and load depending on the system need and battery state of charge (SOC) condition. It also has two zones of utility loads and two PCMs interfacing each of the zones share the zonal load demand. The load center PCMs are assumed to be unidirectional converters which means they cannot allow energy to flow from one bus to the other.

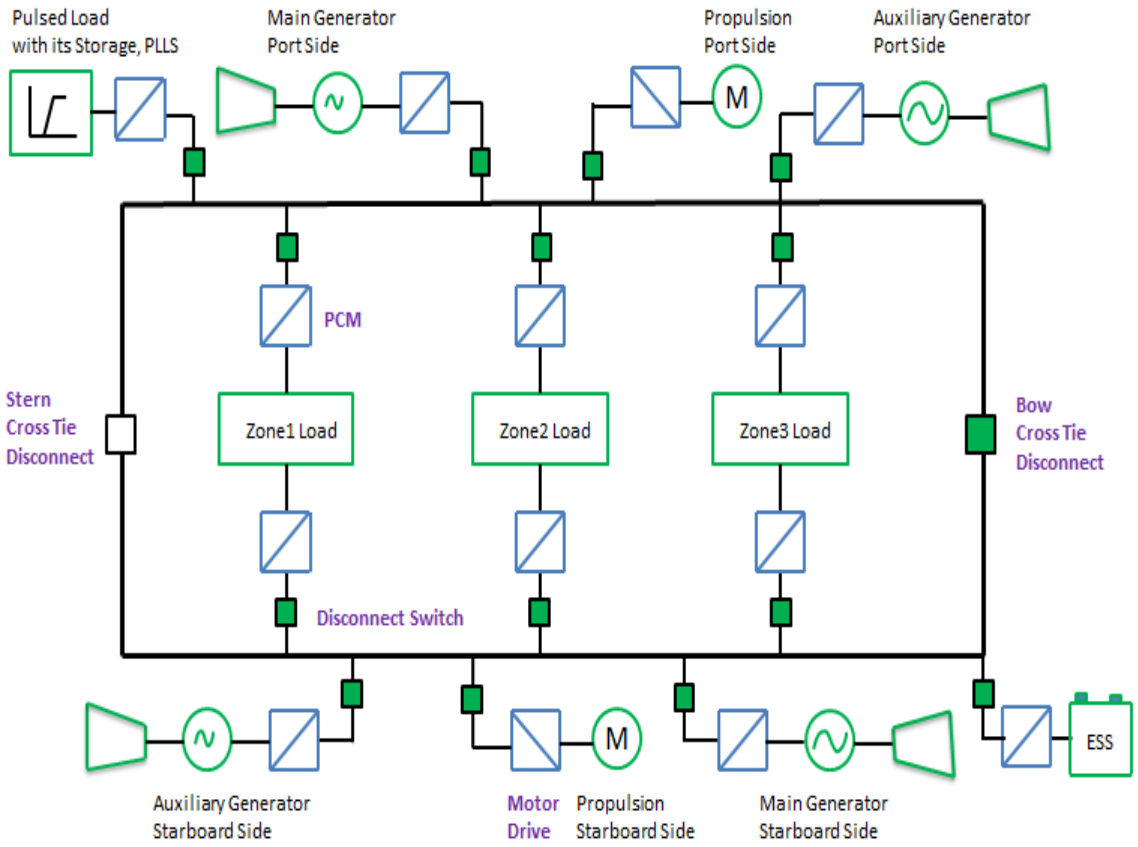

Figure 3.1. Architecture of example Ship Microgrid

The pulsed load is a high priority high energy load and therefore it has its own pulsed load local storage (PLLS). The rate of change of demand due to charging the PLLS is higher than the zonal loads. PLLS mitigates the impact of higher load ramp rates on the main bus. It buffers the power system from pulsed type loads and is charged from the main bus at a tolerable ramp rate [41-42].

An example charging and regeneration profile of a notional PLLS is shown in Figure 3.2. It may operate in Current Control, Power Control or Voltage Control modes. PLLS can also work bi-directionally as ESS, i.e. it can source power to the microgrid if there is a need from the system while no demand from the pulsed load.

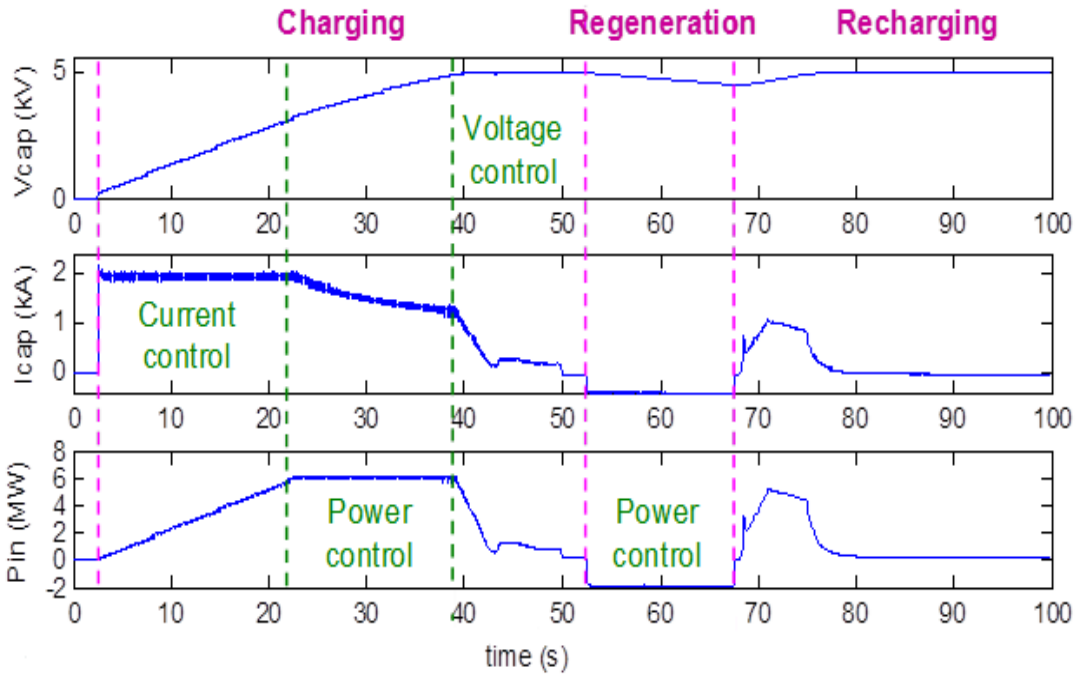

Figure 3.2. Pulsed Load Characteristics

Two main buses form the backbone of the microgrid, the Starboard side bus and the Port side bus. They are connected by two cross-tie disconnect switches. These disconnects are used to connect the two main buses, control flow of energy, maintain voltage levels and to disconnect them as necessary. To ensure control of the above requirements, one of the two cross-ties must be disconnected every moment.

Energy flow in the shipboard system is dictated by the coordination method for the converters. For a zonal system such as this it is desirable to dictate paths of energy flow into each zone and generator loading at the main buses. These flows will be determined by system level objectives in the form of a cost function subject to constraints.

Zonal and main bus level control systems enable flexible routing of energy within the test system. Each zone is managed by a zonal level control with a master-slave sharing scheme. The zonal PCM converter designated as the master for that zone regulates in-

zone voltage while the slave PCM converter tracks a designated percentage of the master converter's output (sharing percentage). System control above the zonal level designates which converter is the master as well as the sharing percentage. Sharing of zonal load by the slave zonal PCM may vary from 0% to 100% depending on the system level optimizer decision. The PCMs connected with the load center are assumed to be unidirectional converters. Control of the system energy flow above the zonal level is accomplished by the main bus level control. Within the main bus level control, a bus-tie controller regulates the total bus-tie current for the sum of all parallel bus-tie branches connecting the two buses. Thus, the system level control can dictate how energy flows into each zone and how energy flows across a bus-tie.

Each zone or load center introduces one variable (sharing variable). Storage as well as Bus-Tie currents also introduce variables into the cost function. These variables determine the role of ESS (either source or load), flow of energy between the main buses through the bus ties, and the sharing into each zone and thereby determine the generators' operating points. An optimization algorithm would be presented that would determine values of these variables dynamically to minimize system loss.

3.2 CERTS MICROGRID

The CERTS microgrid structure assumes an aggregation of loads and microsources operating as a single system. Microsources are power electronic based to provide the required flexibility to insure controlled operation as a single aggregated system. This control flexibility allows the microgrid to present itself to the bulk power system as a single controlled unit, have plug-and-play simplicity for each microsource, and meet the

customers' local needs. Key issues that are part of the microgrid structure include the interface, control and protection requirements for each microsource as well as microgrid

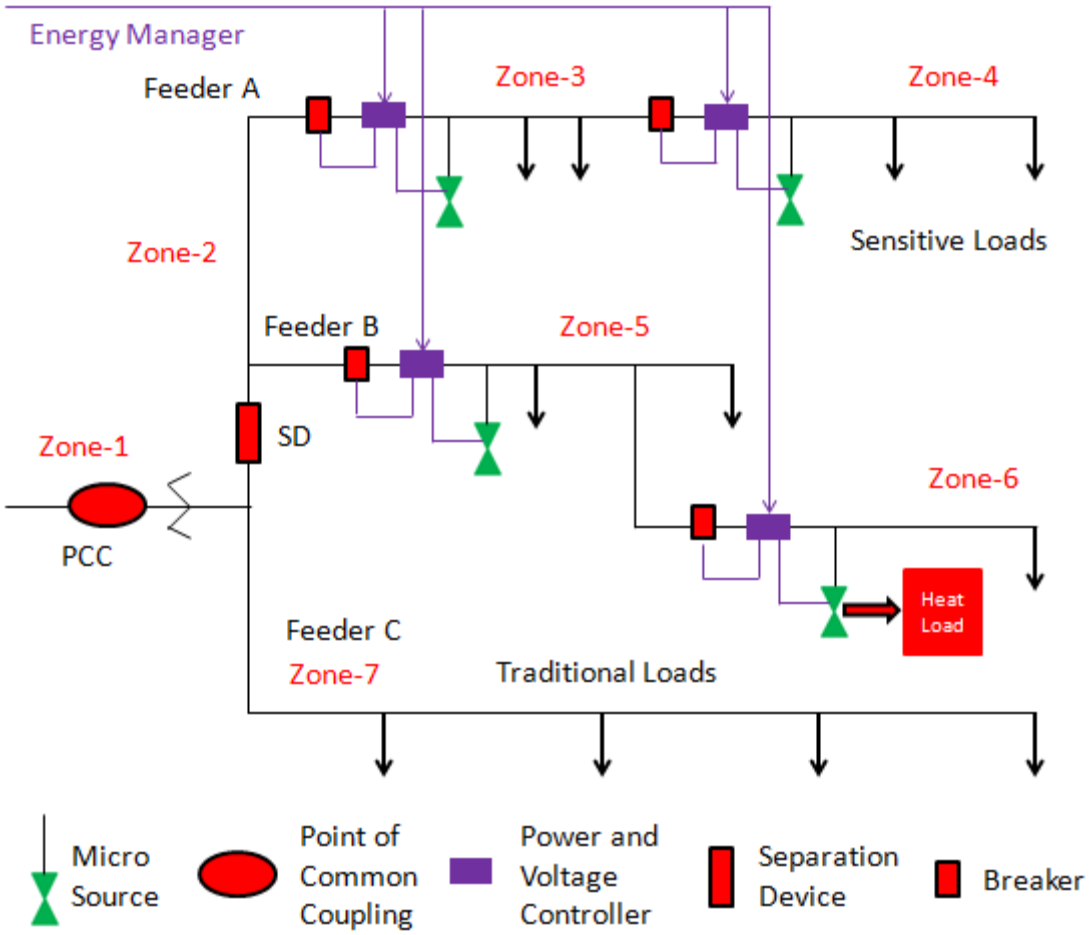

Figure 3.3. CERTS microgrid architecture

voltage control, power flow control, load sharing during islanding, protection, stability, and overall operation. The ability of the microgrid to operate connected to the grid as well as smooth transition to and from the island mode is another important function [1].

The electrical system is assumed to be radial with three feeders – A, B, and C – and a collection of microsources and loads. In Figure 3.3, there are two feeders with

microsources and one without any generation having non-sensitive loads. During disturbances on the bulk power system, Feeders 'A' & 'B' can island using the separation device (SD) to minimize disturbance to the sensitive loads. Of course islanding does not make sense if there is not enough local generation to meet the demands of the sensitive loads. The traditional loads on Feeder 'C' are left to ride through the disturbance. This eliminates nuisance trips of the traditional load when the microgrid islands to protect critical loads. Feeder 'A' & 'B' (Zone – 2, 3, 4, 5 & 6) along with microsources and sensitive loads form the islanded microgrid system. The microsources are either microturbines or fuel cells interfaced to the system through power electronics. The power and voltage controller near each microsource provides the control signals to the source, which regulates feeder power flow and bus voltage at levels prescribed by the Energy Manager. As downstream loads change, the local microsources' power is also changed to hold the total power flow at the dispatched level. Microsource controllers respond in a few milli-seconds. The basic inputs to the microsource controller are set points for power, P, and bus voltage, V. The energy manager is responsible to provide those set points to each microsource controller. The optimization algorithm would work within the energy manager to find out the global optimal set point that would minimize the system loss and ensure overall system efficiency and stability. Feeder 'C' along with the bulk power system gets disconnected while the microgrid runs in islanded mode. According to Figure 3.3, Feeder 'A' & 'B' belongs the same electrical structure. To introduce non-uniformity and for simplicity, Figure 3.4 is the test case that would be discussed later to validate the research objective. Here Feeder 'A' is having a lumped load and a generating system. Feeder 'B' has two lumped loads with two generators.

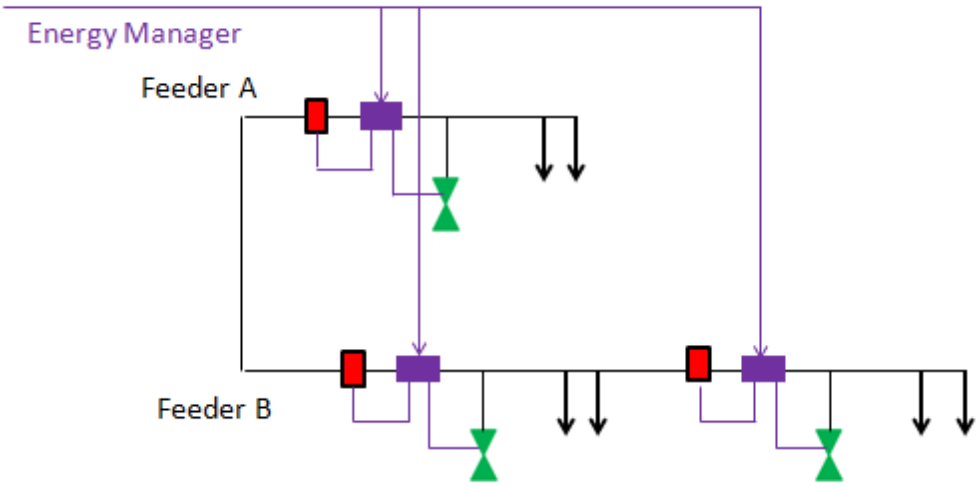

Figure 3.4. CERTS microgrid test case during islanded operation

CHAPTER IV

SYSTEM LOSS OF A POWER SYSTEM AND ITS COMPONENTS

Inefficiency of power system components and heat loss are generally attributed to power system loss. But the actual bulk loss appears from other factors. Generators' set points, impedances and even improper use of storage system cause the largest share of total loss. The most important components of microgrid system losses are briefly discussed in this chapter.

4.1 UNIT COMMITMENT

Unit commitment (UC) aims to schedule the most cost-effective combination of generating units to meet forecasted load and reserve requirements, while adhering to generator and transmission constraints. Generally, UC is completed for a specific time horizon and determines which sources will be operating when. This commitment schedule takes into account the inter-temporal parameters of each generator (minimum run time, minimum down time, ramp rate, notification time, start-up cost etc.) but does not specify production levels. The objective is to minimize the power generation costs while meeting the power demands. The UCP is an important area of research which has attracted increasing interest from the scientific community due to the fact that even small savings in the operation cost for each hour can lead to major overall economic savings.

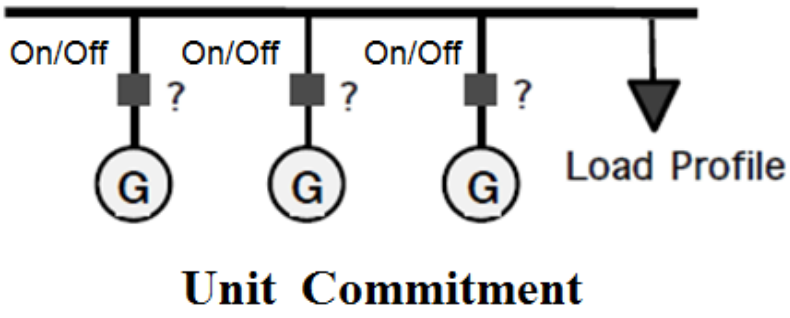

Figure 4.1. Unit Commitment problem

Run/Down time differs significantly over the type of generators. Steam turbine generators have higher run/down time than the gas turbine ones. Start-up cost also varies significantly over the types. In the example microgrid, all the generators are gas turbine based. So run/down times can be ignored. The only parameter that affects commitment for optimization is start-up cost. Unlike steam turbine sources (Steam turbine generators have three levels of start-up costs. They are hot, intermediate and cold start-up cost which takes the shape of step changed discrete values), each gas turbine generator has its own constant start-up cost. Start-up cost has non-zero positive value only when the generator state changes from offline to online [43-44].

4.2 ECONOMIC DISPATCH

Economic Dispatch Problem (ED) has become a crucial task in the operation and planning of power systems. The objective of ED is to schedule the committed generating units output so as to meet the required load demand at minimum cost satisfying all unit and system operational constraints. Improvement in scheduling the unit outputs can lead to significant cost saving.

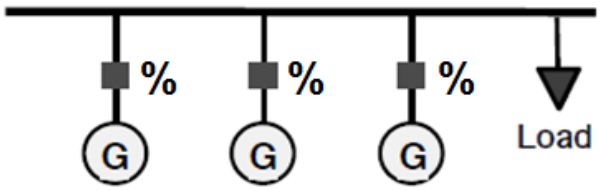

Figure 4.2. Economic Dispatch problem

Efficiency or Fuel Loss factor of any generating system varies over its operating points. Figure 4.3 & Table 4.1 show a typical variation of specific fuel consumption (SFC) in per-unit for a 36 MW MT30 generating system. For this particular curve in Figure 4.3, when the load is 20% of rated power, the specific fuel consumption is about twice the rated SFC [45-46].

Table 4.1. Specific Fuel Consumption of Main Generator

Power (MW)	Power (pu)	SFC (kg/KWhr)
2	0.055555556	0.95
3	0.083333333	0.713
6	0.166666667	0.45
9	0.25	0.356
12	0.333333333	0.313
15	0.416666667	0.275
18	0.5	0.256
21	0.583333333	0.244
24	0.666666667	0.231
27	0.75	0.225
30.5	0.847222222	0.219
33	0.916666667	0.213
36	1	0.206

Efficiency characteristics can be derived from its specific fuel consumption (SFC) data. SFC data provided by the ONR for main generator (gas turbine generator) is shown in Table 4.1.

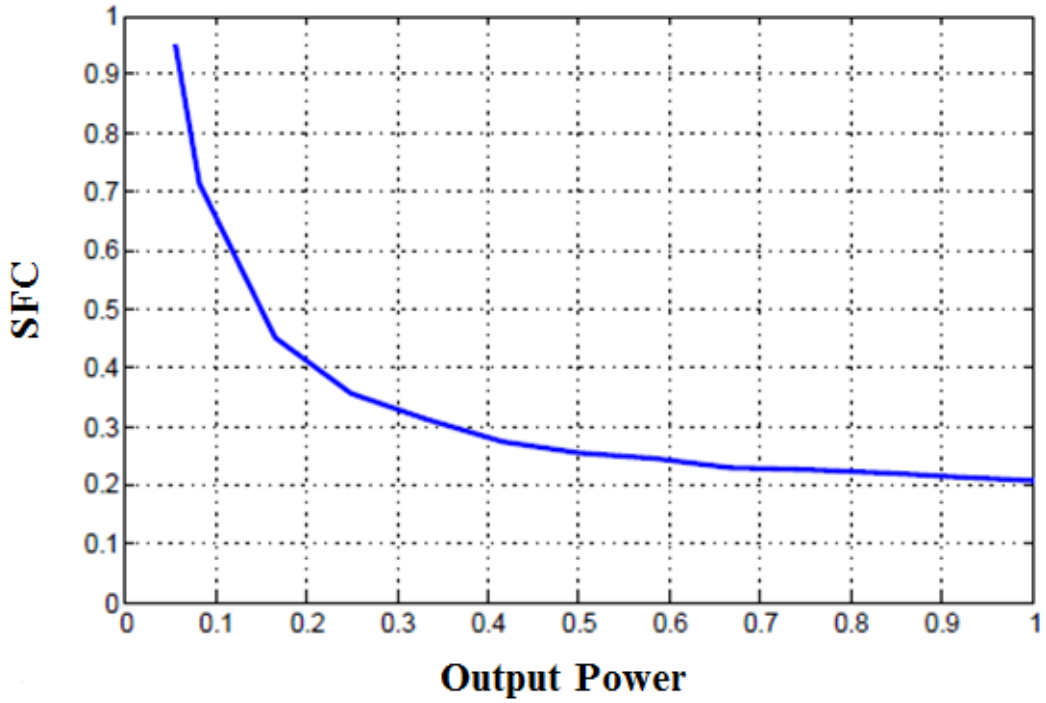

Figure 4.3. Output Power vs Specific Fuel Consumption in p.u. [45]

Heating value of natural gas,

$$HV = 13.8912 \frac{KWh}{Kg} \tag{4.1}$$

Efficiency can be calculated from the given data using the relationship,

$$\eta = \frac{1}{SFC * HV} \tag{4.2}$$

Corresponding fuel loss can be calculated using the relationship,

$$Loss = (\frac{1}{\eta} - 1) * Load \tag{4.3}$$

Operating points and corresponding fuel loss/cost characteristics of the generator can be availed from the data in Table 4.2 & Table 4.3 using 2 degree polynomial trend line.

Table 4.2. Efficiency of the Main Generator

Power (MW)	Power (pu)	SFC (kg/KWhr)	Efficiency
2	0.055555556	0.95	0.075776864
3	0.083333333	0.713	0.100964967
6	0.166666667	0.45	0.15997338
9	0.25	0.356	0.202213543
12	0.333333333	0.313	0.229993678
15	0.416666667	0.275	0.261774623
18	0.5	0.256	0.281203208
21	0.583333333	0.244	0.295032874
24	0.666666667	0.231	0.311636455
27	0.75	0.225	0.319946761
30.5	0.847222222	0.219	0.328712426
33	0.916666667	0.213	0.33797193
36	1	0.206	0.349456414

Table 4.3. Efficiency and Loss of the Main Generator

Power (MW)	Power (pu)	SFC (kg/KWhr)	efficiency	Loss
2	0.055555556	0.95	0.075776864	0.677591111
3	0.083333333	0.713	0.100964967	0.742035467
6	0.166666667	0.45	0.15997338	0.875173333
9	0.25	0.356	0.202213543	0.9863168
12	0.333333333	0.313	0.229993678	1.115981867
15	0.416666667	0.275	0.261774623	1.175033333
18	0.5	0.256	0.281203208	1.2780736
21	0.583333333	0.244	0.295032874	1.393847467
24	0.666666667	0.231	0.311636455	1.472578133
27	0.75	0.225	0.319946761	1.59414
30.5	0.847222222	0.219	0.328712426	1.730174178
33	0.916666667	0.213	0.33797193	1.795590133
36	1	0.206	0.349456414	1.8615872

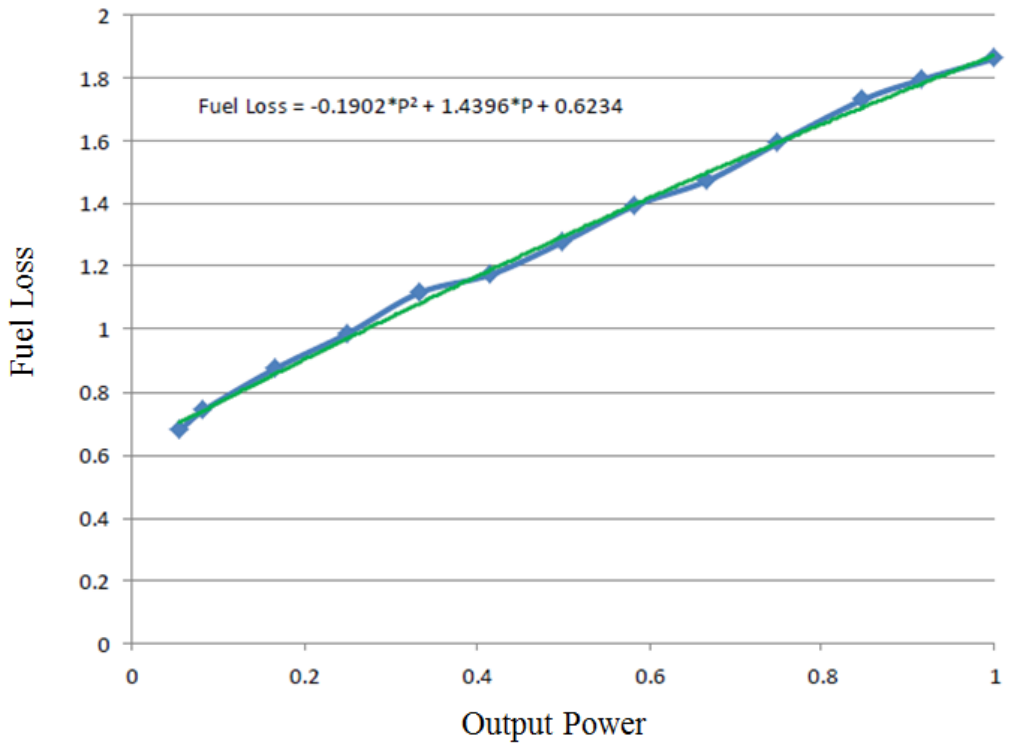

Figure 4.4. Fuel loss characteristics of the Main Generator

Figure 4.4 gives a clear indication (also established by [33]) that cost due to fuel usage inefficiency of an ith generator can be expressed as:

$$C_i = a_i P^2 + b_i P + c_i \tag{4.4}$$

Where ai, bi and ci are turbo-generator dependent constants.

If we assume that the bus-tie impedance of the notional shipboard system is not so significant, cost for the generator systems can be expressed as,

$$C_{gm}(\mathbf{x}) = a_m {I_{gm}}^2 + b_m I_{gm} + c_m \tag{4.5}$$

$$C_{gx}(\mathbf{x}) = a_x {I_{gx}}^2 + b_x I_{gx} + c_x \tag{4.6}$$

Where am, bm, cm, ax, bx, cx are main and auxiliary turbo-generator dependent constants respectively.

The cost function for the system due to fuel usage inefficiency can be expressed as a linear form of the loss components as:

$$C_{fuel}(\mathbf{x}) = C_{gm}(\mathbf{x}) + C_{gx}(\mathbf{x}) \tag{4.7}$$

For overall fuel usage minimization, which is an economic dispatch problem, the weighting of generator loss functions must be equal [47-52].

4.3 DISTRIBUTION LOSS

Distribution or Ohmic loss is the waste of energy due to the impedance of distribution lines. While distribution losses are negligible for a shipboard distribution system virtual impedances can be added to direct energy flow in order to meet operational requirements beyond the fuel cost within the same loss cost function framework.

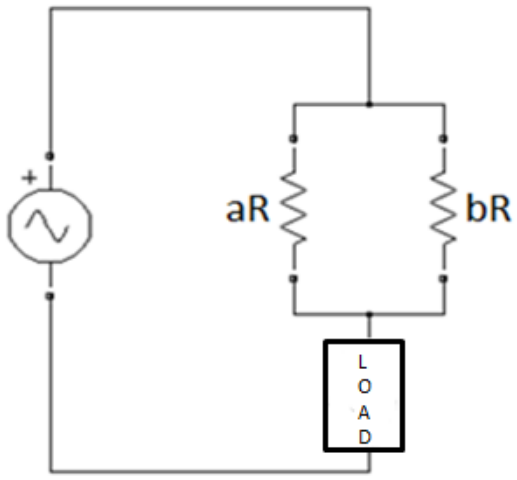

Figure 4.5. Ohmic loss basics

Ohmic loss is a non-linear function of current. Due to its non-linearity, minimization of distribution loss isn't straightforward. A simple electrical circuit is shown in Figure 4.5 to illustrate Ohmic loss problem. Energy can be delivered through both of the ohmic paths 'aR' and 'bR' to the load. Suppose we have the provision to control energy routing through the branches. As distribution loss is a non-linear function of current, optimal solution is not to let the whole energy route through the low impedance path. In real life power system where there are many sources, loads, storages and numerous transmission lines, distribution or ohmic loss minimization itself becomes a complex optimization problem.

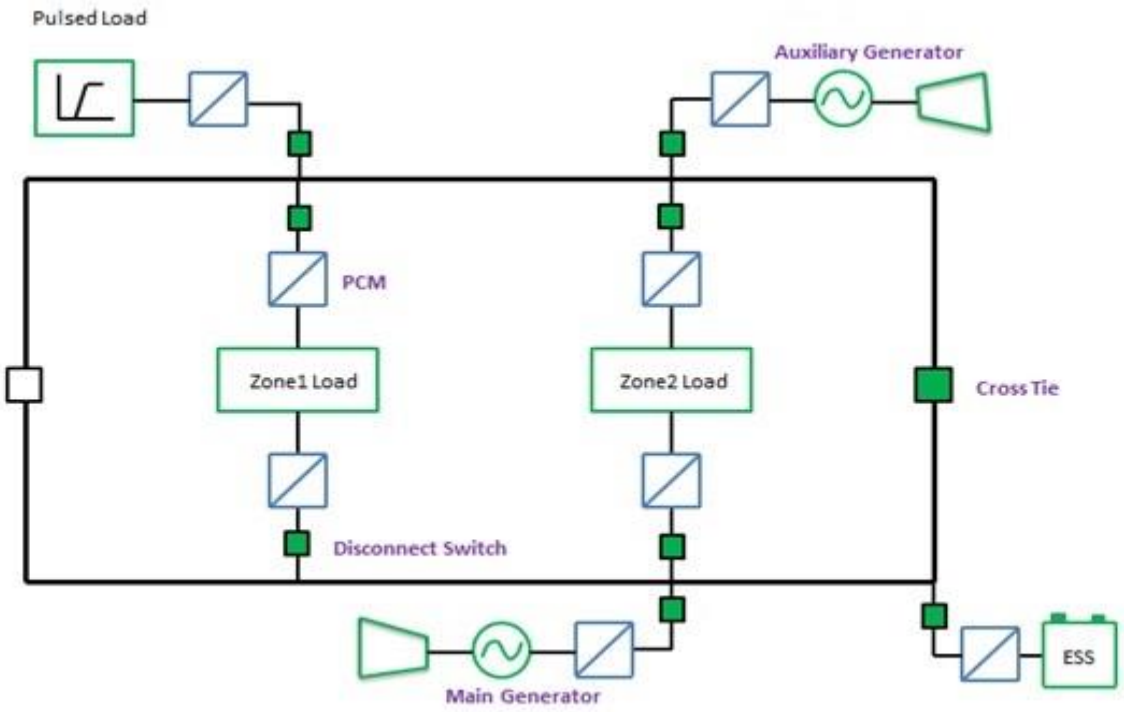

Figure 4.6. Simplified Ship Microgrid

A simpler microgrid with two generators (one main, another auxiliary), one ESS, one Pulsed Load and two zones within the same architecture of the ship system would be

discussed for simplicity. The simplified microgrid in Figure 4.6 covers all the complexities any islanded microgrid can have. Any control algorithm that optimizes this model will equally fit for any other DC microgrid system. Electrical conversion of the example microgrid in Figure 4.6 is shown in Figure 4.7.

Here I_1 is the load of Zone1, I_2 of Zone2, I_5 of pulsed load. I_4 is the maximum charging/discharging current of ESS and I_3 is the maximum allowed cross-tie (inter-bus) current. The variables x, y, z, u are ratios that would determine flow of energy through all the branches and must be optimized by the system controllers in a distributed fashion that would ensure minimal loss of the system. Value of 'x' and 'y' may vary from 0 to 1 with a step size of 0.1; On the other hand, 'z' and 'u' may have any value between -1 to +1 with a step size of 0.2 (as bi-directional). Distribution loss of the mentioned microgrid can be expressed as:

$$\begin{aligned} C_{dr}(\mathbf{x}) &= x^2 I_1^2 (R_1 + R_1' + R_2 + R_2') + y^2 I_2^2 (R_2 + R_2') + z^2 I_3^2 (R_2 + R_2' + R_3) \\ &+ u^2 I_4^2 (R_2 + R_4) - 2xI_1 (I_1 R_1' + I_1 R_2' + I_2 R_2' + I_5 R_1' + I_5 R_2') - 2yI_2 (I_1 + I_2 + I_5) R_2' \\ &- 2zI_3 (I_1 + I_2 + I_5) R_2' + 2xyI_1 I_2 (R_2 + R_2') + 2xzI_1 I_3 (R_2 + R_2') - 2xuI_1 I_4 R_2 \\ &+ 2yzI_2 I_3 (R_2 + R_2') - 2yuI_2 I_4 R_2 - 2zuI_3 I_4 R_2 + \text{Const} \end{aligned} \quad (4.8)$$

where $C_{dr}(\mathbf{x})$ is distribution loss, I_1 is Zone 1 load current, I_2 is Zone 2 load current, I_3 is the maximum allowed cross-tie (inter-bus) current, I_4 is the maximum charging/discharging current of ESS and I_5 is the pulsed load charging current. Variable 'x' controls the flow of energy in Zone1, variable 'y' controls energy routing in Zone2. Variable 'z' determines the amount of energy that needs to be routed through the tie. Variable 'z' may get both positive and negative value to ensure that energy may flow from any bus to the other. Variable 'u' dictates behavior of the ESS. Based on the value of 'u' (positive or negative), ESS may serve as a source or load.

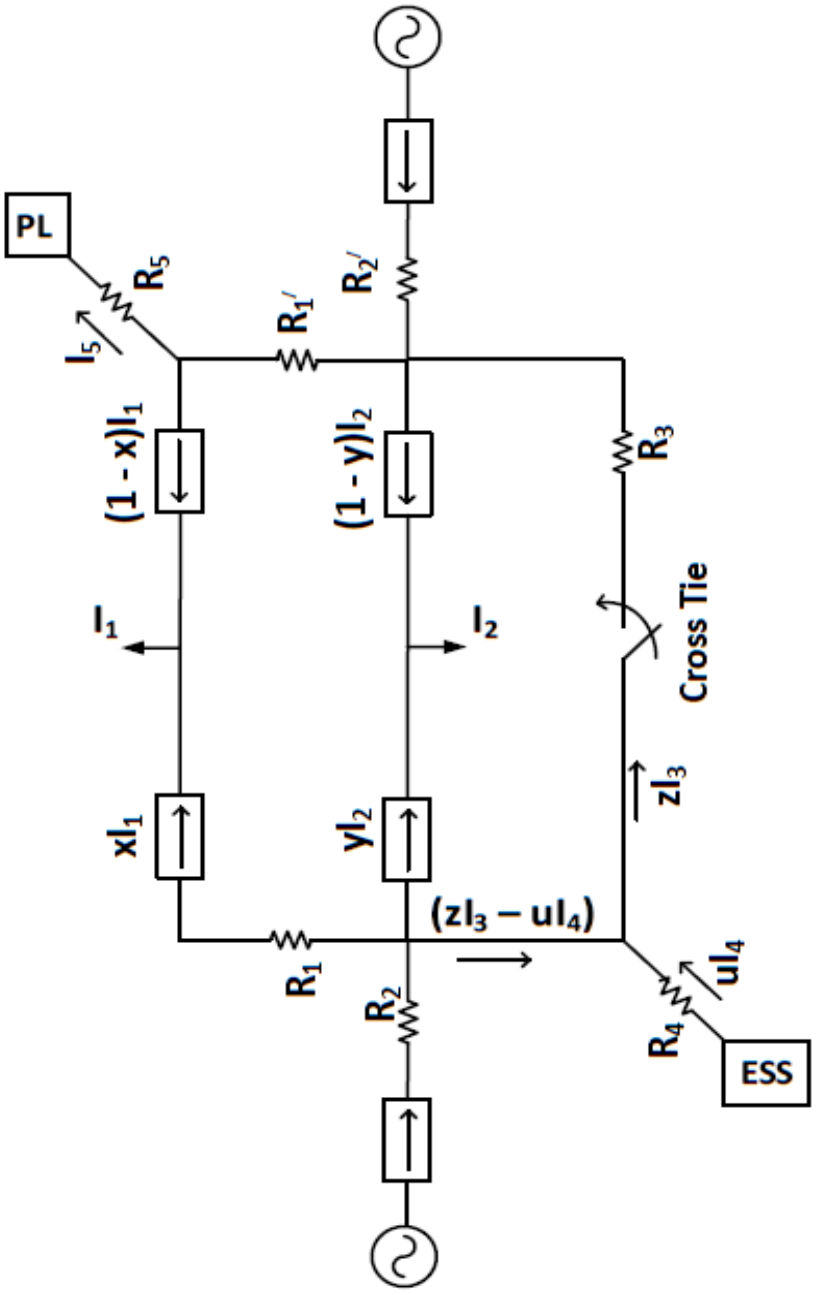

. Figure 4.7. Electrical representation of the simplified ship microgrid

The cost function for the system including fuel and distribution losses can be expressed as a linear form of the loss components as:

$$C_{sys}(\mathbf{x}) = C_{gm}(\mathbf{x}) + C_{gx}(\mathbf{x}) + C_{dr}(\mathbf{x}) \tag{4.9}$$

Supply current limits and ramp rate constraints are

$$g_1(\mathbf{x}) = xI_1 + yI_2 + zI_3 - uI_4 \le (I_{gm})_{\max} \tag{4.10}$$

$$g_2(\mathbf{x}) = (1-x)I_1 + (1-y)I_2 + I_5 - zI_3 \le (I_{gx})_{\max} \tag{4.11}$$

$$g_3(\mathbf{x}) = \Delta I_{gm} \le (\Delta I_{gm})_{\max} \tag{4.12}$$

$$g_4(\mathbf{x}) = \Delta I_{gx} \le (\Delta I_{gx})_{\max} \tag{4.13}$$

where $(I_{gi})_{max}$ denotes the i^{th} generator maximum current and ΔI_{gi} is the rate of change of generator current within the interfacing PCM controller measurement time step.

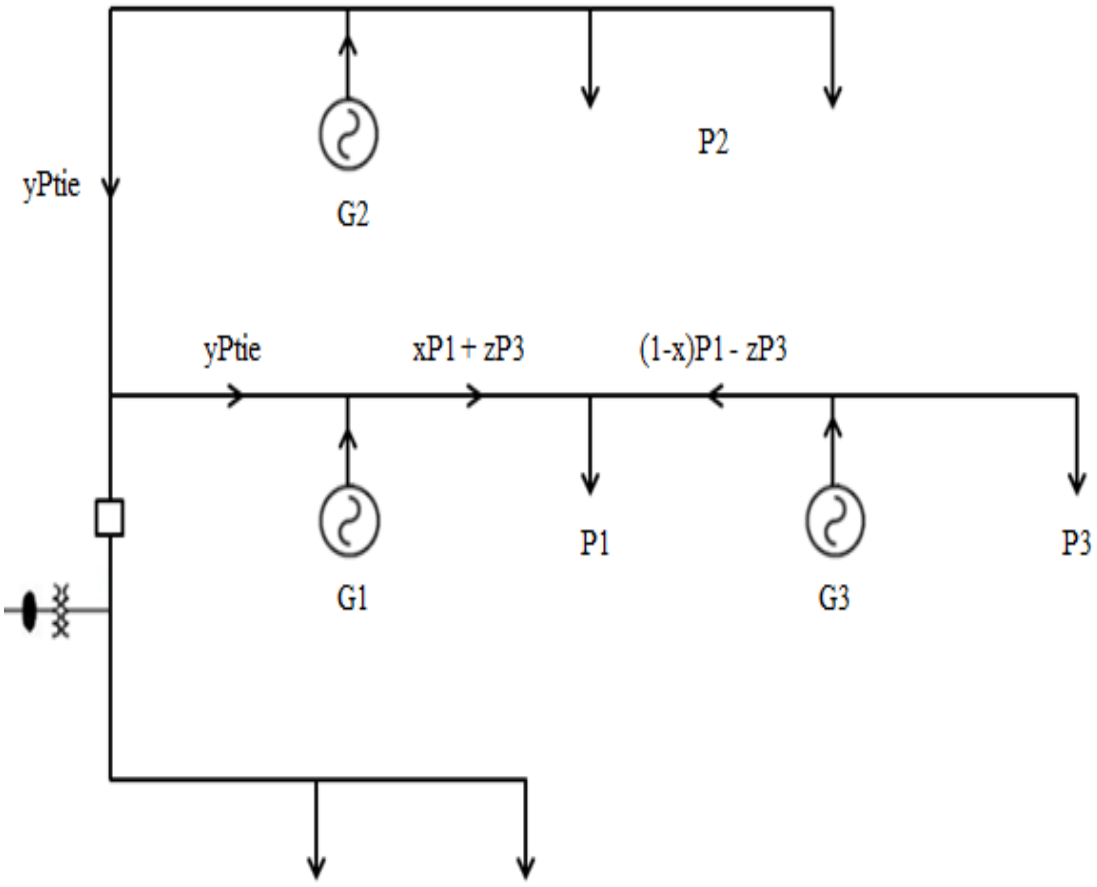

Figure 4.8. Electrical representation of CERTS microgrid test case

Electrical representation of the CERTS microgrid test case is shown in Figure 4.8. Here G1 and G3 have different generation characteristics than G2. P1, P2 & P3 are sensitive loads. Non-sensitive loads are disconnected from the microgrid using the SD to protect the sensitive loads from grid's quality issue.

Generators' fuel usage inefficiency and loss due to line impedances provide similar relations described in Equations (4.4) – (4.8). Cost relations for the CERTS microgrid are described in detail in Appendix B.

4.4 STORAGE SYSTEM LOSS

Static inefficient use of storage system may cause significant loss to the power system. Usually terminal or line impedance of any ESS is much smaller than the distribution system's impedance. So without any intervention storage system appears like an almost lossless source component to the system that always tends to discharge at full capacity in any dynamic system. But we must remember storage gets its energy from others sources which have their fuel cost along with inefficiency characteristics. To address this issue and to ensure most economic use of the ESS, a virtual equivalent fuel consumption impedance is added in series to the terminal resistance R_4 in the Figure 4.7. This virtual impedance changes along with battery SOC. Expression of the battery equivalent fuel consumption virtual impedance is:

$$R_V = (1 - SOC_t) * a \tag{4.14}$$

Here 'a' is the slope by which value of virtual impedance changes. Virtual impedance value is low when SOC is higher. It makes energy from ESS cheaper while fully charged and costlier during low value of SOC [53]. It would have significant effect on the dynamic optimization set points which would be shown elaborately in Chapter VIII.

4.5 OVERALL SYSTEM LOSS

System losses may include many other considerations such as power system components' efficiency, maintenance cost, depreciation etc. Here we would discuss an optimization algorithm that can provide real-time simultaneous solution of Economic Dispatch & Distribution Loss along with dynamic usage of storage system. Unit commitment, maintenance cost, components depreciation is out of the scope of this research objective.

CHAPTER V

OPTIMIZATION ALGORITHM

There are several properties that measure how good a distributed optimization algorithm is. They are: Latency, Convergence, Workload Distribution, Optimality etc. In any real-time dynamic system, latency is one of the most important properties to be dealt with. If a pulsed load appears suddenly and the EMS takes too long time to make decisions, then it may violate the sources' capacity constraints and also the load might not be adequately supplied due to ramp rate limitations. If the algorithm doesn't ensure gradual convergence to global optimal points, then it becomes useless. Distribution of workload can ensure system expandability within time limits [54].

An optimization algorithm has been developed that dynamically determines optimal values of the converter coordinating control variables in a distributed fashion in order to ensure generator system economic dispatch and minimization of distribution loss simultaneously. In any real-time dynamic system, control cycle determinism is one of the most important control system design constraints. Failure of the real-time optimization based system control to converge within the time boundaries means that the system would run with old set points for an indeterminate interval which may violate constraints and destabilize the system. Here the cost function formulation is modified from the initial definition into a framework suitable for a distributed system control. Distribution of workload ensures system expandability within the control system limit.

The granularity of the solution space must be considered for a distributed implementation since distribution of the optimization algorithm requires the use of communication channels. In order to reduce bandwidth requirements the control variables are discretized with a fixed step size. In the example shipboard system values of 'x' and 'y' dictate the zonal PCM sharing ratio and may vary from 0 to 1. They are discretized with a step size of 0.1. The bidirectional variables for bus-tie current and ESS current, 'z' and 'u' may have any value between -1 to +1 with a step size of 0.2.

Optimality and Convergence is guaranteed by this algorithm. If the microgrid has many zonal load centers and number of variables to be dealt with are more, some other pruning techniques like 'reduction of variables', 'sliding' 'check and eliminate' etc. can be adopted that would ensure convergence with sub-optimality.

5.1 SCALING AND CHANGE OF VARIABLES

The objective of this research is to minimize the overall cost/loss of the microgrid. It includes sources' operating cost (fuel cost & cost due to storages' virtual impedance) and distribution loss. Thus the objective function in Equation (4.9) becomes:

$$C_{sys}(\mathbf{x}) = Const + a_{11}x^2 + a_{22}y^2 + a_{33}z^2 + a_{44}u^2 + a_1x + a_2y + a_3z + a_4u + a_{12}xy + a_{13}xz + a_{14}xu + a_{23}yz + a_{24}yu + a_{34}zu \quad (5.1)$$

where 'x', 'y', 'z', 'u' are variables and the rest are load dependent constants.

In Equation (5.1), Loss is a quadratic function where the variables are coupled with each other. As they are not loosely coupled, basic objective function in the straight forward expression is not useful for Distributed Control. This type of problem falls within the category commonly named as 'Mixed Integer Problem' or MIP in short. Depending

on the nature of constraints, MIPs are sub-divided. MIP models with quadratic constraints are called Mixed Integer Quadratically Constrained Programming (MIQCP) problems. Models without any quadratic features are often referred to as Mixed Integer Linear Programming (MILP) problems. MIP models with a quadratic objective function but without quadratic constraints are called Mixed Integer Quadratic Programming (MIQP) problems. As seen in Equations (4.10), (4.11), (4.12) and (4.13), constraints are not quadratic. So our system falls within the category of 'Mixed Integer Quadratic Programming' (MIQP) problem [55-60].

The rate of convergence is enhanced if interaction between the variables can be eliminated or at least reduced by defining new variables in terms of old ones. Changing the scaling of variables to obtain contours circular or parabolic in shape will boost its convergence by enabling the pruning off of a large portion of the search tree. If we assume,

$$z_1 = b_1 x + \frac{k_1}{2} \tag{5.2}$$

$$z_2 = c_1 x + c_2 y + \frac{k_2}{2} \tag{5.3}$$

$$z_3 = d_1 x + d_2 y + d_3 z + \frac{k_3}{2} \tag{5.4}$$

$$z_4 = e_1 x + e_2 y + e_3 z + e_4 u + \frac{k_4}{2} \tag{5.5}$$

where $b_1, k_1, c_1, c_2, k_2, d_1, d_2, d_3, k_3, e_1, e_2, e_3, e_4, k_4$ are load dependent constants, then (5.1) can be redefined as,

$$C_{sys}(\mathbf{x}) = {z_1}^2 + {z_2}^2 + {z_3}^2 + {z_4}^2 = \sum_{i=1}^{n} {z_i}^2 \tag{5.6}$$

In the case of Equation (5.6) it is apparent that $C_{sys}(x)$ is minimized if all 'z_i^2' are minimized independently. Hence the objective is reformulated as n one-dimensional search problem which makes the system distributable and saves a considerable amount of convergence time. In this form, 'z_1' is independent of any other variable and becomes leader to initiate a search tree whereas 'z_2', 'z_3' & 'z_4' acts as consecutive follower.

5.2 SEARCH AND PRUNE

Conversion of the basic variables into 'z_i' domain variables makes them unidirectional interacting. In the basic cost function of Equation (5.1), every variable is coupled and dependent on others; but in the converted cost function in Equation (5.6), this dependency is unidirectional.

All variables are squared in the converted cost function which contributes to total loss in parabolic form. It gives an advantage to prune off a significant number of search trees. Loss due to z_1 is shown in Figure 5.1.

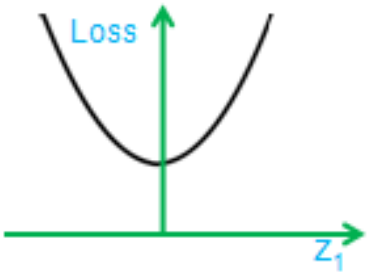

Figure 5.1. Loss due to z_1

As loss due to z_1 is z_1^2, it would always have positive value with a shape of parabola as shown in Figure 5.1. The value of z_1 that makes the loss component minimum is very important, because all lesser values of z_1 would be pruned out.

Figure 5.2. Loss due to pruned z_1

Pruning as shown in Figure 5.2 reduces iteration number significantly and does not introduce any approximation or sub-optimality. Only lesser values of z_1, left to the minimum loss value (depends on the constraint), would be truncated.

Each value of existing 'z_1' would initiate a search tree. This would get another span of 'z_2' values and corresponding loss component for every 'z_1'. Values of 'z_2' would also be pruned as it was done for 'z_1' values and the same would be done for others. The capacity constraint truncates the span of 'z_4' values and negates the need to consider all the available values of 'z4'.

One search tree is shown in Figure 5.3 along with pruning and optimal solution. Dashed line branches are pruned off without introducing any approximation. It provides a significant advantage in computation burden. For example, if there are 4 variables each with 11 steps as in the discussed case:

Number of computation tree without pruning $= 11*11*11*11 = 14641$

Number of computation (around, as observed) tree with pruning $= 4*6*5*1 = 120$

If the number of required operation with the basic cost function is compared, then the reduction is from $(14641*51) = 746,691$ to $(120*11) = 1320$.

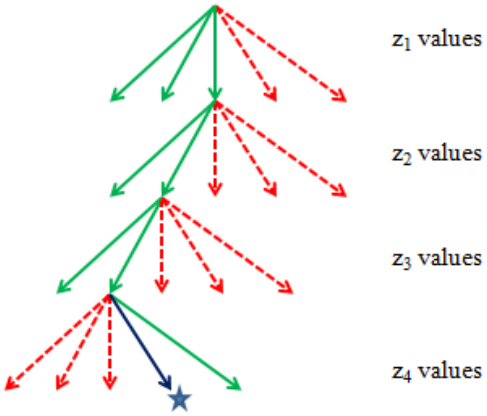

Figure 5.3. Search tree

Thus, this algorithm provides the opportunity to distribute the search tree among the agents with a two-step inter-communication. Each of the agents can solve its part independently without overlapping.

5.3 AGGRESSIVENESS VS SUB-OPTIMALITY

In Figure 5.1 & 5.2, each variable provides clear indication of the optimal cost or loss region. This gives us an opportunity to discard search tree from the opposite region too.

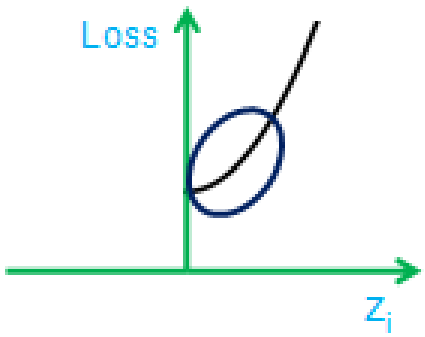

Figure 5.4. Optimal Region

If we do so, we may get closer sub-optimal solution rather than the global optimal. If there were no capacity constraint of the sources, we could have pruned all values other than the ones that provide minimum loss. So it is basically a tradeoff between aggressiveness and sub-optimality. From our observation in simulation, it has been found that the more independent the variable is, the narrower its optimal region becomes.

We can adopt several other attributes which have been found very effective in simulation. 'Sliding' method can reduce the search tree significantly. It extends the pruning area on the next dependent variable (on the left). Suppose we want to slide over z_2. In that case we would consider those values of z_3 that has higher absolute values than those considered for the previous value of z_2. This method has been found very effective though the result isn't always global optimum.

CHAPTER VI

SOFTWARE AGENT AND COMMUNICATION

As mentioned in Chapter I, multi-agent systems (MAS) have been shown to be a viable method for system level distributed control. Thus a MAS framework has been selected to accomplish a communication based implementation of the distributable optimization algorithm presented in Chapter VI. An agent is a software (or hardware) entity that is situated in some environment and capable of autonomously reacting to changes in the environment. Agents are intelligent entities that are capable of communication and are able to alter their behaviors. An agent carries out tasks based on user request and has some intelligence such as choosing optimum strategies to achieve its goals. The concept of agent-hood can be summed up by the following definition:

An agent is a computational entity that,

1) acts on behalf of other entities in an autonomous fashion,
2) performs its actions with some level of proactivity and/or reactiveness,
3) exhibits some level of the key attributes of learning, co-operation and mobility.

A multi-agent system (M.A.S.) is a computerized system composed of multiple interacting intelligent agents within an environment. Multi-agent systems can be used to solve problems that are difficult or impossible for an individual agent. It tends to find the best solution for the problems without intervention, provides enhanced speed and reliability. In other words a multi agent system can be defined as a loosely coupled

network of problem solvers that work together to solve problems that are beyond their individual capabilities. The motivations for the increasing interest in MAS research include the following abilities,

1) to solve problems that are too large for a centralized single agent to do due to resource limitations or the sheer risk of having one centralized system;
2) to enhance speed (if communication is kept minimal), reliability (capability to recover from the failure of individual components, with graceful degradation in performance), extensibility (capability to alter the number of processors applied to a problem), the ability to tolerate uncertain data and knowledge;
3) to offer conceptual clarity and simplicity of design [61-67].

6.1 COMMUNICATION OF THE DISCUSSED ALGORITHM

A simple communication diagram for three agents is shown in Figure 6.1. The number of agents could be equal or less than the number of converters. Load information is collected by the sensors at the converters. If there is any change in system load (Zone1 or Zone2 or Pulsed Load or Battery Condition), new measurement is passed to the agent. Each agent then starts intercommunication, passes its own measurement value to other agents. At this point all the agents have the knowledge of the system. Each agent runs its own algorithm, works individually without any interaction with others to find out its local optimal solution. Local solutions are string of 4 values in the converted 'z_i' domain (for example in the shipboard test system z_1, z_2, z_3, z_4). After getting the local solutions, agents send those local values (string of z_1, z_2, z_3, z_4) to another agent who is responsible to compare and find out global optimal solution. This is a very quick process taking time

in the μs level only. Global optimal solutions which are the optimal value for each 'z_i' are then passed to the individual agents. Agents then convert the 'z_i' domain variable back to plant domain variable and send the command to the converters.

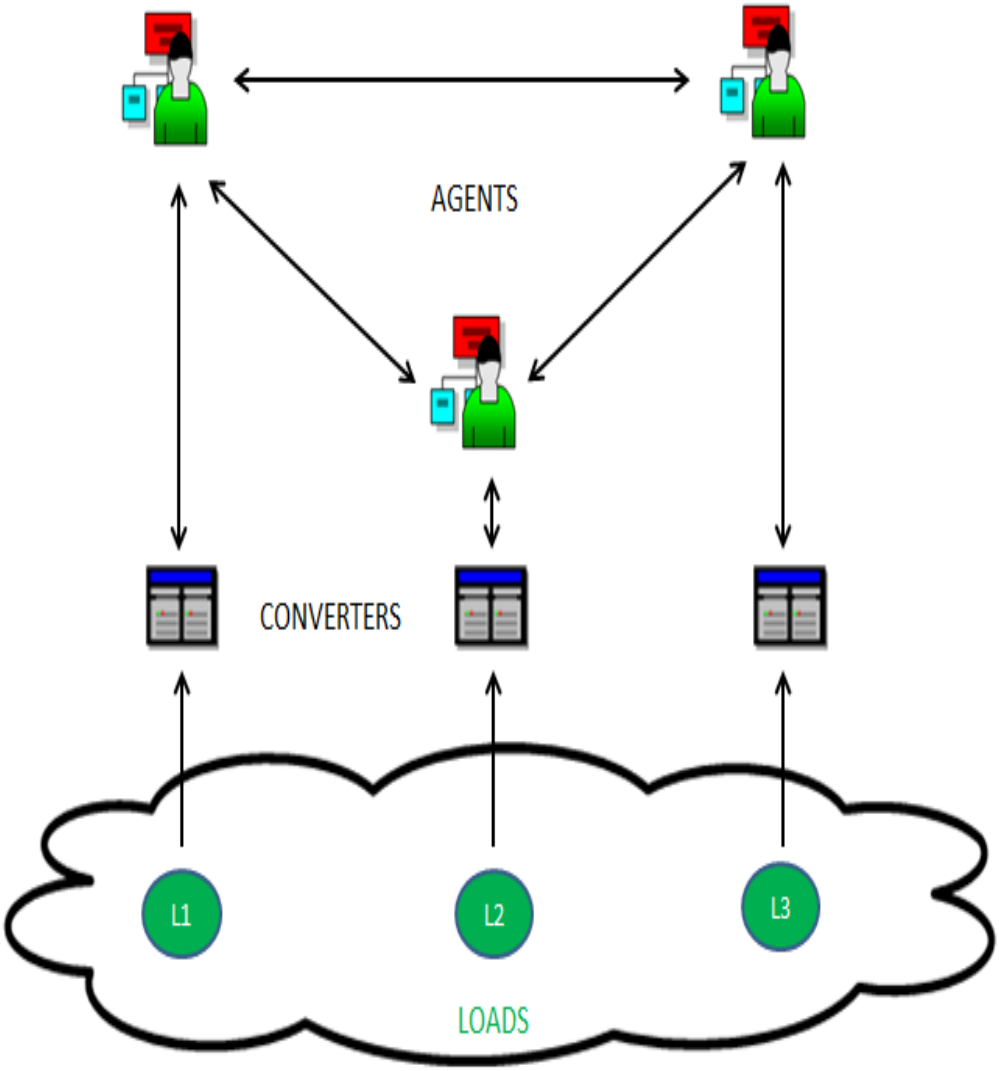

Figure 6.1. Communication design of the control system [35]

Flow diagram of the communication system is shown in Figure 6.2.

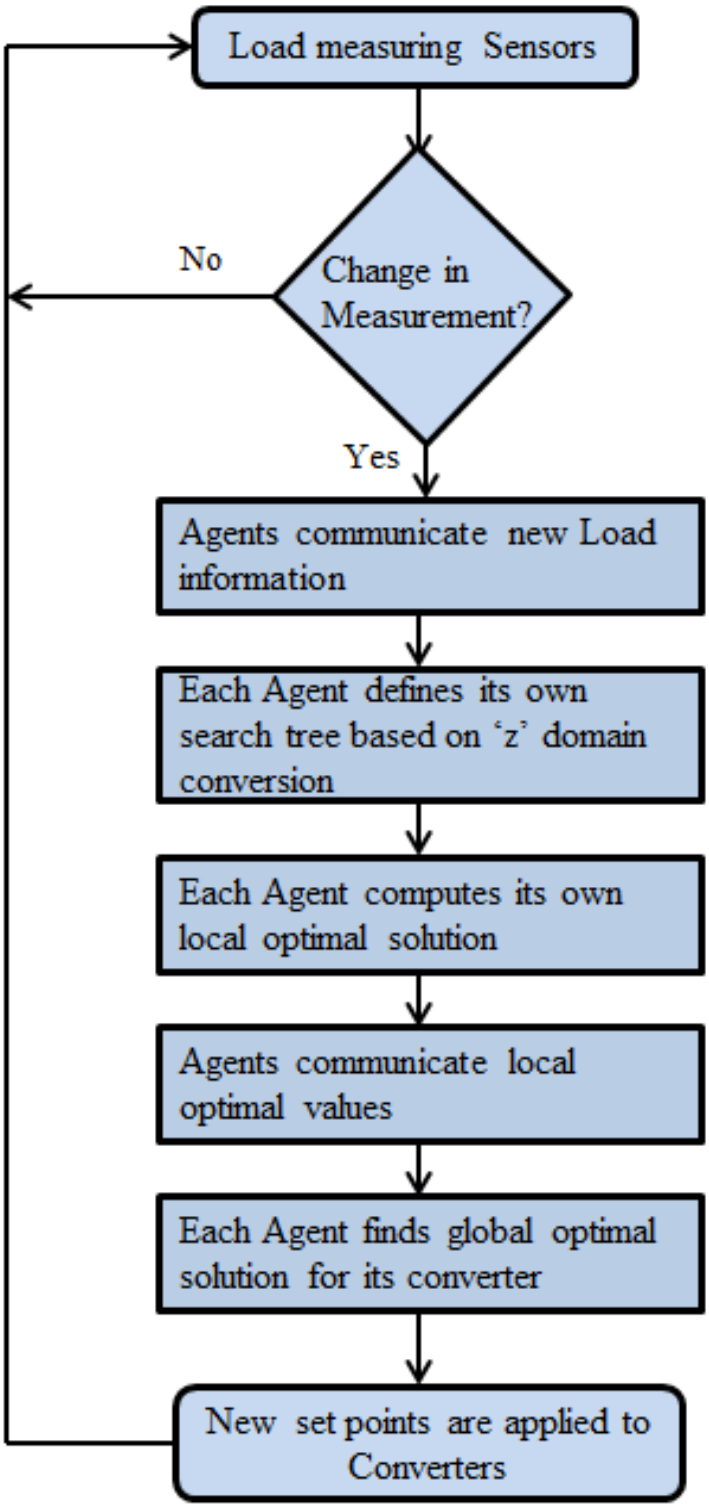

Figure 6.2. Flow diagram of the distributed control

6.2 MULTI-AGENT BASED COMMUNICATION

Communication design of intelligent agent systems for real-time coordination of power converters in microgrid has been extensively discussed in [62]. The authors have highlighted and compared among several methods like Belief-Desire Intention, Facilitator Agent, Publish/Subscribe Technology etc. To manage the coordination among local controllers, a message count is defined and used as a metric value to evaluate system complexity and calculate the upper-time limit for task management. Applying agent technology for optimization and comparing its complexity with the other algorithms using metric values indicate that publish-subscribe technology is one of the most efficient and scalable agent-based solution for each controller action in the case study system.

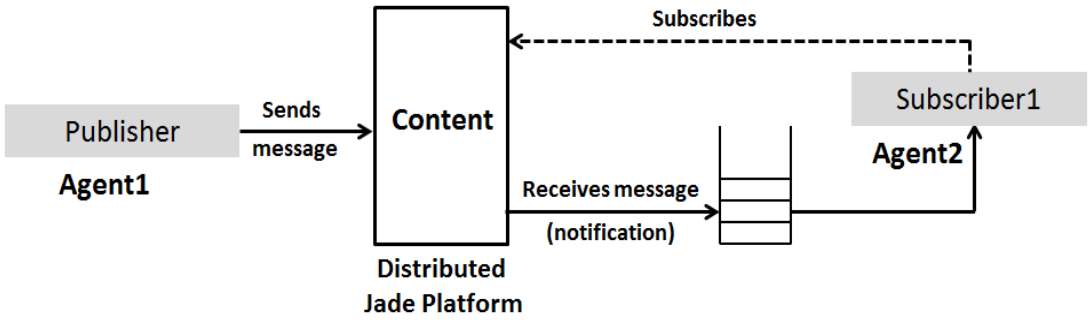

Figure 6.3. Asynchronous message passing paradigm based on content-based publish-subscribe design

Publish-subscribe technology as indicates in Figure 6.3 is a messaging pattern where senders (publishers) program the messages to be sent directly to specific receivers (subscribers) [63]. Subscribers express their interest in some topics or contents in advance and receive only those messages. Publish-subscribe model decouples time, space, and flow between senders and receivers and reduces program complexity and resource consumption.

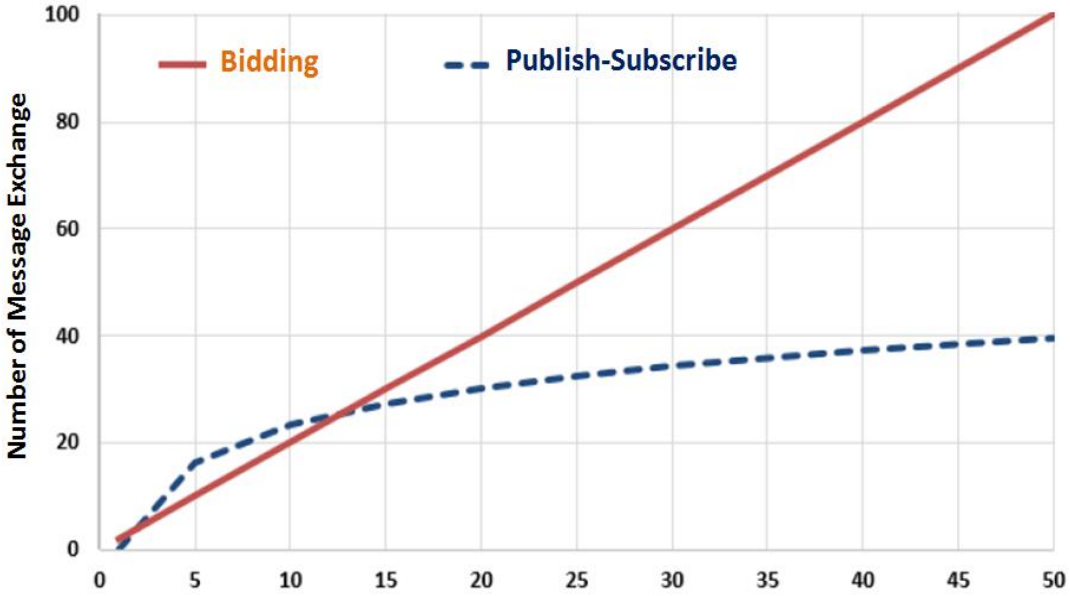

Figure 6.4. Comparison between complexity of bidding and publish-subscribe agent technologies

Figure 6.4 displays a computational comparison between complexities of two agent technologies for a microgrid with a variation from 1 to 50 converters. As seen variable number of converters does not affect the upper-time limits of message exchange in publish-subscribe model compared to one of the most used agent technologies known as bidding algorithm. Assuming a network consisting of N nodes, publish-subscribe can route to the numerically closest node to a given key in less than $\log_2{}^b N$ steps under normal operation (2^b is a configuration parameter with typical value 2, and N is the number of nodes). The number of message counts for bidding algorithm is calculated by 2^N which grows faster than publish-subscribe method by increasing the number of nodes. Agent platform is designed using JADE that is compatible with publish-subscribe technology and capable of developing communication with hardware devices and simulators such as MATLAB. In addition, all of the Java libraries are accessible through

JADE that led to increasing its functionality. The adopted communication paradigm is the asynchronous message passing. Receiver (subscriber) agents send messages to supplier (publisher) agents to request a variable. Each agent has a sort of mailbox (the agent message queue) where the JADE runtime posts messages sent by other agents. Whenever a message is posted in the message queue, the receiving agent is notified. A receiver agent which is previously subscribed for a particular content activates an action method to start communication if there is any matching message, while ignoring all non-matching messages.

Figure 6.5 illustrates a high level design of agent-based system where four converters are individually assigned to converter agents who communicate through the agent platform. Converter agents are grouped in two containers based on system design. Two other agents including Directory Facilitator (DF) and Agent Management System (AMS) run in the main container. DF provides a directory who announces which agents are available on the platform. AMS is the only one that is able to create and destroy other agents, destroy containers and stop the platform. Coordinator agent (AgCo) is developed to facilitate communication among Simulink ports and the agent platform, optimized values then return to the Simulink model and converters. All of routing tables are located in AgCo that communicates with the other agents at the beginning and the end of optimization processes.

Figure 6.6 displays the top level flowchart of designing agent based control system simulated using MATLAB. Load values measured by the converter activate the agent model. Consequently the JADE platform creates four individual agents called Ag1, Ag2, Ag3, and Ag4 upon trigger receipt through AgCo. These agents use individual search

trees to optimize values of z_1, z_2, z_3, and z_4. Since all of the agents run simultaneously, they concurrently extract z_i optimization values from input values (current values of Zone1, Zone2, pulsed load and ESS that are represented as I_1, I_2, I_5 and I_4 respectively in Figure 4.7). Subsequently the four agents communicate and exchange data based on publish-subscribe design. After each agent optimization routine has completed, agents with the minimum z_i values locate received data from peer agents. This agent calculates x, y, z, u values and send them back to Simulink through a AgCo. After receiving the confirmation of data delivery, each agent terminates and finishes its life cycle.

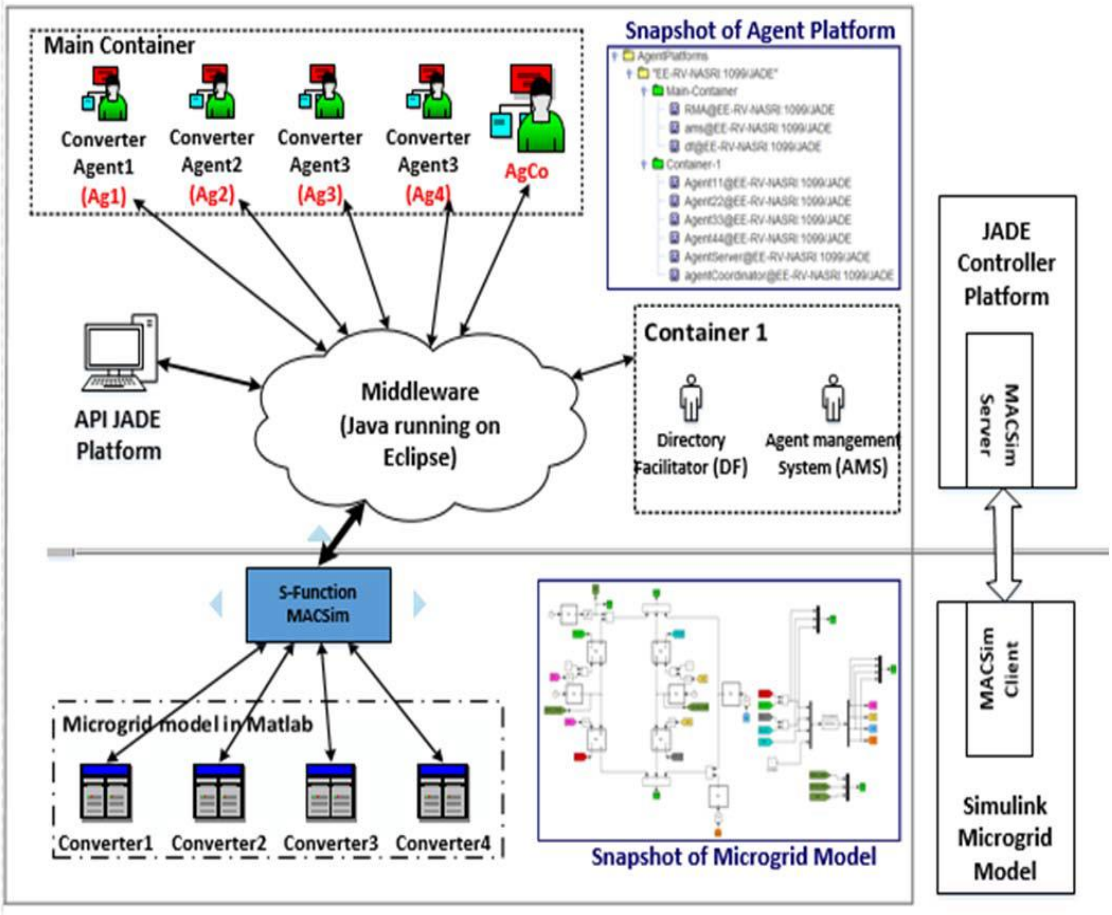

Figure 6.5. Integrated agent-based system including MATLAB model in lower section and JADE platform in upper section, joined using MACSim toolbox

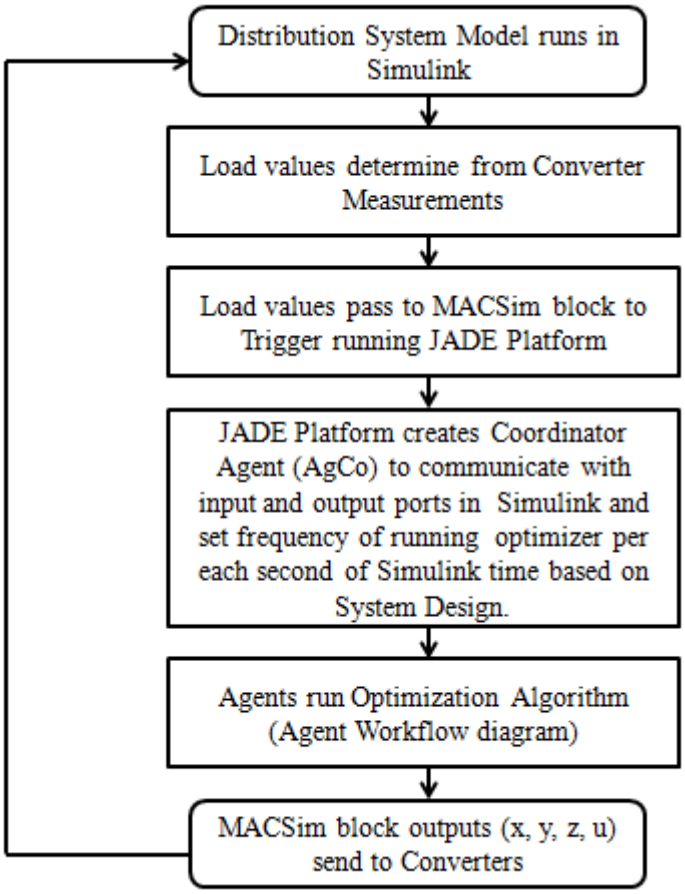

Figure 6.6. Work flow diagram of designing integrated agent-based controller

CHAPTER VII

RESULTS

Simulation results have been obtained for several case studies using the notional DC distribution system and the CERTS microgrid. The algorithm provides optimal set points for the converters which in turn control energy flow through each of the zones, branches, manage inter-bus energy flow, dictates storage behavior and thereby enforce sources' generation settings. Generators impose capacity limits and ramp rate constraints and minimum generation setting to the algorithm. Results would be shown and discussed step by step for the below four different cases:

1) Minimization of Distribution Loss
2) Economic Dispatch and minimization of Distribution Loss simultaneously
3) Economic Dispatch and minimization of Distribution Loss simultaneously considering minimum generation setting
4) System Loss minimization of CERTS Microgrid.

Tests for both the Shipboard system and CERTS microgrid were conducted with the MATLAB Simulink models shown in Figure 7.1 & Figure 7.2. Figure 7.1 shows electrical plant with converters, controllers (Zone1 Control, Zone2 Control, Pulsed Load Control, Battery Control) and the system optimizer. The algorithm for the energy management system runs within the System Optimizer. Outputs of the system optimizer feed the input of the controllers.

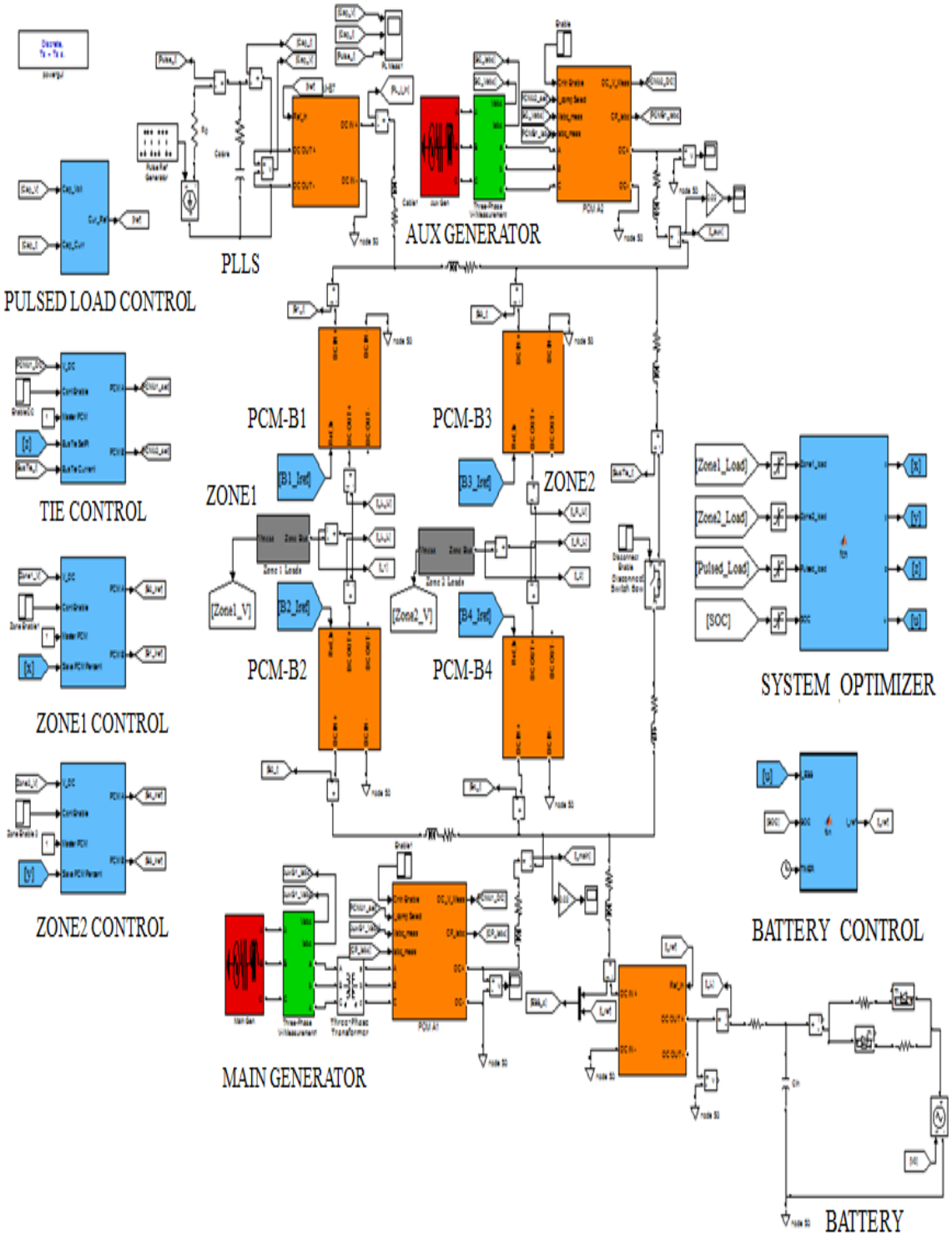

Figure 7.1. Shipboard Power system for the test scenario

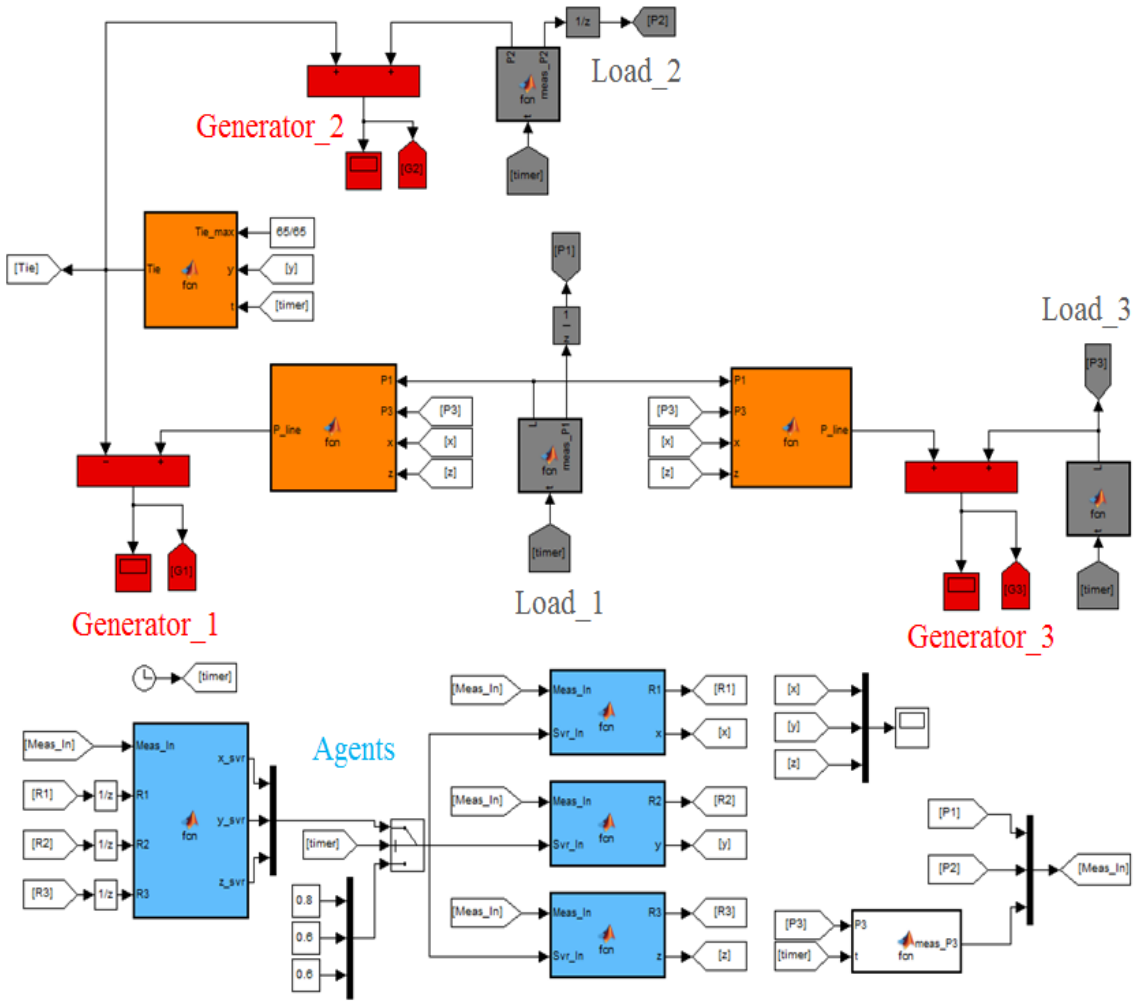

Figure 7.2. CERTS Microgrid for the test scenario

7.1 MINIMIZATION OF DISTRIBUTION LOSS

The first test case minimizes only the distribution losses described by Equation (4.8) with capacity limits and ramp rate constraints. Neither fuel cost nor the minimum generation setting for the generators have been considered in this case. Load profile and corresponding output of the notional Shipboard DC Distribution system is shown is Figure 7.3 and Figure 7.4 respectively. In normal operating condition, any of the two bus-

ties would be disconnected. The following results have been obtained keeping the stern cross-tie disconnect open and the port cross-tie closed.

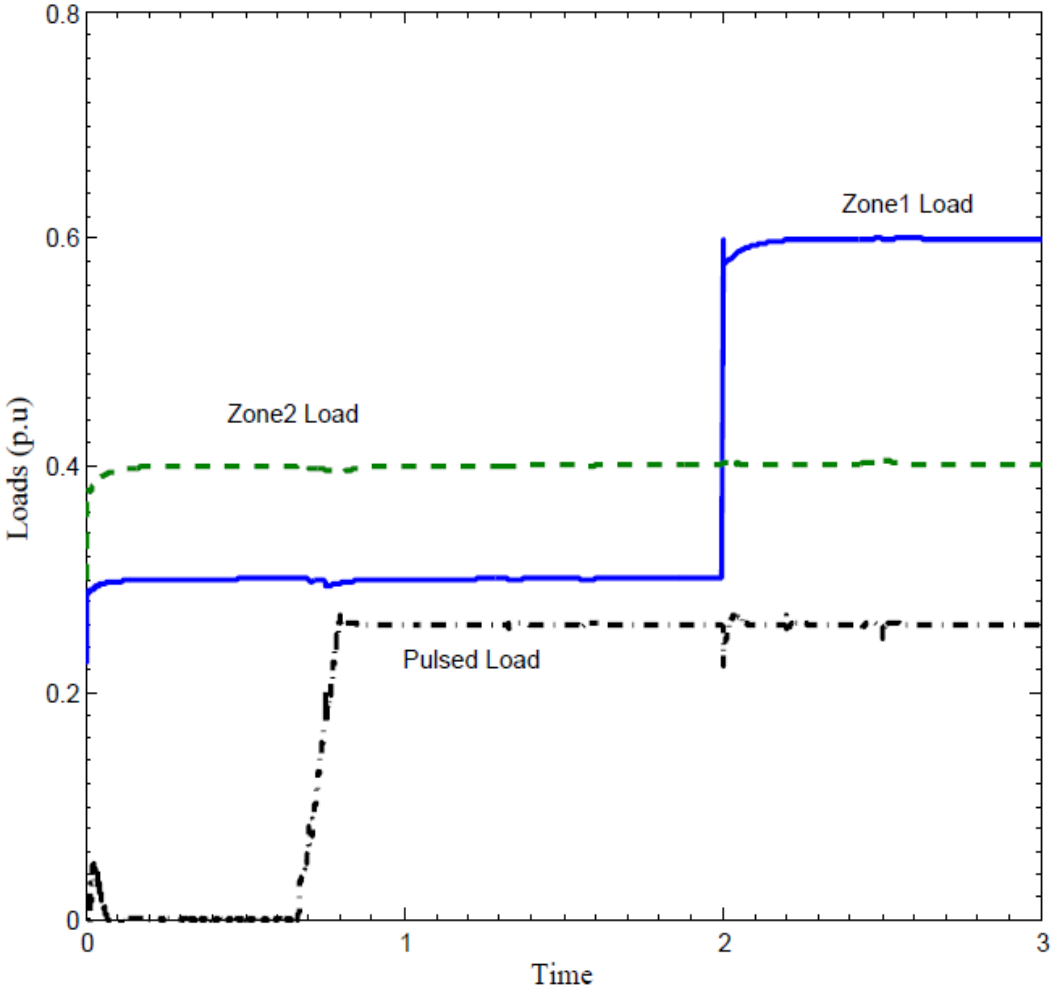

Figure 7.3. Load profiles in the shipboard system for the test scenario

The pulsed load storage system is charged rapidly beginning at time t=0.67s. Due to new loading conditions, the ESS increases its supply and Zone1 sharing variable changes twice to ensure minimum distribution loss. At time t=2s when Zone1 load changes, all system configuration changes. To ensure maximum efficiency, Zone1 sharing variable decreases, Zone2 sharing variable increases, the ESS increases its supply to its maximum

limit and Starboard side bus provides 20% of its maximum allowable inter-bus energy flow to the Port side bus.

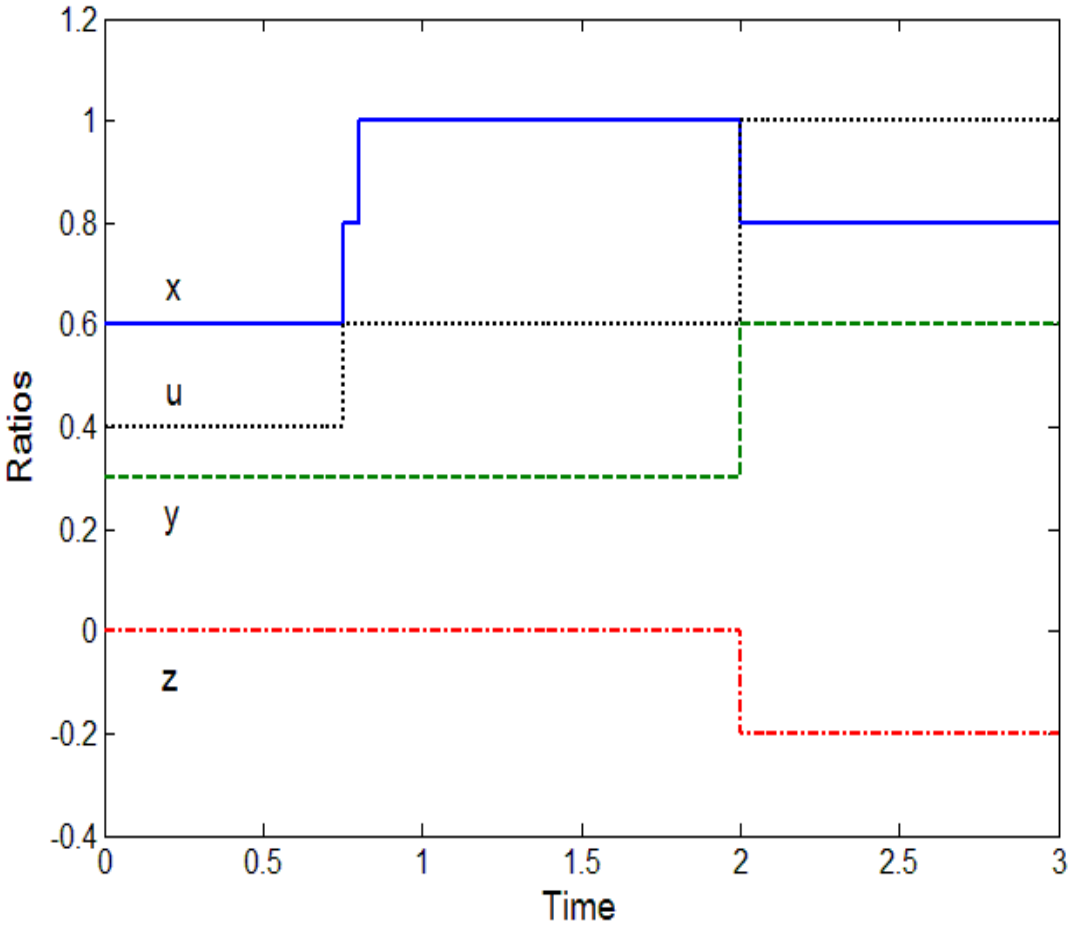

Figure 7.4. Converter operating points for minimization of Distribution Loss

Sharing of load between zone1 converters is shown in Figure 7.5. This load sharing is dictated by the value of 'x' (Zone1 ratio). As the value of 'x' increases as shown in Figure 7.4, we see the corresponding change in load sharing in Figure 7.5. At around 0.8 sec when 'x' becomes 1, one converter carries 100% of zone1 load and the other one runs at no load (0% load). Zone1 Load changes at t=2 sec, so does the ratio 'x'. Similar change in load sharing is observed in Figure 7.5.

As seen in Figure 7.4, value of 'y' (zone2 ratio) is 0.3 and it doesn't change until t=2 sec. So PCM-B4 is carrying 30% and PCM-B3 the rest 70% of the Zone2 load till t=2 sec. At t=2 sec, its value switches to 0.6. Zone2 Load sharing exactly follows the new set point. PCM-B4 now carries 60% and PCM-B3 the rest 40% of the Zone2 load.

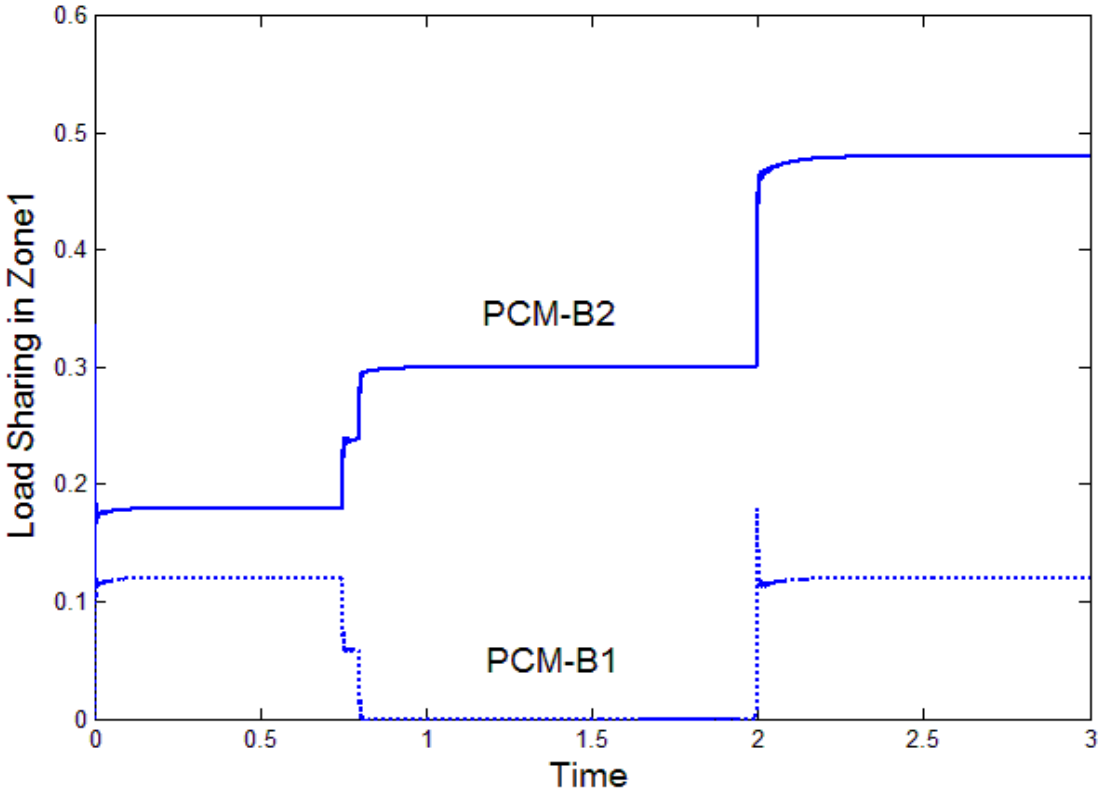

Figure 7.5. Load sharing in Zone1

Generators settings are shown in Figure 7.7. Generators impose capacity limit and ramp rate constraint only (not fuel cost) in the discussed case. That is why Auxiliary generator is providing more energy than the Main generator most of the time. Both of the generators contribute to the charging of the pulsed load local storage. When Zone1 load doubles up at t=2 sec, both of the generators respond to the new set points maintaining the ramp rate limitation.

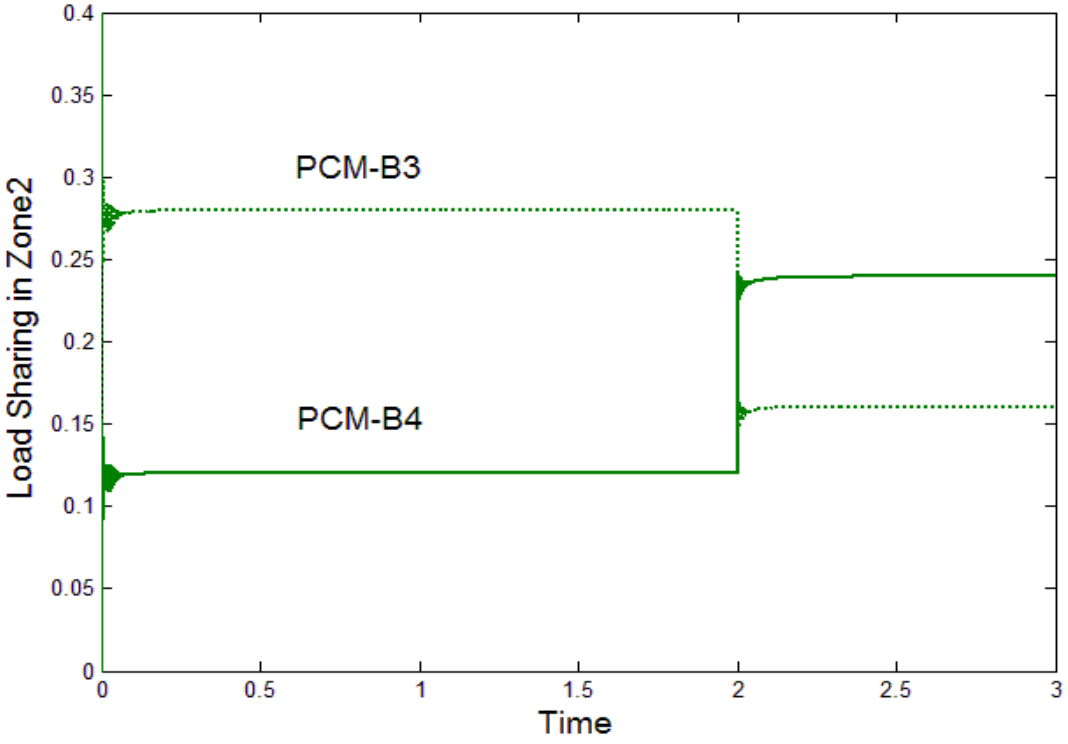

Figure 7.6. Load sharing in Zone2

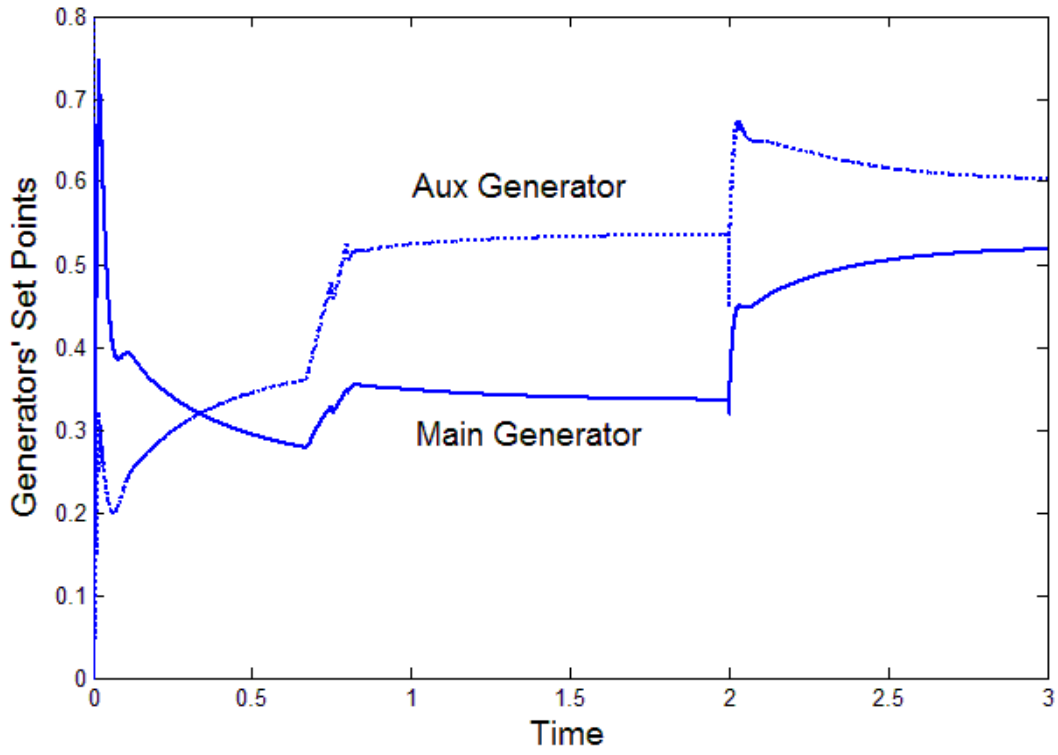

Figure 7.7. Generators' contribution for minimization of Distribution Loss

Zonal voltages have been shown in Figure 7.8. Zone voltages are maintained at 400V DC. We see some minor shifts due to change in loads and operating points which are quickly recovered by the controllers.

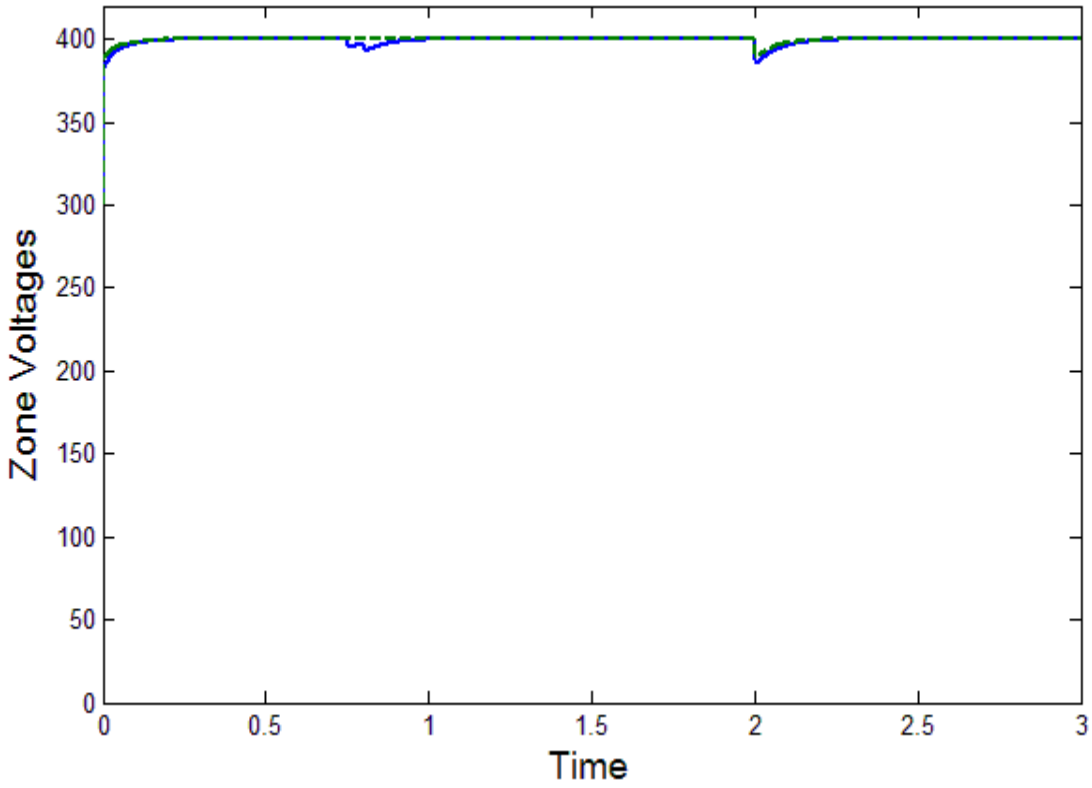

Figure 7.8. Zonal Voltages

7.2 ECONOMIC DISPATCH AND MINIMIZATION OF DISTRIBUTION LOSS SIMULTANEOUSLY

This test case minimizes fuel usage and the distribution losses simultaneously with generators' capacity limits and ramp rate constraints. Fuel usage cost has been extracted from the data at Table 4.3. The same Load profile, used for minimization of distribution loss of the notional Shipboard DC Distribution system, has been used here. It would enable us to visualize clearly the change of the system configurations or set points.

Outputs of the distributed coordinating control system for converter operating points are shown in Figure 7.9. As seen in Figure 7.3 Zone1 load (solid line) is almost 0.3 per-unit until t=2s. It doubles at t=2s. Zone2 load (dashed line) is 0.4 per-unit and it remains unchanged throughout the entire simulation time frame. The pulsed load storage system is charged rapidly beginning at time t=0.67s. The PLLS is in the current control mode of the charging cycle shown in Fig. 4.2.

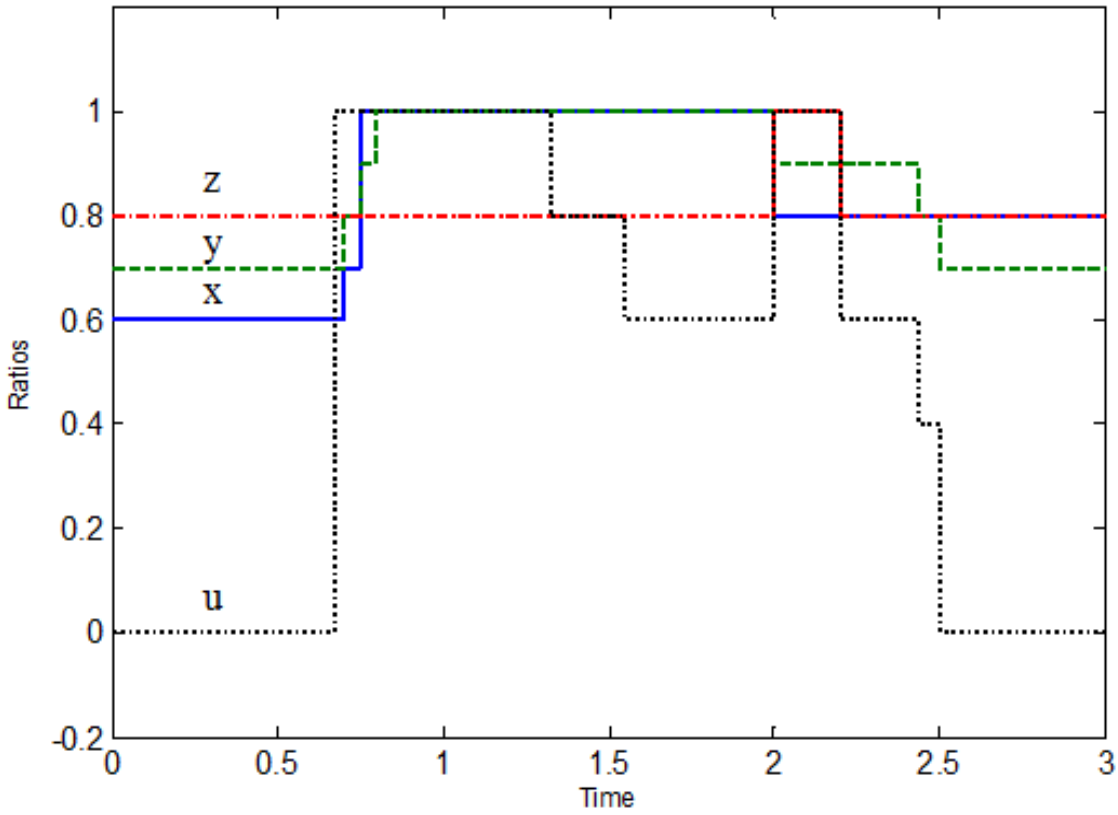

Figure 7.9. Converter operating points dictated by the system control

Outputs of the system control, shown in Figure 7.9, correspond to the control variable labels of Figure 4.7. Initially the Storage system is kept idle until the PLLS begins the charging mode. Optimal value of 'x (solid line in Figure 7.9)', 'y (dashed line)' and 'z

(dash-dot line)' ensure economic dispatch of the fuel based sources and minimum distribution loss of the microgrid simultaneously. As the PLLS begins charging at t=0.67s, several set point changes are observed until the system loads comes to fixed values at t=0.77s. Though both of the zonal loads remain unchanged during this period, both zonal settings change to ensure minimum system loss during this period. ESS set point steps to its maximum as it has very low inertia and enables enforcement of ramp rate constraints when the PLLS charging cycle begins. After t=0.77s, there is no change in system load until t=2s. Still several changes in the ratio values can be observed. This is because of the cost of ESS varies with respect to the change of its SOC. ESS current and SOC are shown in Figures 7.10 & 7.11. The controller keeps track of the battery SOC and corresponding change in the cost function by modification of a virtual resistance at the coupling point of the ESS to the system. The virtual resistance is added to R_4 in Figure 4.7. During low SOC values, which results in higher values of cost by increase of R_4, it becomes optimal for the system to reduce ESS participation. Due to change in Zone1 load starting at t=2s, all of the system variables change to ensure minimum cost within the constraints. At this point there is sudden rise of ESS participation despite low SOC to support generators' ramp rate limitations. At t=2.5s, ESS stops to source any energy as it reaches its lower SOC boundary.

Generators settings are shown in Figure 7.12. Before t=0.67s, the main generator sources all the demand of the system. During this period, ESS is idle and it becomes more efficient to run the main generator only. As the PLLS charging begins at t=0.67s, auxiliary generator just starts to contribute whereas main generator's contribution changes along with the sharing of ESS and keeping ramp rate constraint met. As Zone1

load doubles up at t=2s, contribution from both of the generators keep rising smoothly. As ESS stops to source any demand at t=2.5s due to its lower SOC limit, that energy must be supplied by other sources. The balance is fully supplied from the Auxiliary generator as the Main generator has already reached its full load condition.

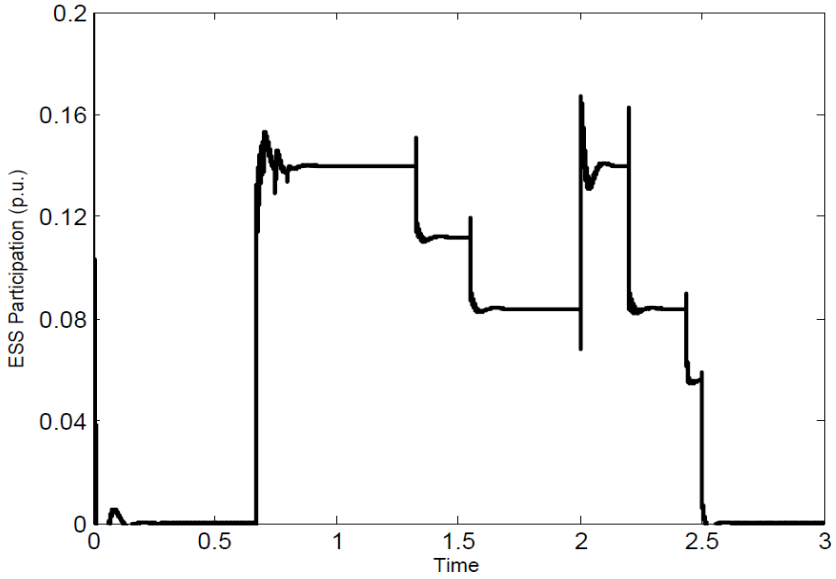

Figure 7.10. Power contribution of ESS due to different loading conditions in the shipboard system

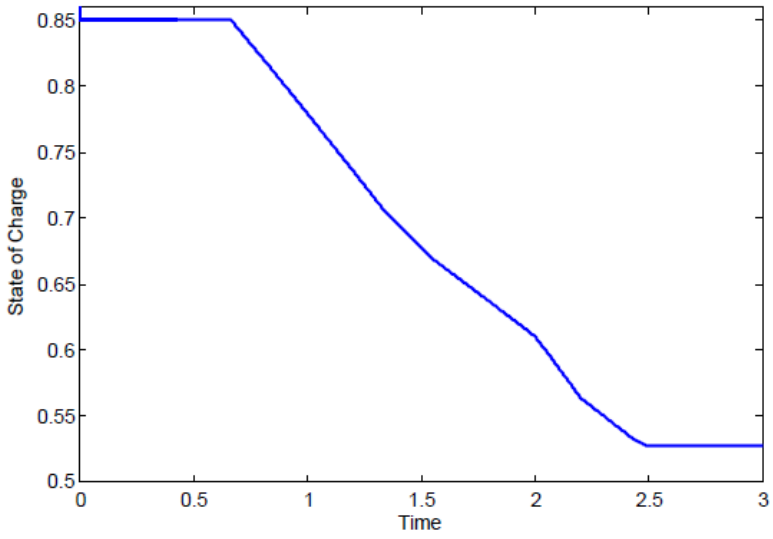

Figure 7.11. Change of SOC due to discharge of the ESS

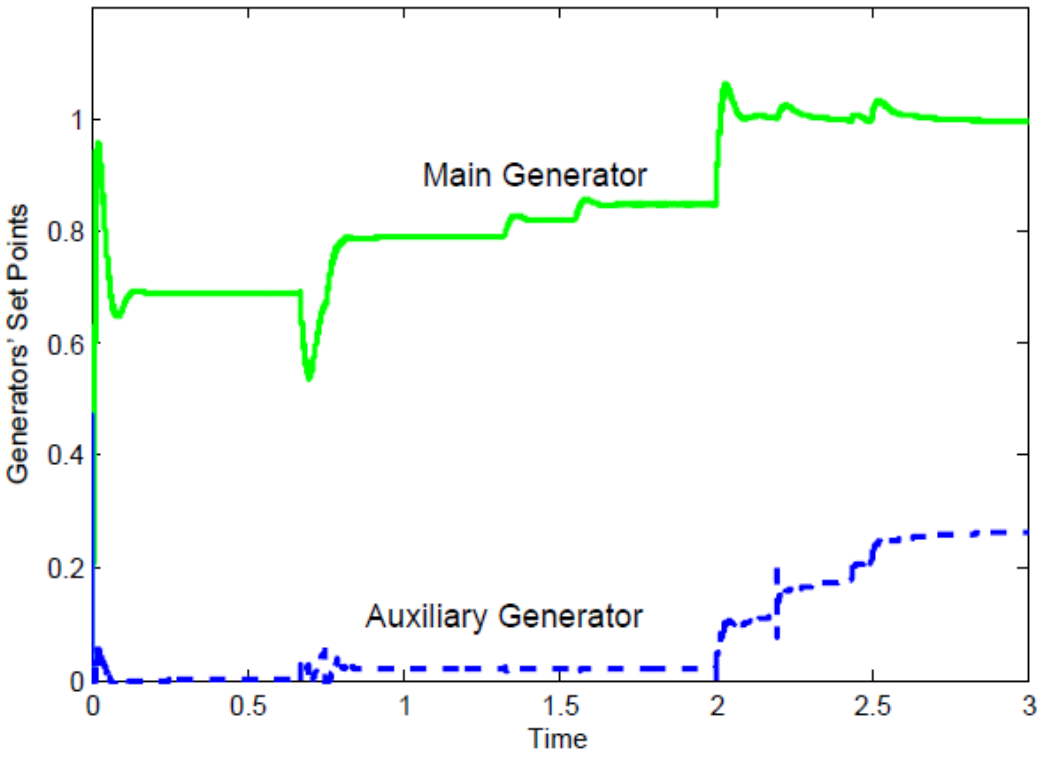

Figure 7.12. Generators' contributions in the shipboard system

All these generator set points come indirectly from the optimal converter setting due to dynamic loading condition so that the system cost is always minimum. It would save a good amount of fuel/cost than using traditional source or converter rating based power sharing. Comparison of loss due to dynamic optimization vs traditional rating based energy sharing has been plotted in Figure 7.13. Rated capacity of the Main generator has been considered as the base for this discussion. The solid line stands for the actual loss in p.u. due to Optimization based coordination (neglecting virtual resistance), dashed line stands for the loss in p.u. due to Optimization based coordination considering virtual resistance and the dashed-dot line stands for the loss due to traditional rating based equivalent sharing. Cost incurred due to the set points during t <= 0.67s is slightly more

than 1.5 per unit. If the same load had been supplied using sources' and converters' rating based equivalent sharing where Auxiliary generator contributes 60% of the Main generator, zonal converters share equally and ESS contributes only to buffer the sources' ramp rate limitation, it would cause loss to be around 1.9 p.u. So the optimization based sharing has the potential to save almost 25% of the loss by using the dynamic distributed algorithm.

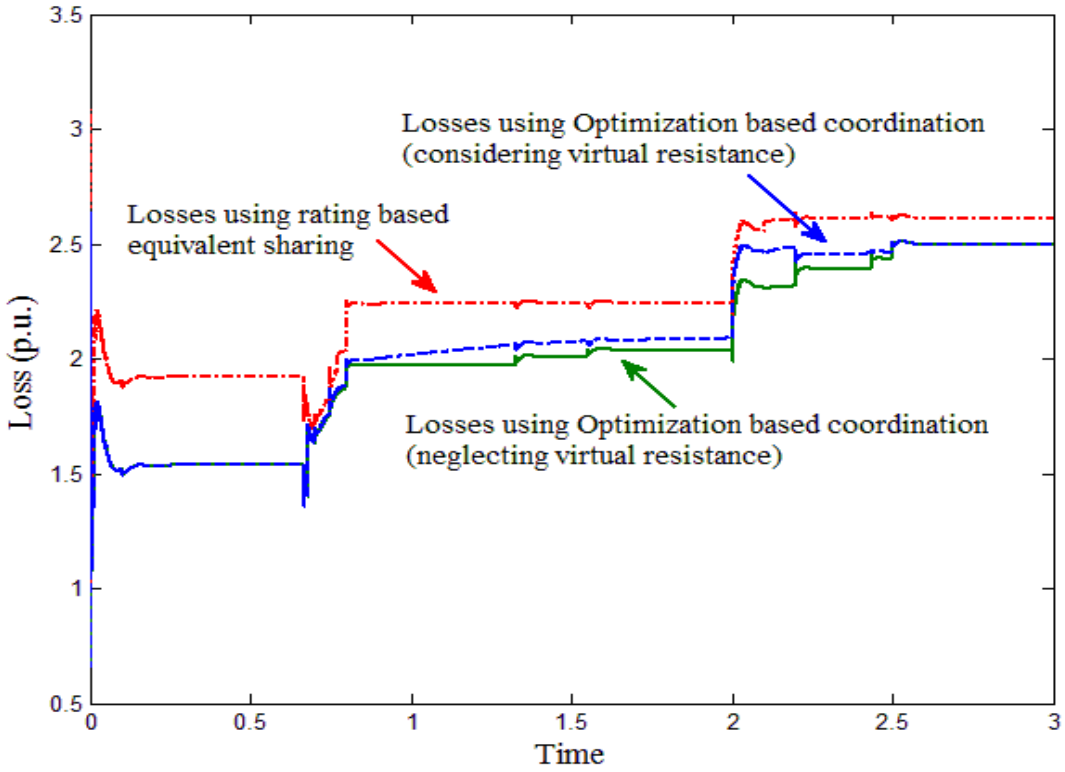

Figure 7.13. Comparison of loss due to dynamic optimization vs rating based sharing

After the pulsed load saturates at t=0.77s, a continuous increase in dynamic loading cost considering virtual resistance is observed until t=2s. This is due to continuous change of battery SOC and corresponding increase of the virtual battery resistance. After t=2.5s, both of the Optimization based sharing curves merge as the battery is offloaded at

that period. Optimization based coordination saves a significant amount of loss throughout the simulation time.

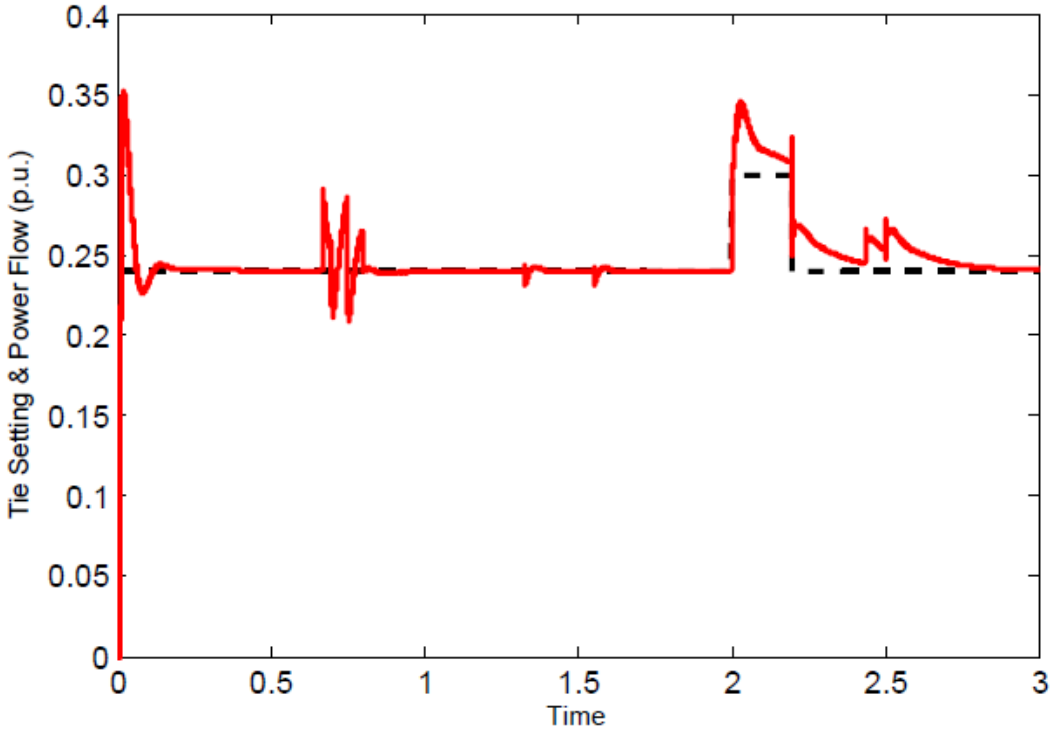

Figure 7.14. Bus cross-tie current

Figure 7.14 shows flow of energy from one bus to the other through the tie. As seen in Figure 7.9, the value of 'z' (dash-dot line) is 0.8 until t=2s. The positive value indicates that energy is flowing here from the bus connected to the Main Generator to the bus connected to the Auxiliary Generator.

Load current sharing between the PCMs that supply Zone 1 and Zone 2 are shown in Figure 7.15 & 7.16 respectively. The solid line stands for the master PCM and the dashed line for the slave. Load currents follow control variables as expected. For example, the value of Zone1 sharing variable 'x' is 0.6 up to t=0.67 sec. Thus, one converter is sharing

0.18 per-unit and the other 0.12 per-unit of the load current. The value of Zone 2 sharing variable 'y' is 0.7 up to t=0.67 sec. and master converter is sharing 0.28 per-unit and the slave 0.12 per-unit of load current.

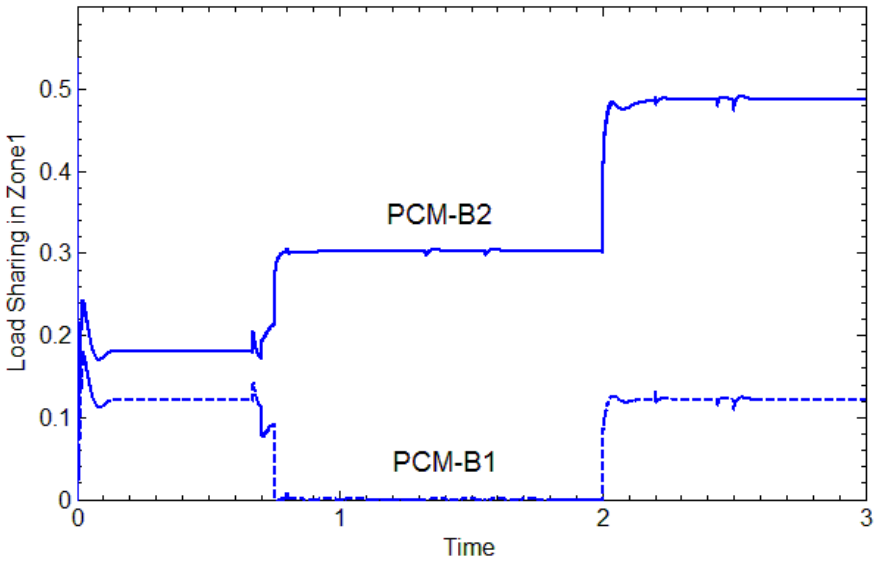

Figure 7.15. Load sharing in Zone1

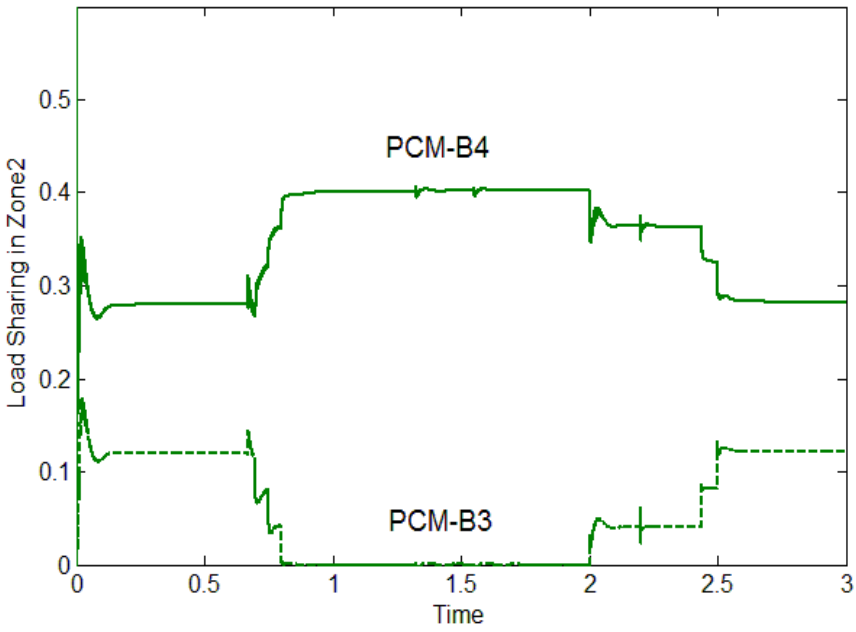

Figure 7.16. Load sharing in Zone2

7.3 ECONOMIC DISPATCH AND MINIMIZATION OF DISTRIBUTION LOSS SIMULTANEOUSLY CONSIDERING MINIMUM GENERATION SETTING

This test case minimizes fuel usage and the distribution losses simultaneously considering generators' capacity limits, ramp rate constraints and minimum generation settings. A minimum generating set point has been considered on the Main Generator as an added constraint. In power industry, even in the case of Hybrid Electric vehicle, fuel based generating system has minimum loading set point. Load profile used for Economic Dispatch and minimization of Distribution Loss simultaneously considering minimum Generation setting is shown in Figure 7.17.

Outputs of the control system for converter operating points are shown in Figure 7.18. As seen in Figure 7.17, both Zone1 load (solid line) and Zone2 load (dashed line) are 0.6 per-unit until t=1.8s. Then Zone1 load changes to 0.2 per-unit and remains unchanged the entire time frame. Zone2 load changes twice, once at t=1.8 sec to 0.5 per-unit and then at t=2.2 sec to 0.2 per-unit. The pulsed load storage system is charged rapidly beginning at time t=0.67s. The PLLS is in the current control mode of the charging cycle.

Outputs of the system control, shown in Figure 7.18, correspond to the control variable labels of Figure 4.7. Optimal value of ‘x (solid line in Figure 7.18)’, ‘y (dashed line)’, ‘z (dash-dot line)’ and ‘u (dotted line)’ ensure economic dispatch of the sources and minimum distribution loss of the microgrid simultaneously. As the PLLS begins charging at t=0.67s and cost of energy from the ESS keeps increasing, several set point changes are observed before the zonal load changes. This is because of the cost of ESS varies with respect to the change of its SOC. ESS current and SOC are shown in Figure 7.19 & 7.20. As the SOC decreases which results in higher values of cost by increase of

the virtual impedance to R4, it becomes optimal for the system to reduce ESS participation.

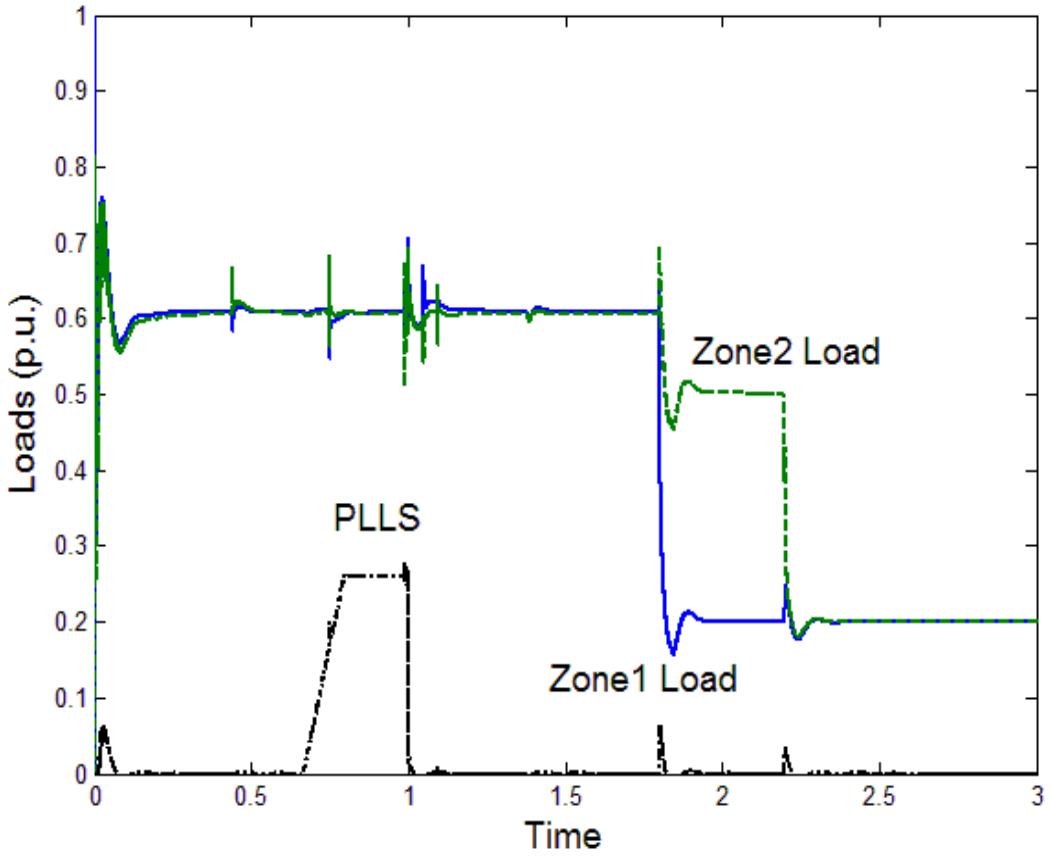

Figure 7.17. Load profiles in the shipboard system for the test scenario

Due to change in both Zone1 and Zone2 load at t=1.8s, all of the system variables change to ensure minimum cost within the constraints. At this point there is sudden rise of ESS participation despite low SOC and higher corresponding impedance because it becomes more efficient to increase bus-tie energy flow. At t=2.2s, ESS starts to respond as a load and charge itself with the additional energy that the Main Generator is producing due to its minimum generation setting.

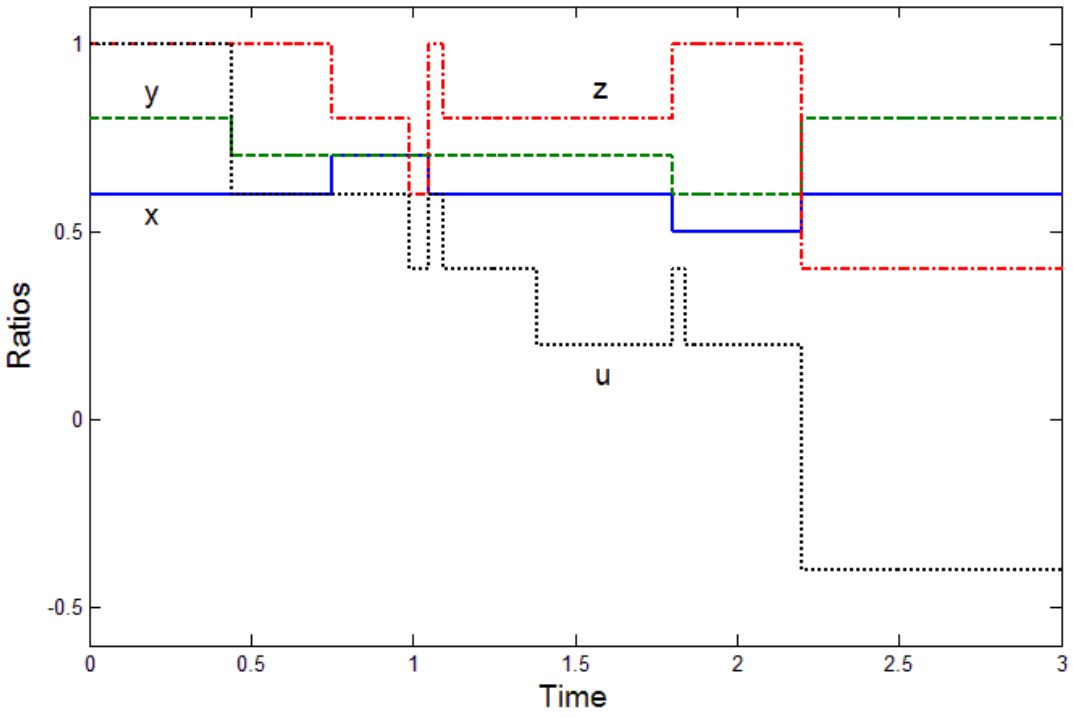

Figure 7.18. Converter operating points dictated by the system control

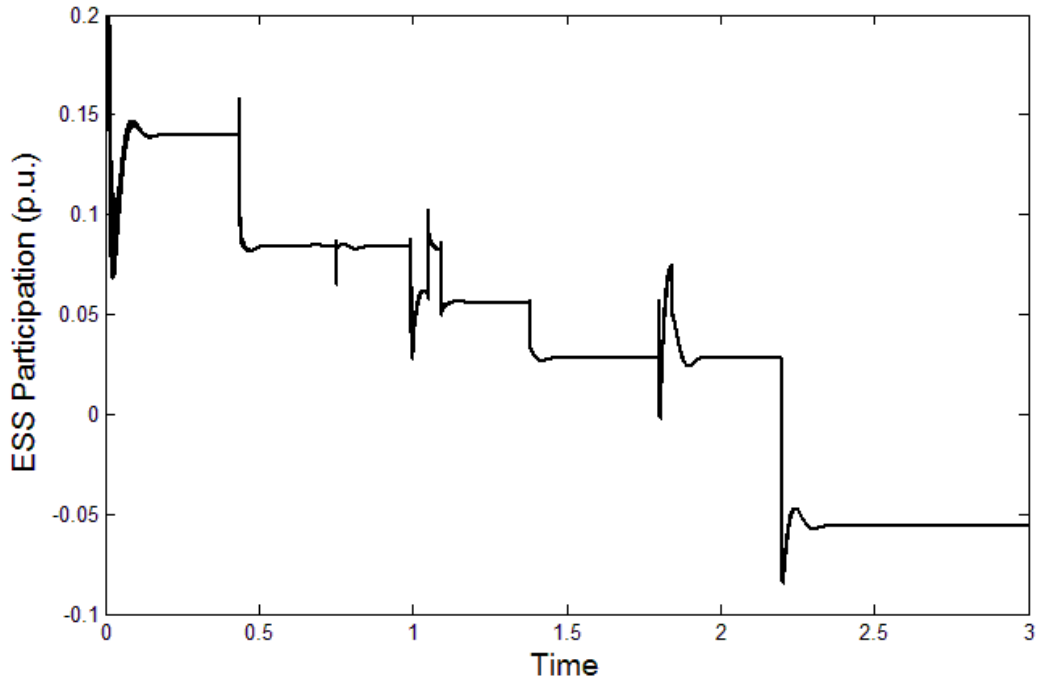

Figure 7.19. Power contribution of ESS due to different loading conditions in the shipboard system

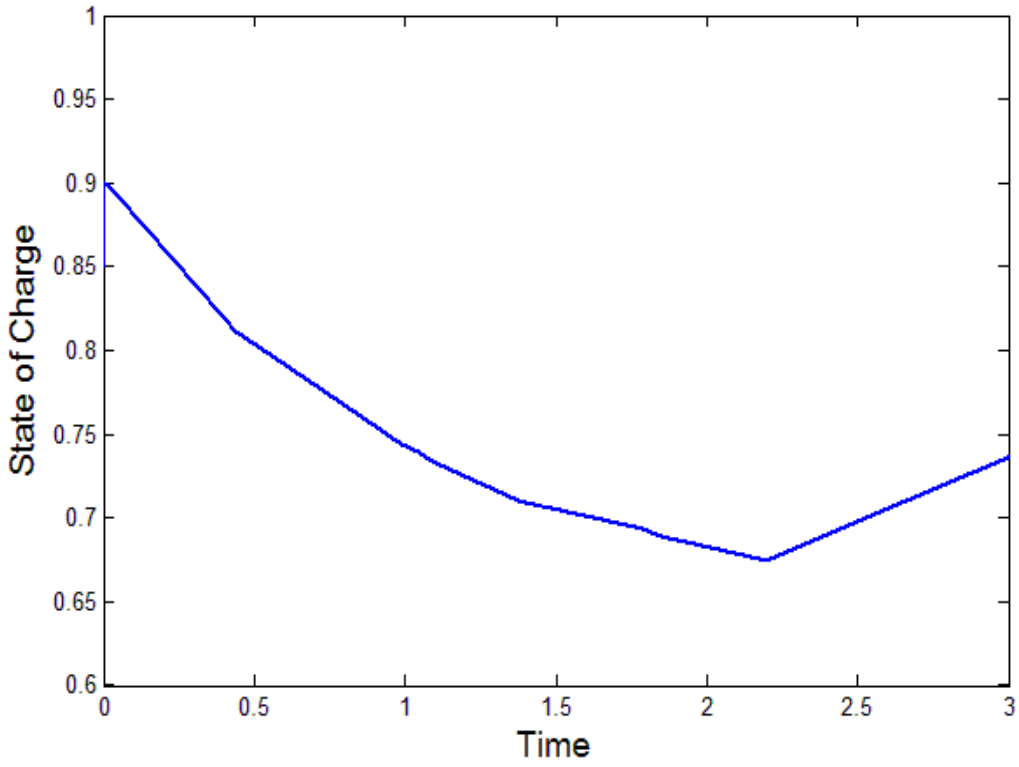

Figure 7.20. Change of SOC due to discharge of the ESS

Generators settings are shown in Figure 7.21. The main generator is running close to its rated power condition until t=1.8s. So we observe PLLS energy is mostly balanced by the Auxiliary generator. ESS keeps changing it participation to meet the system cost efficient along with buffering ramp rate constraint. As both of the zonal loads drop significantly at t=1.8s, it becomes most cost effective to produce energy from the Main generator along with a little contribution from ESS. At t=2.2s Zone2 load drops once more to 0.2s which hits the minimum generation setting of the Main Generator. The balance is obtained as the ESS starts to behave as a load and keeps charging as shown in Figure 7.19. ESS had been discharging at various rates until t=2.2s which causes SOC to drop to 0.7. SOC rises again after t=2.2s as the ESS is charging at this stage.

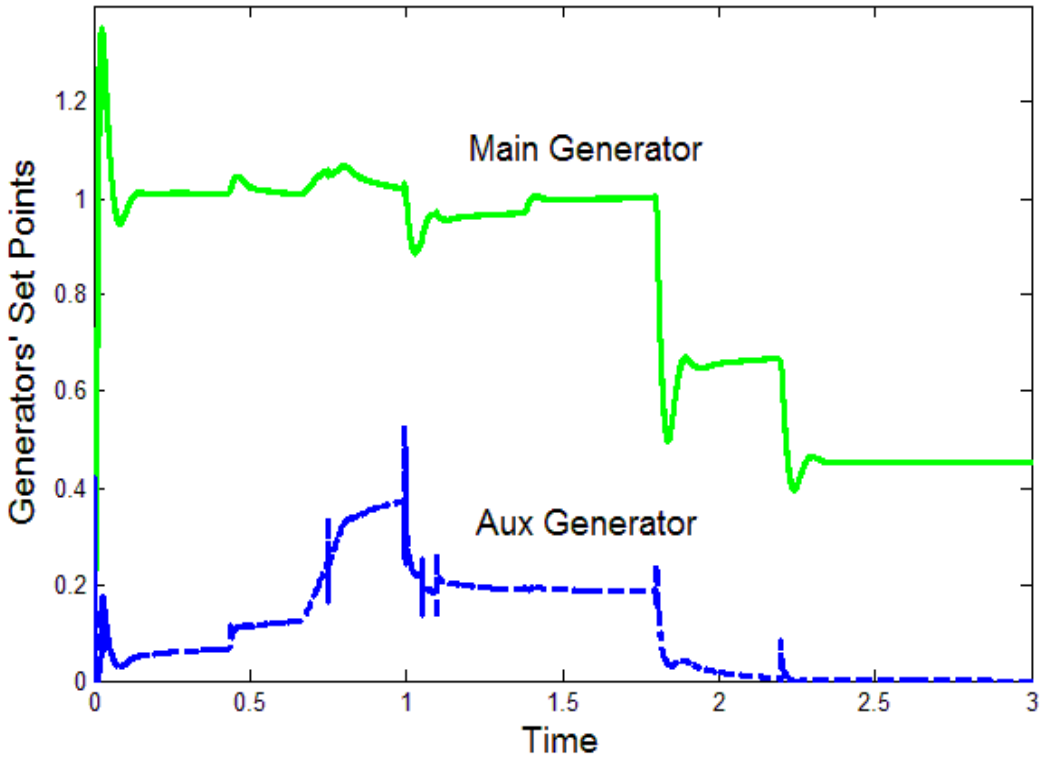

Figure 7.21. Generators' contributions in the shipboard system

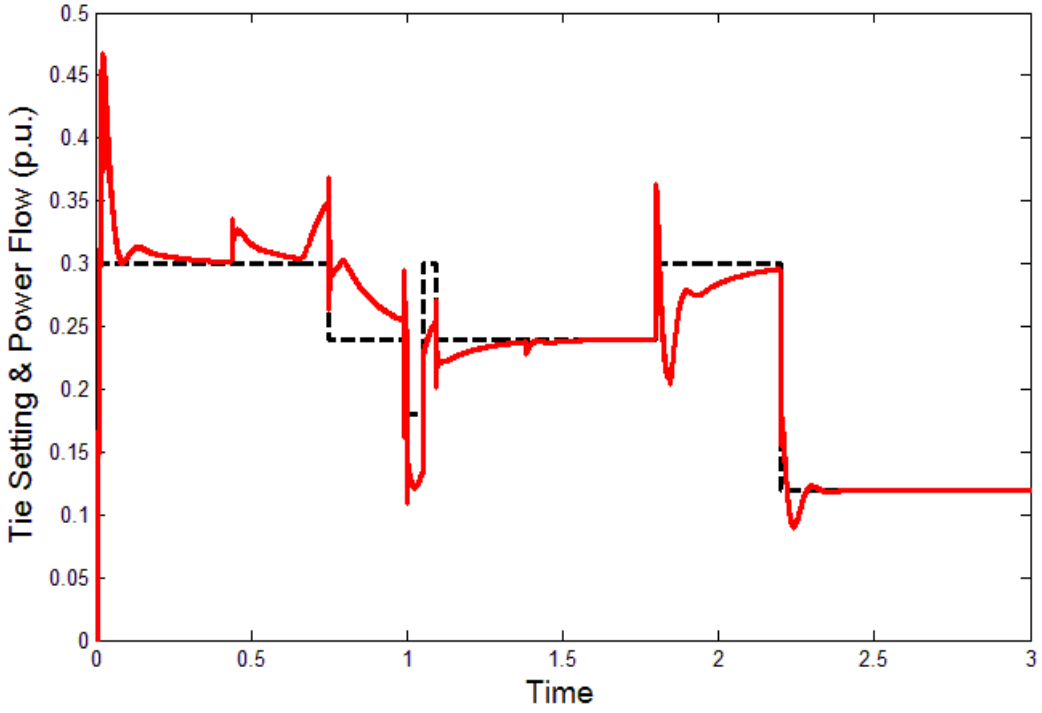

Figure 7.22. Bus cross-tie current

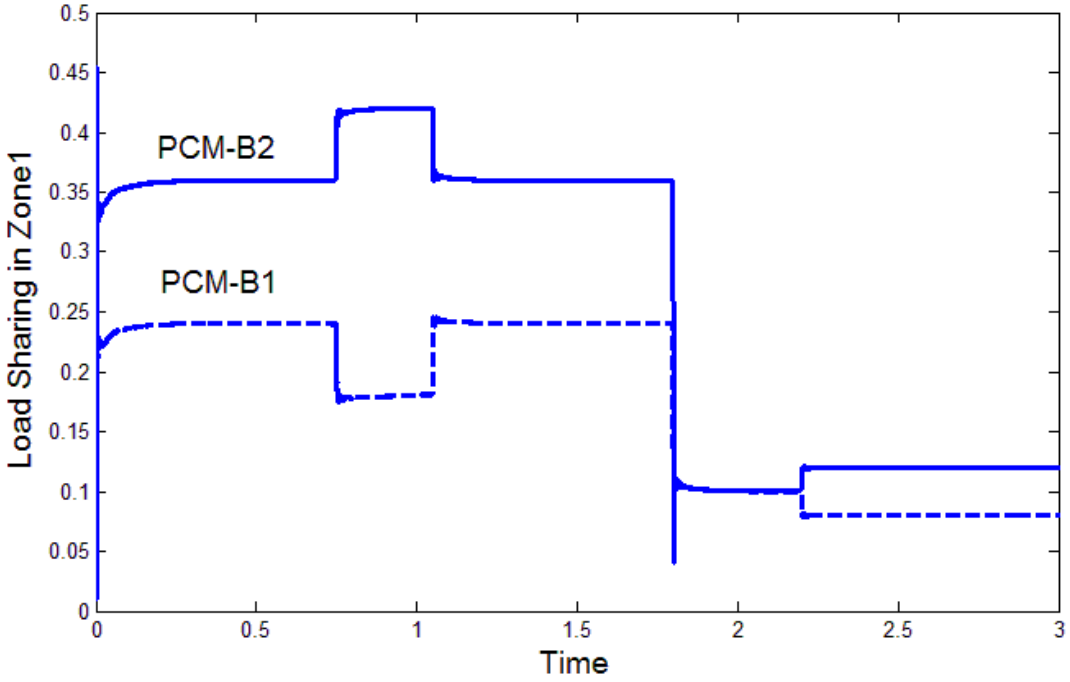

Figure 7.23. Load sharing in Zone1

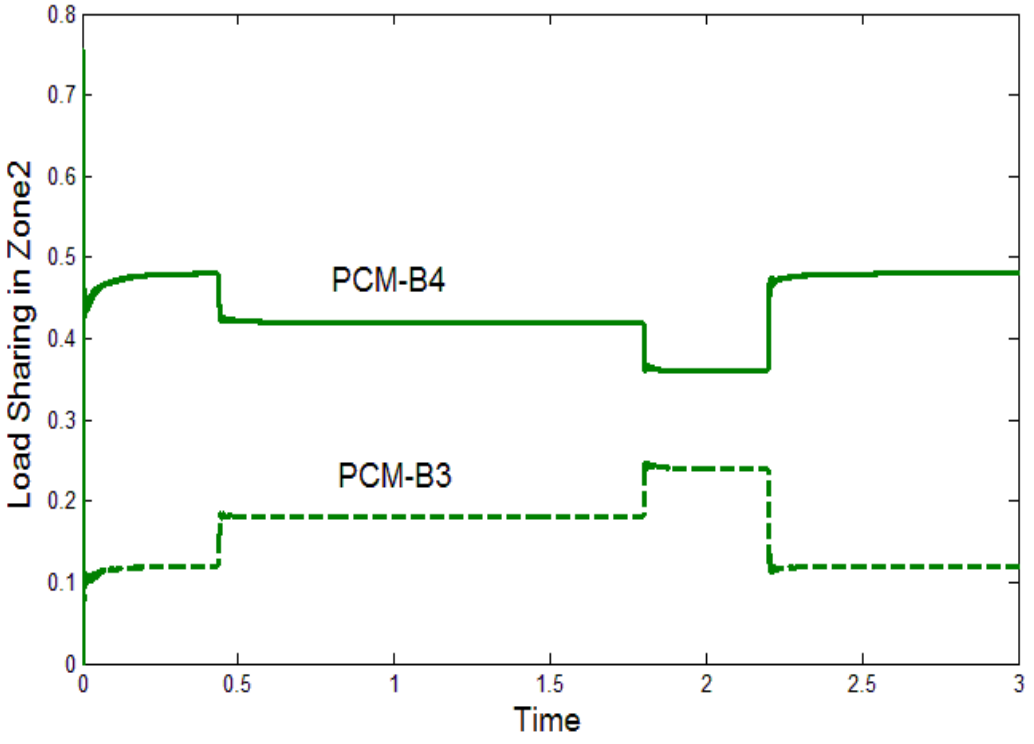

Figure 7.24. Load sharing in Zone2

Load sharing between the PCMs that supply Zone 1 and Zone 2 are shown in Figure 7.23 & 7.24 respectively. Solid line stands for the master PCM and the dashed line for the slave. Load currents follow control variables as expected.

7.4 SYSTEM LOSS MINIMIZATION OF CERTS MICROGRID

Load changes and corresponding optimal ratios of the CERTS Microgrid are shown in Figure 7.25 and Figure 7.26 respectively. Optimal ratios are the decisions of the energy manager to the generating system's controllers. Figure 7.25 shows dc values of the dynamic loads and corresponding generators' set points are shown in Figure 7.27.

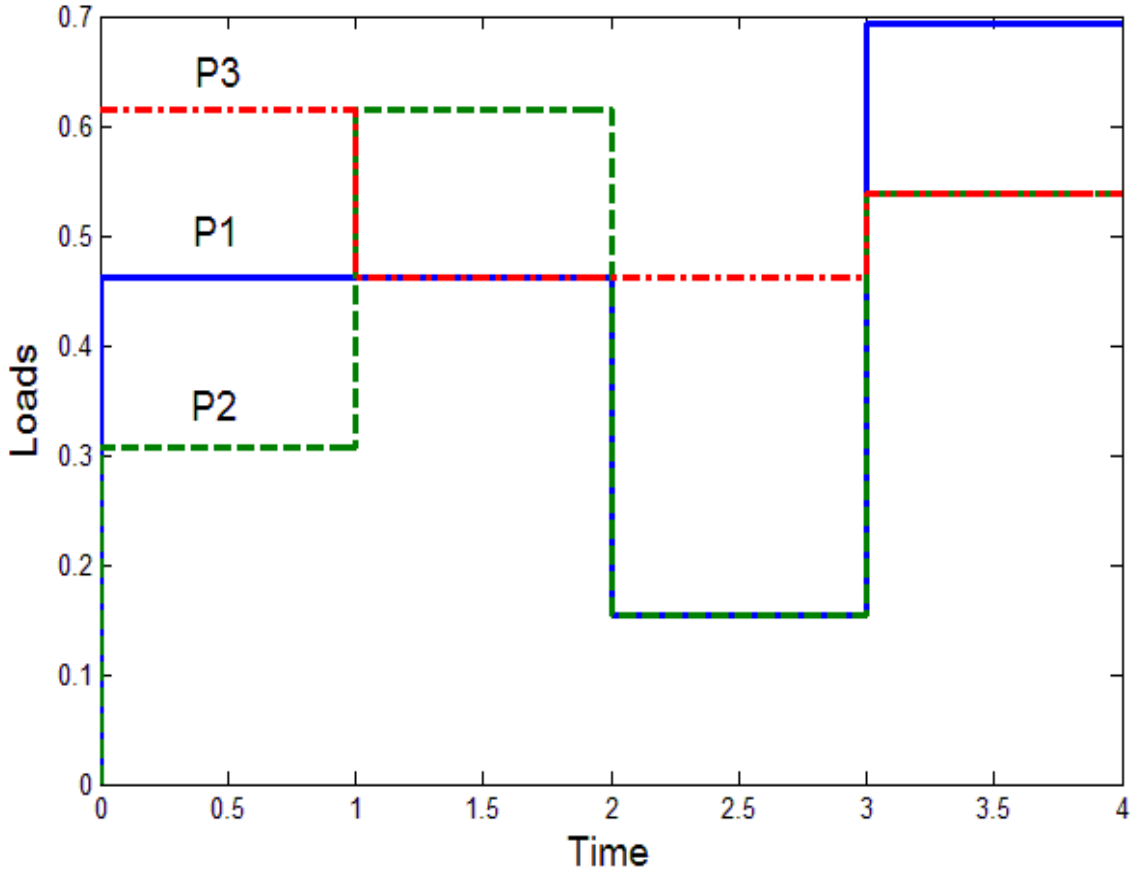

Figure 7.25. Loads in the CERTS Microgrid

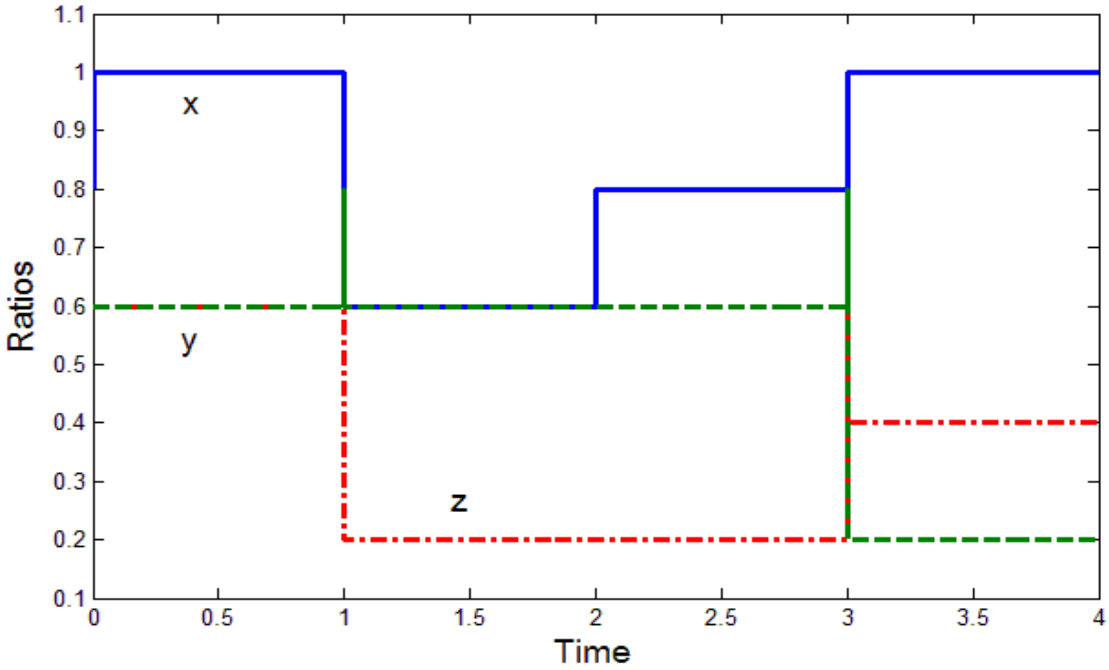

Figure 7.26. Optimal Ratios

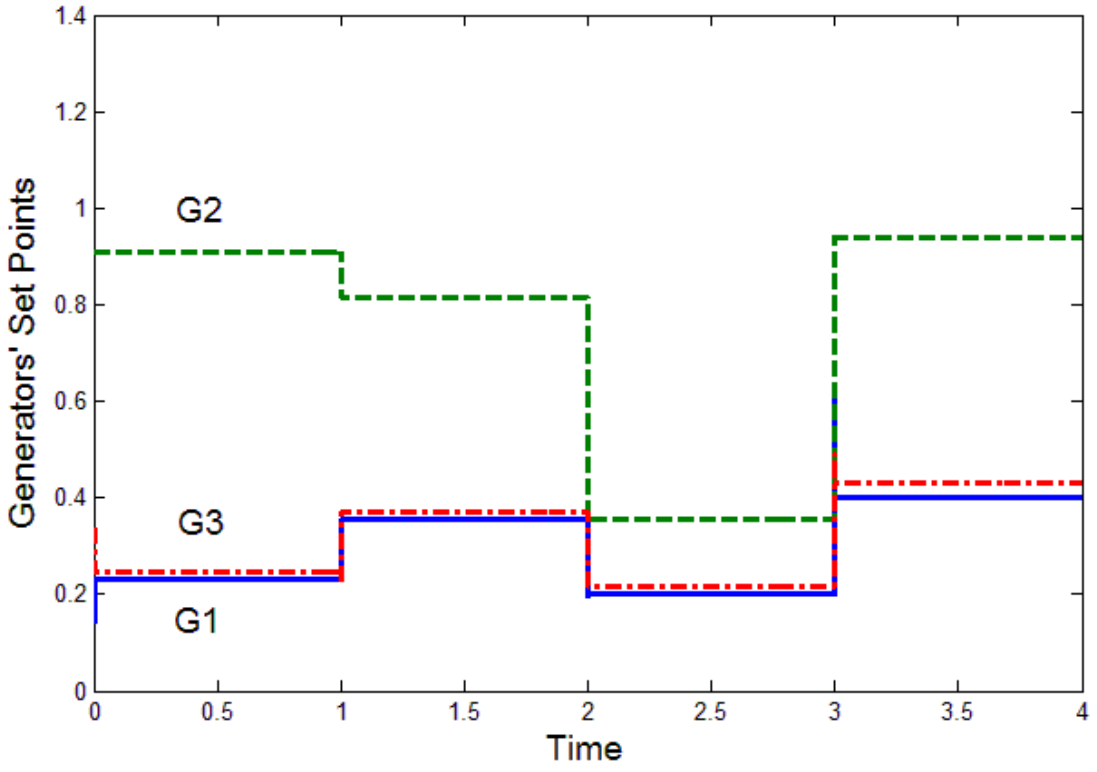

Figure 7.27. Generators' Set Points

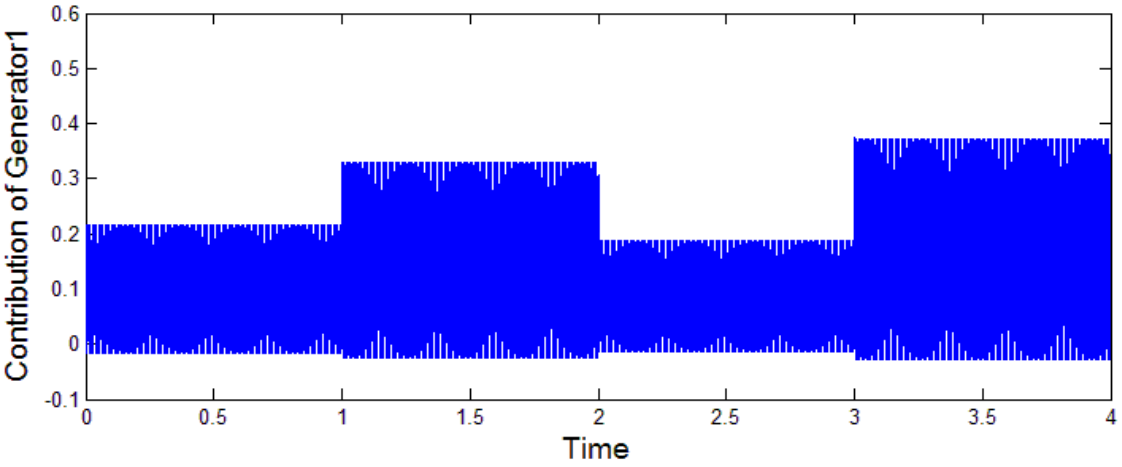

Figure 7.28. Generator1's Contribution

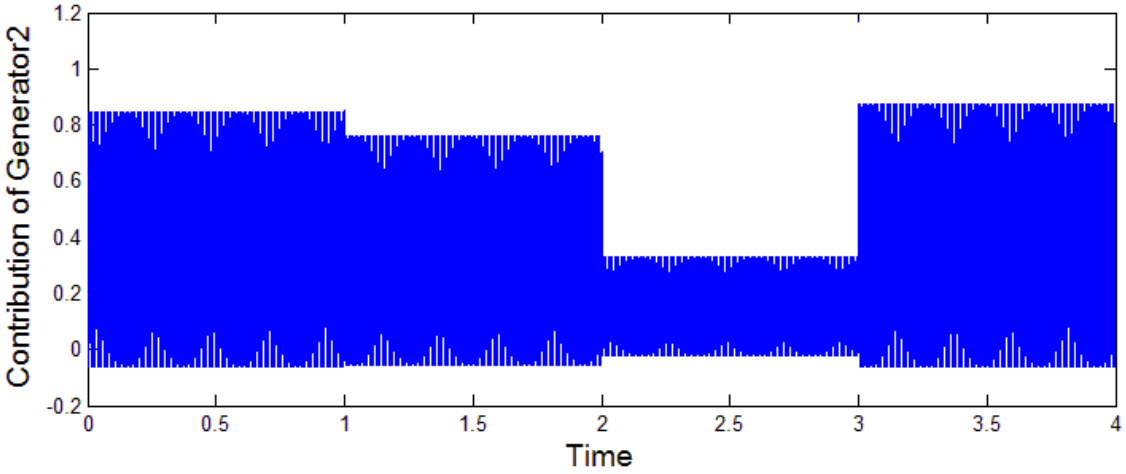

Figure 7.29. Generator2's Contribution

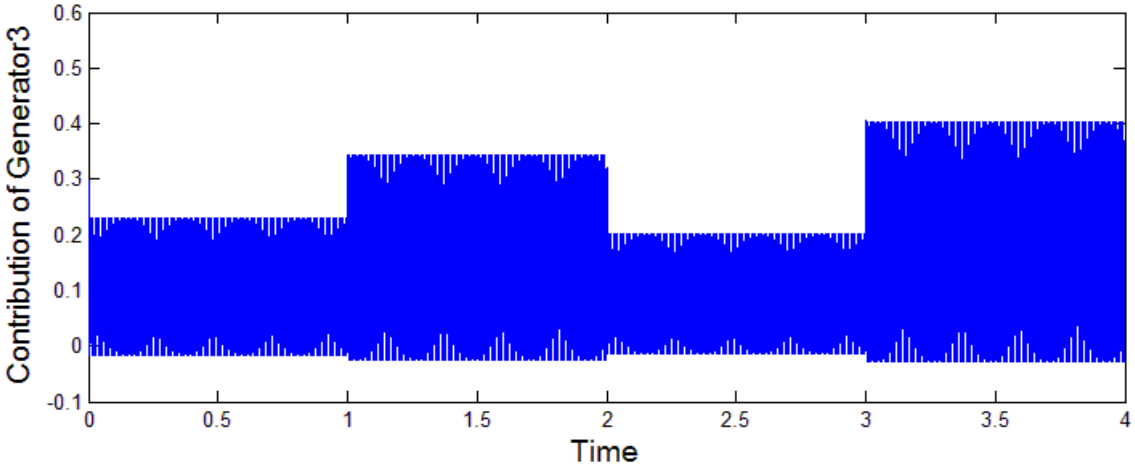

Figure 7.30. Generator3's Contribution

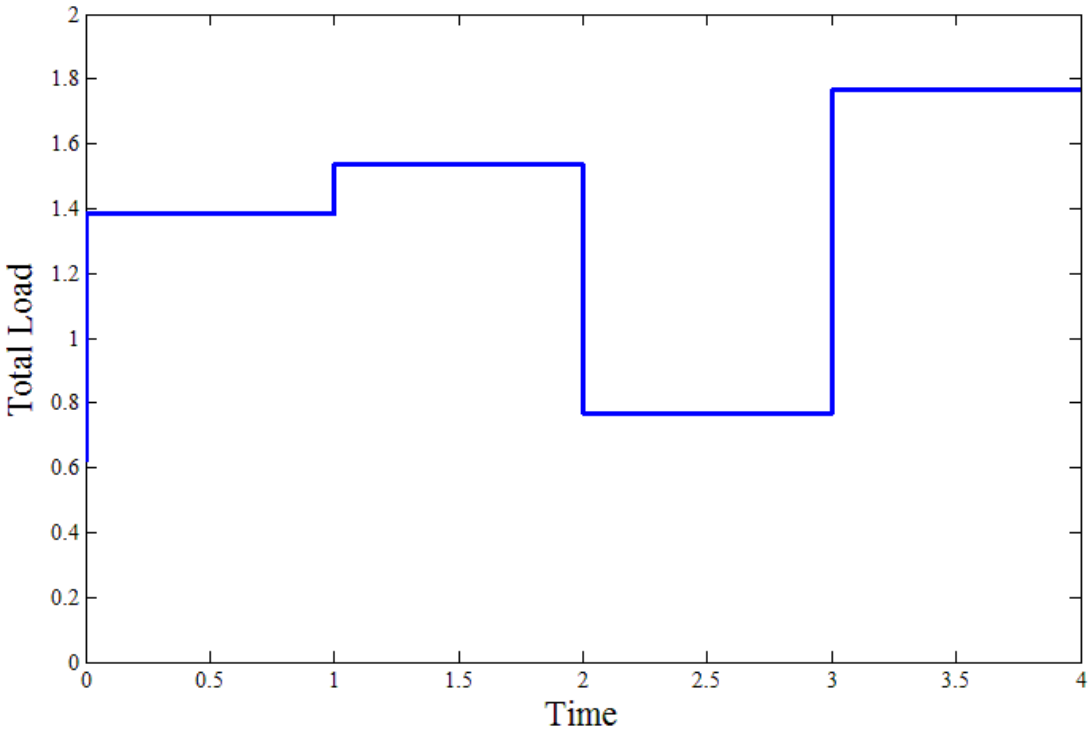

Figure 7.31. Total Load of the System

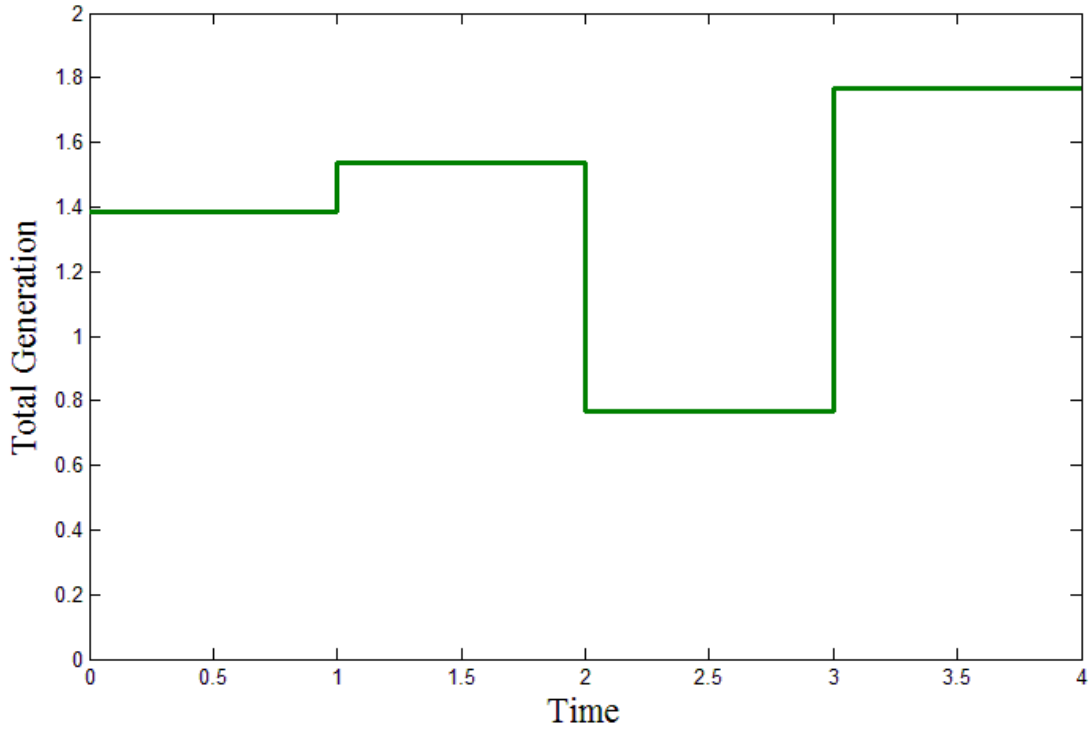

Figure 7.32. Total Generation of the System

AC values of the generators' contributions are shown in Figure 7.28, 7.29 & 7.30. Total load and total generation have been shown in Figure 7.31 & Figure 7.32. As we have used an averaged Model for CERTS Microgrid and the energy manager works perfectly, the load and generation matches exactly as shown in the two figures.

CHAPTER VIII

CONCLUSION

A distributed optimization based system control for microgrids with many power electronic converter interfaces has been developed and validated in this dissertation. The optimization algorithm ensures the most economic fuel usage and simultaneous minimization of distribution loss in microgrids by coordination of the power electronic converters.

In order for an optimization method to be used for system control it must converge to solutions in a time-frame sufficiently small for real-time system level control. The developed system is based on an appropriately framed Mixed Integer Quadratic Programming optimization algorithm that can be solved dynamically with each local converter controller solving a subset of the resulting search tree. Furthermore, the method prunes off significant number of search trees in order to reduce communication requirements between control nodes. It also offers scope to use other more aggressive pruning methods like reduction of variables, sliding over variables, greedy algorithm etc. within its structure that would make it useful for larger power systems as well.

The developed distributed control method was applied to two microgrid test systems, a shipboard power distribution system and CERTS (Consortium of Electric Reliability Technology Solutions) microgrid structure. These two test systems have attributes that

form a superset of attributes found in many other microgrids. As shown in the results, dynamic load management could save a significant amount of fuel usage. A storage system has also been used dynamically with state-of-charge based control, instead of being operated as a traditional peak shaver. An equivalent fuel cost function has been scaled and added to the energy storage system to ensure its best use. Simulation results demonstrate the effectiveness of the proposed distributed coordinating control in managing energy flow within the test systems.

The unit commitment problem is not incorporated into the developed objective function. The optimization algorithm can work on both linear and two degree non-linear function still not equipped to work with exponential terms. As start-up costs of the thermal units can be expressed as exponent of time, it must have the ability to deal with both two degree functions along with exponentials to achieve the simultaneous solution of Unit Commitment, Economic Dispatch and Distribution Loss.

The test microgrids do not have any renewable energy sources. Renewables have different characteristics cost curve than fuel based sources. Though the cost of generation for the renewables is almost free, their investment cost along with depreciation is incorporated into the characteristic cost curves. Renewables have not been discussed in this research, however, future work could add Unit Commitment along with the addition of renewables to the optimization cost function.

REFERENCES

[1] Kueck, John D., Robert H. Staunton, Solomon D. Labinov and Brendan J. Kirby, "Microgrid Energy Management System," Consultant Report prepared for the California Energy Commission, 2003.

[2] Josep M. Guerrero, "AC and DC Microgrids," Paris 31, March 2010.

[3] Ali Feliachi, Karl Schoder, Shilpa Ganesh and Hong-Jian Lai, "Distributed Control Agents Approach to Energy Management in Electric Shipboard Power Systems," *IEEE Transaction on Energy Conversion,* 2006.

[4] Xianyong Feng, Takis Zourntos, Karen L. Butler-Purry and Salman Mashayekh, "Dynamic Load Management for NG IPS Ships," *Power and Energy Society General Meeting,* 2010 IEEE.

[5] Firas Alkhalil, Philippe Degobert, Frederic Colas and Benoit Robyns, "Fuel consumption optimization of a multimachines microgrid by secant method combined with IPPD table," *European Association for the Development of Renewable Energies,* Environment and Power Quality, Valencia (Spain), 15th to 17th April, 2009.

[6] Leandro dos Santos Coelho and Chu-Sheng Lee, "Solving Economic load Dispatch problems in power systems using chaotic and Gaussian particle swarm optimization approaches," *Elsevier,* vol 30, issue 5, June 2008.

[7] Hao Liang, Bong Jun Choi, Atef Abdrabou, Weihua Zhuang and Xuemin Shen, "Decentralized Economic Dispatch in Microgrids via Heterogeneous Wireless Networks," *IEEE Journal on selected areas in communications,* vol. 30, no. 6, July 2012.

[8] Liu Xiaoping, Ding Ming, Han Jianghong, Han Pingping, and Peng Yali, "Dynamic Economic Dispatch for Microgrids Including Battery Energy Storage," *2nd IEEE International Symposium on Power Electronics for Distributed Generation Systems*, 2010.

[9] Sundari Ramabhotla, Stephen Bayne and Michael Giesselmann, "Economic Dispatch Optimization of Microgrid in Islanded Mode," *IEEE Energy and Sustainability Conference* (IESC), 2014.

[10] Yann Riffonneau, Seddik Bacha, Franck Barruel and Stephane Ploix, "Optimal Power Flow Management for Grid Connected PV Systems with Batteries," *IEEE Transactions on Sustainable Energy,* vol. 2, No. 3, July 2011.

[11] Min Dai, "Control of Power Converters for Distributed Generation Applications," Ohio State University, PhD Dissertation 2005.

[12] Marwali, M.N., Jin-Woo Jung and Keyhani A., "Control of distributed generation systems - Part II: Load sharing control," *IEEE Transactions on Power Electronics,* vol.19, no.6, pp. 1551- 1561, Nov. 2004.

[13] K. De Brabendere, K.Vanthournout, J.Driesen,G.Deconinck, and R. Belmans, "Control of microgrids," *Proc. IEEE Power Eng. Soc. General Meet.*, 2007, pp. 1–7.

[14] Farid Katiraei, Reza Iravani, Nikos Hatziargyriou and Aris Dimeas, "Microgrids Management," *IEEE Power and Energy Magazine,* May 2008.

[15] F Katiraei and M. R. Iravani, "Power Management Strategies for a Microgrid with Multiple Distributed Generation Units," *IEEE Transactions on Power Systems,* vol. 21, no. 4, November 2006.

[16] Josep M. Guerrero, Juan C. Vasquez, Jose Matas, Miguel Castilla and Luis Garcia de Vicuna, "Control Strategy for Flexible Microgrid based on Parallel Line-Interactive UPS Systems," *IEEE Transactions on Industrial Electronics,* vol 56, no. 3, March 2009.

[17] Taylan Ayken and Jun-ichi Imura, "Asynchronous Distributed Optimization of Smart Grid," *SICE Annual Conference,* August 2012, Akita University, Akita, Japan.

[18] I. Vechiu1, A. Llaria, O. Curea and H. Camblong, "Control of Power Converters for Microgrids," *Ecologic Vehicles Renewable Energies,* Monaco, March 26-29 2009.

[19] H. L. Ginn, F. Ponci and A. Monti, "Multi-Agent Control of PEBB Based Power Electronic Systems," *Proc. PowerTech,* 2011 IEEE Trondheim, pp. 1 – 6.

[20] S. Green, L. Hurst, B. Nangle, P. Cunningham, F. Somers, and R. Evans, "Software agents: A review," Technical Report TCD-CS-1997-06, Technical Report of Trinity College, University of Dublin, 1997.

[21] H yacinth S. Nwana, "Software agents: An overview," *Knowledge Engineering Review*, Vol. 11, No 3, pp. 205-244, October/November 1996.

[22] Robert A Huggins, "Energy Storage," Springer, 2010 edition..

[23] Shuo Pang, Jay Farrell, Jie Du, and Matthew Barth, "Battery State-of-Charge Estimation," *Proceedings of the American Control Conference*, Arlington VA June 25-27, 2001.

[24] R.E. Hebner, et. al. "Energy Storage in Future Electric Ships," A report from the Electric Research and Development Consortium, Jan. 2008.

[25] V Pop, H. J. Bergveld, P. H. L. Notten, and P. P. L. Regtien, "State-of-the-art of battery state-of-charge determination," *Meas. Sci. Technol.*, vol. 16, no. 12, pp. R93–R110, Dec. 2005.

[26] S. Kawachi, J. Baba, T. Kikuchi, E. Shimoda, S. Numata, E. Masada and T. Nitta, "State of Charge Control for Energy Storage by use of Cascade Control System for Microgrid," *International conference on clean electrical power*, 2009. p. 370–75.

[27] W. Chang, "The state of charge estimating methods for battery: A review," vol. Hindawi Publishing Corporation ISRN Applied Mathematics (2013) http://dx.doi.org/10.1155/2013/953792 Article ID: 953792.

[28] N. Watrin, B. Blunier, and A. Miraoui, "Review of adaptive systems for lithiumbatteries state-of-charge and state-of-health estimation," *Proceedings of IEEE Transportation Electrification Conference and Expo*, pp. 1–6, Dearborn, Mich, USA, June 2012.

[29] H. Guo, J. Jiang, and Z. Wang, "Estimating the state of charge for Ni-MH battery in HEV by RBF neural network," *Proceedings of the International Workshop on Intelligent Systems and Applications* (ISA '09), pp. 1–4,Wuhan, China, May 2009.

[30] T. Hansen and C. J. Wang, "Support vector based battery state of charge estimator," *Journal of Power Sources*, vol. 141, no. 2, pp. 351–358, March 2005.

[31] I. H. Li, W. Y. Wang, S. F. Su, and Y. S. Lee, "A merged fuzzy neural network and its applications in battery state-of-charge estimation," *IEEE Transactions on Energy Conversion*, vol. 22, no. 3, pp. 697–708, 2007.

[32] M. W. Yatsui and H. Bai, "Kalman filter based state-of-charge estimation for lithium-ion batteries in hybrid electric vehicles using pulse charging," *Proceedings of the 7th IEEE Vehicle Power and Propulsion Conference* (VPPC '11), pp. 1–5, Chicago, Ill, USA, September 2011.

[33] L. Xu, J. P. Wang, and Q. S. Chen, "Kalman filtering state of charge estimation for battery management system based on a stochastic fuzzy neural network battery model," *Energy Conversion and Management*, vol. 53, no. 1, pp. 33–39, 2012.

[34] J. Zhang and C. Xia, "State-of-charge estimation of valve regulated lead acid battery based on multi-state unscented Kalman filter," *International Journal of Electrical Power & Energy Systems*, vol. 33, no. 3, pp. 472–476, 2011.

[35] W. He, D. Huang, and D. Feng, "The prediction of SOC of lithium batteries and varied pulse charge," *Proceedings of IEEE International Conference on Mechatronics and Automation* (ICMA '09), pp. 1578–1582, Changchun, China, August 2009.

[36] Md Moinul Islam, Md Rishad Hossain, Roger A. Dougal and Charles W. Brice, "Analysis of real-world power quality disturbances employing time-frequency distribution," *Proceedings of Power Systems Conference* (PSC), *IEEE*, Clemson University, 2016.

[37] A. J. Salkind, C. Fennie, P. Singh, T. Atwater, and D. E. Reisner, "Determination of state-of-charge and state-of-health of batteries by fuzzy logic methodology," *Journal of Power Sources*, vol. 80, no. 1-2, pp. 293–300, 1999.

[38] N. Doerry, " Naval Power Systems", *IEEE Electrification Magazine*, vol. 3, No. 2, June 2015, pp. 12-21.

[39] R.E. Hebner, et. al. "Energy Storage in Future Electric Ships" A report from the Electric Research and Development Consortium, Jan. 2008.

[40] T. J. McCoy, "Integrated Power Systems- An Outline of Requirements and Functionalities for Ships", *Proceedings of the IEEE*, Vol. 103, No. 12, Dec 2015, pp. 2276-2284.

[41] R. E. Hebner, K. Davey, J. Herbst, D. Hall, J. Hahne, D. D. Surls and A Ouroua, "Dynamic Load and Storage Integration," *Proceedings of the IEEE*, Vol. 103, No. 12, Dec 2015, pp. 2344-2353.

[42] L. N. Domaschk, A. Ouroua, R.E. Hebner and O.E. Bowlin, "Coordination of large plused loads on future electric ships," *IEEE Trans. Magn.*, Vol. 43, Jan. 2007, pp. 450-4755.

[43] Brittany Wright, "A review of unit commitment," Online Available: http://www.ee.columbia.edu/ lavaei/Projects/Brittany_Wright.pdf.

[44] A. Sima Uyar and Belgin Turkay, "Evolutionary Algorithms for the Unit Commitment Problem," *Turk J Elec. Engin.*, vol. 16 n. 3, 2008, pp. 239-255.

[45] Dan Li, Roger A. Dougal, Eshwarprasad Thirunavukarasu and A. Ouroua, in "Variable Speed Operation of Turbogenerators to Improve Part-load Efficiency," *Electric Ship Technologies Symposium* (ESTS), 2013 IEEE.

[46] Amita Mahor, Vishnu Prasad and Saroj Rangnekar "Economic dispatch using particle swarm optimization: A review," *Renewable and Sustainable Energy Reviews*, vol. 13, issue 8 (2009), pp. 2134–2141.

[47] Noel Augustine, Sindhu Suresh, Prajakta Moghe and Kashif Sheikh, "Economic dispatch for a microgrid considering renewable energy cost functions," *Innovative Smart Grid Technologies* (ISGT), IEEE PES, 2012.

[48] Mimoun Younes, Riad L Kherfene and Fouad Khodja, "Environmental/Economic Power Dispatch Problem /renewable energy Using firefly algorithm," *Proceedings of the 2013 International Conference on Environment, Energy, Ecosystems and Development*.

[49] Nguyen Thi Phuong Thao and Nguyen Trung Thang, "Environmental Economic Load Dispatch with Quadratic Fuel Cost Function Using Cuckoo Search Algorithm," *International Journal of u- and e- Service, Science and Technology*, Vol.7, No.2 (2014), pp.199-210.

[50] Amita Mahor, Vishnu Prasad and Saroj Rangnekar, "Economic dispatch using particle swarm optimization: A review," *Renewable and Sustainable Energy Reviews*, 13 (2009) 2134–2141.

[51] K.T. Chau and Y.S. Wong, "Overview of power management in hybrid electric vehicles," *Energy Conversion and Management*, 43 (2002) 1953–1968.

[52] Emiliano Dall'Anese, Hao Zhu and Georgios B. Giannakis, "Distributed Optimal Power Flow for Smart Microgrids," *IEEE Transactions Smart Grid*, vol. 4, no. 3, pp. 1464–1475, Sep. 2013.

[53] Gao Jianping, Zhu GG, Strangas EG and Sun Fengchun, "Equivalent fuel consumption optimal control of a series hybrid electric vehicle," *Proceedings of the institution of mechanical engineers*, part D. J Autom Eng, 2009, 223:1003–18.

[54] G. Couloris, J. Dollimore, and T. Kindberg, "Distributed Systems Concepts and Design," 3rd ed., Addison-Wesley, 2001.

[55] Donald A. Pierre, "Optimization Theory with Applications," Mineola, N.Y., Dover Publications, 1986.

[56] Optimizing MIP Problems, Gurobi Optimization.

[57] D. P. Bertsekas and J. N. Tsitsiklis, "Parallel and Distributed Computation: Numerical Methods," Englewood Cliffs, NJ: Prentice-Hall, 1989.

[58] Dimitri P. Bertsekas, "Nonlinear Programming," Athena Scientific, 1995.

[59] Dimitri P. Bertsekas, "Dynamic Programming and Optimal Control," Athena Scientific, Belmont, Massachusetts. Volumes 1 and 2.

[60] Dimitri P. Bertsekas, "Distributed Dynamic Programming", *IEEE Transaction on Automatic Control*, Vol.AC-27, NO.3, June 1982.

[61] Maryam Nasri, Herbert L. Ginn and Mehrdad Moallem, "Application of Intelligent Agent Systems for Real-time Coordination of Power Converters (RCPC) in Microgrids," *IEEE Energy Conversion Congress and Exposition* (ECCE), 2014.

[62] S. D.J. McArthur, E.M. Davidson, V.M. Catterson, A.L. Dimeas, N.D. Hatziargyriou, F. Ponci and T. Funabashi, "Multi-agent systems for power engineering applications—Part I: concepts, approaches, and technical challenges," *IEEE Transactions on Power System* (2007), pp. 1743–1752

[63] Sasu Tarkoma, "Publish/subscribe Systems, Design and Principles," Chapters 7 & 8, Textbook, Wiley Press, 2012.

[64] M. Nasri, Md Rishad Hossain, Herbert L. Ginn and Mehrdad Moallem, "Agent-based Real-time Coordination of Power Converters in a DC Shipboard Power

System" in the *proceedings of Electric Ship Technologies Symposium* (ESTS), IEEE, VA, 2015.

[65] M. Nasri, Mehrdad Moallem, Md Rishad Hossain and Herbert L. Ginn, "Distributed Control of Converters in a DC Microgrid Using Agent Technology," P*roceedings of Power Systems Conference* (PSC), IEEE, Clemson University, 2016.

[66] MR. Hossain and HL. Ginn, "Real-time Distributed Coordination of Power Electronic Converters for Optimization of DC Shipboard Distribution Systems," *Electric Ship Technologies Symposium (ESTS) conference*, IEEE, 2015, VA.

[67] Md. Rishad Hossain and Herbert L Ginn III, "Real-time Distributed Coordination of Power Electronic Converters in a DC Shipboard Distribution System," *IEEE Transactions on Energy Conversion*, Submitted.

[68] M. R. Hossain, Y. Luo, M. H. Ali, and R. Hovsapian, "Power System Stabilization by Controlled Supercapacitor Energy Storage System," *IEEE Transactions on Energy Conversion*, Submitted.

APPENDIX A - LOSS IN SHIPBOARD MICROGRID

Fuel usage cost of a turbo-generator is expressed as:

$$C_i = a_i P^2 + b_i P + c_i \tag{A.1}$$

where a_i, b_i and c_i are turbo-generator dependent constants.

If we assume that the bus-tie impedance of the notional shipboard system is not so significant, cost for the Main and Auxiliary generator systems can be expressed as:

$$C_{gm}(\mathbf{x}) = a_m {I_{gm}}^2 + b_m I_{gm} + c_m \tag{A.2}$$

$$C_{gx}(\mathbf{x}) = a_x {I_{gx}}^2 + b_x I_{gx} + c_x \tag{A.3}$$

Again in the shipboard system, current through the Main generator,

$$I_{gm} = xI_1 + yI_2 + zI_3 - uI_4 \tag{A.4}$$

and current through the Auxiliary generator,

$$I_{gx} = (1-x)I_1 + (1-y)I_2 + I_5 - zI_3 \tag{A.5}$$

Putting the expression of I_{gm} from Equation (A.4) into Equation (A.2), we get fuel usage cost of the Main generator,

$$C_{gm}(\mathbf{x}) = (a_m I_1^2)x^2 + (a_m I_2^2)y^2 + (a_m I_3^2)z^2 + (a_m I_4^2)u^2 + (b_m I_1)x + (b_m I_2)y + (b_m I_3)z - (b_m I_4)u + 2a_m I_1 I_2 xy + 2a_m I_1 I_3 xz - 2a_m I_1 I_4 xu + 2a_m I_2 I_3 yz - 2a_m I_2 I_4 yu - 2a_m I_3 I_4 zu + c_m \quad \text{(A.6)}$$

Putting the expression of I_{gx} from Equation (A.5) into Equation (A.3), we get fuel usage cost of the Auxiliary generator,

$$C_{gx}(\mathbf{x}) = (a_x I_1^2)x^2 + (a_x I_2^2)y^2 + (a_x I_3^2)z^2 - (2a_x I_t I_1 + b_x I_1)x - (2a_x I_t I_2 + b_x I_2)y - (2a_x I_t I_3 + b_x I_3)z + 2a_x I_1 I_2 xy + 2a_x I_1 I_3 xz + 2a_x I_2 I_3 yz + (c_x + b_x I_t + a_x I_t^2) \quad \text{(A.7)}$$

where, $I_t = I_1 + I_2 + I_5$

Distribution loss of the notional shipboard power system,

$$C_{dr}(\mathbf{x}) = x^2 I_1^2 (R_1 + R_1' + R_2 + R_2') + y^2 I_2^2 (R_2 + R_2') + z^2 I_3^2 (R_2 + R_2' + R_3) + u^2 I_4^2 (R_2 + R_4) - 2xI_1 (I_1 R_1' + I_1 R_2' + I_2 R_2' + I_5 R_1' + I_5 R_2') - 2yI_2 (I_1 + I_2 + I_5) R_2' - 2zI_3 (I_1 + I_2 + I_5) R_2' + 2xyI_1 I_2 (R_2 + R_2') + 2xzI_1 I_3 (R_2 + R_2') - 2xuI_1 I_4 R_2 + 2yzI_2 I_3 (R_2 + R_2') - 2yuI_2 I_4 R_2 - 2zuI_3 I_4 R_2 + \text{Const} \quad \text{(A.8)}$$

So the System loss (fuel usage and distribution loss) becomes,

$$C_{sys}(\mathbf{x}) = (a_m I_1^2)x^2 + (a_m I_2^2)y^2 + (a_m I_3^2)z^2 + (a_m I_4^2)u^2 + (b_m I_1)x + (b_m I_2)y + (b_m I_3)z - (b_m I_4)u + 2a_m I_1 I_2 xy + 2a_m I_1 I_3 xz - 2a_m I_1 I_4 xu + 2a_m I_2 I_3 yz - 2a_m I_2 I_4 yu - 2a_m I_3 I_4 zu + (a_x I_1^2)x^2 + (a_x I_2^2)y^2 + (a_x I_3^2)z^2 - (2a_x I_t I_1 + b_x I_1)x - (2a_x I_t I_2 + b_x I_2)y - (2a_x I_t I_3 + b_x I_3)z + 2a_x I_1 I_2 xy + 2a_x I_1 I_3 xz + 2a_x I_2 I_3 yz + x^2 I_1^2 (R_1 + R_1' + R_2 + R_2') + y^2 I_2^2 (R_2 + R_2') + z^2 I_3^2 (R_2 + R_2' + R_3) + u^2 I_4^2 (R_2 + R_4) - 2xI_1 (I_1 R_1' + I_1 R_2' + I_2 R_2' + I_5 R_1' + I_5 R_2') - 2yI_2 (I_1 + I_2 + I_5) R_2' - 2zI_3 (I_1 + I_2 + I_5) R_2' + 2xyI_1 I_2 (R_2 + R_2') + 2xzI_1 I_3 (R_2 + R_2') - 2xuI_1 I_4 R_2 + 2yzI_2 I_3 (R_2 + R_2') - 2yuI_2 I_4 R_2 - 2zuI_3 I_4 R_2 + (c_m + c_x + b_x I_t + a_x I_t^2) + \text{Const} \quad \text{(A.9)}$$

APPENDIX B - LOSS IN CERTS MICROGRID

Power flow from Generator1,

$$P_{g1} = xP_1 - yP_{tie} + zP_3 \tag{B.1}$$

Putting this expression of P_{g1} into Equation (A.1), we get fuel cost due to Generator1,

$$C_{g1} = (a_1P_1^2)x^2 + (a_1P_{tie}^2)y^2 + (a_1P_3^2)z^2 + (b_1P_1)x - (b_1P_{tie})y + (b_1P_3)z - (2a_1P_1P_{tie})xy + (2a_1P_1P_3)xz - (2a_1P_{tie}P_3)yz + c_1 \tag{B.2}$$

Power flow from Generator2,

$$P_{g2} = P_2 + yP_{tie} \tag{B.3}$$

which gives cost due to Generator2,

$$C_{g2} = (a_2P_{tie}^2)y^2 + (2a_2P_2P_{tie} + b_2P_{tie})y + (a_2P_2^2 + b_2P_2 + c_2) \tag{B.4}$$

Contribution from Generator3,

$$P_{g3} = P_1 + P_3 - xP_1 - zP_3 \tag{B.5}$$

This gives cost due to Generator3,

$$C_{g3} = (a_3P_1^2)x^2 + (a_3P_3^2)z^2 - [2a_3P_1(P_1 + P_3) + b_3P_1]x - [2a_3P_3(P_1 + P_3) + b_3P_3]z + (2a_3P_1P_3)xz + (b_3P_1 + b_3P_3 + a_3P_1^2 + a_3P_3^2 + 2a_3P_1P_3 + c_3) \tag{B.6}$$

So, system loss of the CERTS Microgrid,

$$
\begin{aligned}
C_{sys} &= (a_1 P_1^2)x^2 + (a_1 P_{tie}^2)y^2 + (a_1 P_3^2)z^2 + (b_1 P_1)x - (b_1 P_{tie})y + (b_1 P_3)z \\
&-(2a_1 P_1 P_{tie})xy + (2a_1 P_1 P_3)xz - (2a_1 P_{tie} P_3)yz + c_1 + (a_2 P_{tie}^2)y^2 \\
&+(2a_2 P_2 P_{tie} + b_2 P_{tie})y + (a_2 P_2^2 + b_2 P_2 + c_2) + (a_3 P_1^2)x^2 + (a_3 P_3^2)z^2 \\
&-[2a_3 P_1 (P_1 + P_3) + b_3 P_1]x - [2a_3 P_3 (P_1 + P_3) + b_3 P_3]z + (2a_3 P_1 P_3)xz \\
&+(b_3 P_1 + b_3 P_3 + a_3 P_1^2 + a_3 P_3^2 + 2a_3 P_1 P_3 + c_3) + C_{dr}
\end{aligned}
\tag{B.7}
$$

And the constraints are,

$$g_1(\mathbf{x}) = xP_1 - yP_{tie} + zP_3 \le (P_{g1})_{\max} \tag{B.8}$$

$$g_2(\mathbf{x}) = P_2 + yP_{tie} \le (P_{g2})_{\max} \tag{B.9}$$

$$g_3(\mathbf{x}) = (1-x)P_1 + (1-z)P_3 \le (P_{g3})_{\max} \tag{B.10}$$

APPENDIX C - SCALING AND CHANGE OF VARIABLES

Let,

$$z_1^{/} = b_1 x \tag{C.1}$$

$$z_2^{/} = c_1 x + c_2 y \tag{C.2}$$

$$z_3^{/} = d_1 x + d_2 y + d_3 z \tag{C.3}$$

$$z_4^{/} = e_1 x + e_2 y + e_3 z + e_4 u \tag{C.4}$$

Equation (5.1) can then be converted as,

$$C_{sys} = z_1^{/2} + k_1 z_1^{/} + z_2^{/2} + k_2 z_2^{/} + z_3^{/2} + k_3 z_3^{/} + z_4^{/2} + k_4 z_4^{/} + Const \tag{C.5}$$

where k_1, k_2, k_3 and k_4 are load dependent constants.

If we assume,

$z_1 = [z_1^{/} + \frac{k_1}{2}]$, $z_2 = [z_2^{/} + \frac{k_2}{2}]$, $z_3 = [z_3^{/} + \frac{k_3}{2}]$, $z_4 = [z_4^{/} + \frac{k_4}{2}]$, Equation (5.1) can then be expressed as,

$$C_{sys} = z_1^2 + z_2^2 + z_3^2 + z_4^2 + Const - \frac{1}{4}(k_1^2 + k_2^2 + k_3^2 + k_4^2) \tag{C.6}$$

We need to optimize variable portion of the cost function only. So the ultimate cost function that needs to be taken care of is,

$$C_{sys}(\mathbf{x}) = z_1{}^2 + z_2{}^2 + z_3{}^2 + z_4{}^2 = \sum_{i=1}^{n} z_i{}^2 \tag{C.7}$$